

# UNCLASSIFIED

AD NUMBER
AD907152
NEW LIMITATION CHANGE
TO Approved for public release, distribution unlimited
FROM Distribution authorized to U.S. Gov't. agencies only; Test and Evaluation; 01 DEC 1972. Other requests shall be referred to Air Force Weapons Lab., Kirtland AFB, NM.
AUTHORITY
CEEDO USAF ltr 29 Jun 1977

THIS PAGE IS UNCLASSIFIED

THIS REPORT HAS BEEN DELIMITED  
AND CLEARED FOR PUBLIC RELEASE  
UNDER DOD DIRECTIVE 5200.20 AND  
NO RESTRICTIONS ARE IMPOSED UPON  
ITS USE AND DISCLOSURE.

DISTRIBUTION STATEMENT A

APPROVED FOR PUBLIC RELEASE;  
DISTRIBUTION UNLIMITED.

AD907152  
AFWL-TR-72-61

AFWL-TR-  
72-61

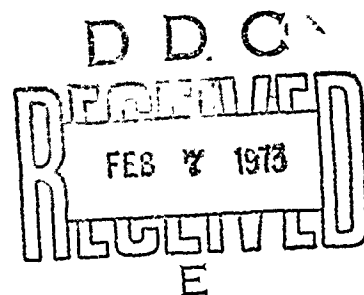
## PAVEMENT CRATERING STUDIES

Asbjorn Kvammen, Jr.      Raman Pichumani  
The Eric H. Wang Civil Engineering Research Facility  
University of New Mexico

James L. Dick, Jr.  
Capt.      USAF  
Air Force Weapons Laboratory

TECHNICAL REPORT NO. AFWL-TR-72-61

December 1972

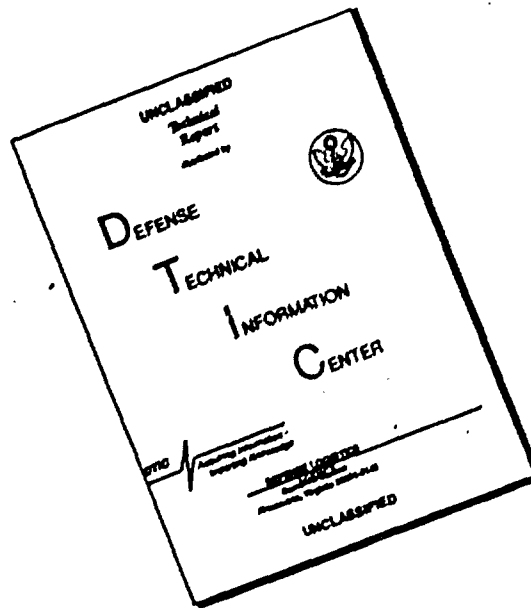


AIR FORCE WEAPONS LABORATORY

Air Force Systems Command  
Kirtland Air Force Base  
New Mexico

Distribution limited to U.S. Government agencies only because of test and evaluation (1 Dec 72). Other requests for this document must be referred to AFWL (DEZ), Kirtland AFB, NM.

# DISCLAIMER NOTICE



THIS DOCUMENT IS BEST QUALITY AVAILABLE. THE COPY FURNISHED TO DTIC CONTAINED A SIGNIFICANT NUMBER OF PAGES WHICH DO NOT REPRODUCE LEGIBLY.

AFML-TR-72-61

AIR FORCE WEAPONS LABORATORY  
Air Force Systems Command  
Kirtland Air Force Base  
New Mexico 87117

When US Government drawings, specifications, or other data are used for any purpose other than a definitely related Government procurement operation, the Government thereby incurs no responsibility nor any obligation whatsoever, and the fact that the Government may have formulated, furnished, or in any way supplied the said drawings, specifications, or other data, is not to be regarded by implication or otherwise, as in any manner licensing the holder or any other person or corporation, or conveying any rights or permission to manufacture, use, or sell any patented invention that may in any way be related thereto.

DO NOT RETURN THIS COPY. RETAIN OR DESTROY.

AFWL-TR-72-61

PAVEMENT CRATERING STUDIES

Asbjorn Kvammen, Jr.

Raman Pichumani

The Eric H. Wang Civil Engineering Research Facility  
University of New Mexico

James L. Dick, Jr.  
Capt. USAF

Air Force Weapons Laboratory

TECHNICAL REPORT NO. AFWL-TR-72-61

Distribution limited to U.S. Government agencies only because of test and evaluation (1 Dec 72). Other requests for this document must be referred to AFWL (DEZ), Kirtland AFB, NM.

FOREWORD

This report was prepared by the Eric H. Wang Civil Engineering Research Facility, University of New Mexico, Albuquerque, New Mexico, under Contract F29601-72-C-0024. The research was performed under Program Element 63723F, Project 683M, Subtask 4.6.110.

Inclusive dates of research were January 1971 through January 1972. The report was submitted 10 November 1972 by the Air Force Weapons Laboratory Project Officer, Captain James L. Dick (DEZ-S).

This technical report has been reviewed and is approved.



JAMES L. DICK  
Captain, USAF  
Project Officer



OREN G. STROM  
Lt Colonel, USAF  
Chief, Aerospace Facilities Branch



WILLIAM B. LIDDICOET  
Colonel, USAF  
Chief, Civil Engineering Research  
Division

# ABSTRACT

## (Distribution Limitation Statement B)

The objectives of this research effort were twofold: (1) to define the damage to airfield pavement systems caused by a wide range of C-4 Charges and bombs when detonated at various depths below the pavement surface (i.e., determine the extent of damage expected from these explosives), and (2) to investigate the feasibility of scaling pavement systems and explosive in order to more economically study cratering effects on different pavement systems. The first objective was implemented by a series of tests using 5 , 15 , and 25-lb C-4 charges placed at various depths under pavement surfaces in two abandoned airfields (Fort Sumner and Hays) and three sizes of bombs at the Hays test site. Damage such as the repair volumes, true crater depths, etc., were plotted as a function of charge size and depth-of-burst. Three types of craters were found: (1) shallow depth-of-burst craters of hemispherical shape, (2) deep depth-of-burst craters with no apparent crater and little ejecta, and (3) intermediate depth-of-burst craters exhibiting some of the characteristics of both the shallow and the deep craters. The crater dimensions from Fort Sumner (sandy silt subgrade) were, in general, smaller than those from Hays (clay subgrade) for all C-4 charges. A similitude analysis was conducted using the test data from the C-4 charges (Hays) to ascertain if a scaling factor or a distortion factor could be determined. The study revealed that the scaling factor varied widely when scaling the maximum damage depth-of-burst, the radius of the crater at the surface, and the crater volumes. To accomplish the second objective, small-scale tests were conducted modeling the full-scale experimental tests performed at CERF in 1969. This study also indicated variations in scaling factors.



## CONTENTS

<u>Section</u>	<u>Page</u>
I INTRODUCTION	1
II TEST SITES	3
III EXPLOSIVES	8
IV CRATER PARAMETERS	10
V TEST PROCEDURES	13
VI FULL-SCALE FIELD TEST DATA	17
1. Crater Types	17
2. Fort Sumner Test Results	17
3. Hays Test Results	25
VII DATA ANALYSIS	56
1. Fort Sumner Data	56
2. Hays Data	59
VIII SMALL-SCALE MODEL FEASIBILITY STUDY	84
1. Literature Survey	84
2. Preliminary Model Study	86
IX CONCLUSIONS AND RECOMMENDATIONS	96
Appendixes:	
I Fort Sumner Subsurface Exploration Data	99
II Hays Subsurface Exploration Data	109
III Fort Sumner Crater Data	118
IV Hays Crater Data	132
V Model Study Data	164
References	173

## ILLUSTRATIONS

<u>Figure</u>		<u>Page</u>
1	Fort Sumner Test Site	4
2	Fort Sumner Test Section	5
3	Hays Test Site	6
4	Hays Test Section	7
5	C-4 Charges Used at Fort Sumner and Hays	8
6	Bombs Used at Hays	9
7	Typical Crater	11
8	Typical Crack Pattern of Concrete with Joints	12
9	2.5-lb C-4 Shape Charge	13
10	Auger and Typical C-4 Charge	14
11	Placement of 500-lb Bomb	14
12	Crater Types	18
13	True Soil and Concrete Crater Volumes versus Depth-of-Burst for 5-lb Charge (Fort Sumner)	20
14	Crater Radii versus Depth-of-Burst for 5-lb Charge (Fort Sumner)	20
15	Crater from Detonation of 5-lb Charge (Fort Sumner)	21
16	True Soil and Concrete Crater Volumes versus Depth-of-Burst for 15-lb Charge (Fort Sumner)	22
17	Crater Radii versus Depth-of-Burst for 15-lb Charge (Fort Sumner)	22
18	Craters from Detonation of 15-lb Charge (Fort Sumner)	23
19	True Soil and Concrete Crater Volumes versus Depth-of-Burst for 25-lb Charge (Fort Sumner)	26
20	Crater Radii versus Depth-of-Burst for 25-lb Charge (Fort Sumner)	26
21	Crater from Detonation of 25-lb Charge (Fort Sumner)	27
22	True Soil and Concrete Crater Volumes versus Depth-of-Burst for 5-lb Charge Under 8-Inch-Thick Concrete (Hays)	28

# ILLUSTRATIONS (Cont'd)

<u>Figure</u>		<u>Page</u>
23	Crater Radii versus Depth-of-Burst for 5-lb Charge Under 8-Inch-Thick Concrete (Hays)	28
24	Craters from Detonation of 5-lb Charge Under 8-Inch-Thick Concrete (Hays)	30
25	True Soil and Concrete Crater Volumes versus Depth-of-Burst for 5-lb Charge Under 11-Inch-Thick Concrete (Hays)	32
26	Crater Radii versus Depth-of-Burst for 5-lb Charge Under 11-Inch-Thick Concrete (Hays)	32
27	True Soil and Concrete Crater Volumes versus Depth-of-Burst for 15-lb Charge Under 8-Inch-Thick Concrete (Hays)	33
28	Crater Radii versus Depth-of-Burst for 15-lb Charge Under 8-Inch-Thick Concrete (Hays)	33
29	Craters from Detonation of 15-lb Charge Under 8-Inch-Thick Concrete (Hays)	34
30	True Soil and Concrete Crater Volumes versus Depth-of-Burst for 15-lb Charge Under 11-Inch-Thick Concrete (Hays)	37
31	Crater Radii versus Depth-of-Burst for 15-lb Charge Under 11-Inch-Thick Concrete (Hays)	37
32	Craters from Detonation of 15-lb Charge Under 11-Inch-Thick Concrete (Hays)	39
33	True Soil and Concrete Crater Volumes versus Depth-of-Burst for 25-lb Charge Under 8-Inch-Thick Concrete (Hays)	40
34	Crater Radii versus Depth-of-Burst for 25-lb Charge Under 8-Inch-Thick Concrete (Hays)	40
35	Craters from Detonation of 25-lb Charge Under 8-Inch-Thick Concrete (Hays)	41
36	True Soil and Concrete Crater Volumes versus Depth-of-Burst for MK-81 Bomb (Hays)	44
37	Crater Radii versus Depth-of-Burst for MK-81 Bomb (Hays)	44
38	Craters from Detonation of MK-81 Bomb (Hays)	45
39	True Soil and Concrete Crater Volumes versus Depth-of-Burst for MK-82 Bomb (Hays)	48
40	Crater Radii versus Depth-of-Burst for MK-82 Bomb (Hays)	48

# ILLUSTRATIONS (Cont'd)

<u>Figure</u>		<u>Page</u>
41	Craters from Detonation of MK-82 Bomb (Hays)	49
42	True Soil and Concrete Crater Volumes versus Depth-of-Burst for M-117 Bomb (Hays)	53
43	Crater Radii versus Depth-of-Burst for M-117 Bomb (Hays)	53
44	Craters from Detonation of M-117 Bomb (Hays)	54
45	Crater Damage versus Charge Size (Fort Sumner)	57
46	Ratio of Average Concrete Repair Volume to Average Combined Repair Volume versus C-4 Charge Size (Fort Sumner)	60
47	Area of Concrete to be Removed versus Depth-of-Burst for C-4 Charges (Fort Sumner)	61
48	True Crater Depth versus Depth-of-Burst (Fort Sumner)	62
49	Aspect Ratio versus Depth-of-Burst for C-4 Charges (Fort Sumner)	63
50	Crater Damage versus Charge Size (Hays)	65
51	Ratio of Average Concrete Repair Volume to Average Combined Repair Volume versus C-4 Charge Size (Hays)	67
52	Area of Concrete to be Removed versus Depth-of-Burst for C-4 Charges (Hays)	68
53	Aspect Ratio versus Depth-of-Burst for C-4 Charges (Hays)	70
54	Crater Damage versus Bomb Size (Hays)	75
55	Area of Concrete to be Removed versus Depth-of-Burst for Bombs (Hays)	78
56	Apparent Crater Depth versus Depth-of-Burst for Bombs (Hays)	79
57	Ejecta versus Depth-of-Burst for Bombs (Hays)	80
58	Apparent Crater Volume versus Depth-of-Burst for Bombs (Hays)	81
59	True Crater Depth versus Depth of-Burst for C-4 Charges and Bombs (Hays)	83
60	Full-Scale Rigid Pavement System [after Pichumani (ref. 1)]	87

# ILLUSTRATIONS (Concl'd)

<u>Figure</u>		<u>Page</u>
61	Models of Rigid Pavement System	89
62	Location of Borings (Fort Sumner)	100
63	Location of Borings (Hays)	110

# TABLES

<u>Table</u>		<u>Page</u>
I	Summary of Average Damage Quantities for C-4 Charges (Fort Sumner)	19
II	Summary of Average Damage Quantities for C-4 Charges (Hays)	29
III	Summary of Average Damage Quantities for Bombs (Hays)	42
IV	Shallowest and Maximum Damage Depth-of-Burst Data for C-4 Charges (Fort Sumner)	56
V	Shallowest and Maximum Damage Depth-of-Burst Data for C-4 Charges (Hays)	64
VI	Scaling and Distortion Factors for C-4 Charges (Hays)	73
VII	Shallowest and Maximum Damage Depth-of-Burst Data for Bombs (Hays)	74
VIII	Summary of Apparent Crater Damage for Bombs (Hays)	82
IX	Model Study Test Data	92
X	Summary of True Crater Damage for Model Tests	93
XI	Summary of Test Results from Reference 1	95
XII	Computed Scaling Factors from Model Study	95
XIII	Soil Test Data (Fort Sumner)	101
XIV	Concrete Test Data (Fort Sumner)	108
XV	Soil Test Data (Hays)	111
XVI	Summary of In-Place Density Tests (Hays)	115
XVII	Concrete Test Data (Hays)	117
XVIII	Damage Quantities for C-4 Charges (Fort Sumner)	119
XIX	Damage Quantities for C-4 Charges (Hays)	133
XX	Damage Quantities for Bombs (Hays)	135

## ABBREVIATIONS AND SYMBOLS

C	linear parameter
D	true crater depth
$E_c$	modulus of elasticity of concrete
$G_s$	specific gravity
H	apparent crater depth
$R_1$	surface crater radius (calculated)
$R_2$	crater repair radius (calculated)
$R_3$	maximum radius at any depth
V	volume
W	weight of explosive
$f'_c$	compressive strength of concrete
m	distortion factor
n	scaling factor
w	moisture content
$\gamma$	density of media
$\gamma_d$	dry soil density

## SECTION I

### INTRODUCTION

#### 1. BACKGROUND

Development of expedient techniques for rapidly repairing airfield pavements damaged by small and large weapons has recently acquired great importance. A prerequisite for this development is the proper understanding of the damage parameters of pavement cratering. A preliminary study of these parameters was carried out by the Air Force Weapons Laboratory (AFWL) in conjunction with the University of New Mexico at the Eric H. Wang Civil Engineering Research Facility (CERF) (ref. 1). In this study small cratering charges (1-1/2 lb of C-4 explosive) were used to simulate the BLU-67, an aerially delivered cratering device. These charges were detonated at a constant depth of 30 in. below different pavement systems. The effect of different pavement systems on the resulting craters was studied as well as the effect of detonation under joints and joint intersections.

Subsequent requirements have necessitated an expanded program to test the effects of large charges detonated at various depths below pavement surfaces. Test sites were selected to provide a variation in subgrade and pavement thickness similar to the European theater of operations.

#### 2. OBJECTIVES

The first objective of this effort was to define the damage parameters that can be expected from a variety of charges and bombs detonated at various depths below the surface of airfield pavements. These damage parameters are of paramount importance in formulating repair techniques and in designing repair equipment to encompass all possible situations. The effects of the subgrade and pavement thickness on the resulting craters were also of primary concern. The second objective was to determine the feasibility of scaling the damage expected in different pavement systems by varying explosive charges to lower the cost of experimentation.

#### 3. APPROACH

To achieve the above mentioned objectives, two parallel research programs were undertaken: (1) full-scale field tests at two abandoned airfields, and



(2) small-scale model studies consisting of a feasibility study, including a literature survey, and a model study of the full-scale field tests. (In this report only the feasibility study of the small-scale models is included. The model study of the full-scale field tests has not been conducted.)

The full-scale field tests consisted of a series of shots with a military plastic explosive (C-4) having a charge weight of 15 lb detonated at 10, 30, 50, 70, 90, and 110 in. below the pavement surface. This initial series was repeated a number of times. After the necessary data were accumulated, the depth-of-burst causing the maximum crater volume was noted. Since the scaling factor for cratering in pavement systems has not yet been determined, cube-root scaling used in general cratering problems was used to calculate the depth-of-burst for the other charges (5- and 25-lb C-4 explosive). Two additional depths-of-burst for both the 5- and 25-lb charges were arbitrarily set at  $1/2$  and  $3/2$  of the chosen scaled depth-of-burst. Each of the three depths-of-burst was used three times for a total of nine shots for each of the two charges.

Of critical importance in this research effort was the definition of the range of runway damage developed from the detonation of bombs. To define this damage, three bombs were tested--the MK-81 (250-lb bomb), the MK-82 (500-lb low-drag bomb), the M-117 (750-lb general purpose bomb). Six of each were tested. The depths-of-burst chosen were calculated from cube-root scaling of the depth-of-burst giving maximum damage from the 25-lb uncased C-4 charge. Subsequent depths-of-burst were selected after each crater was excavated and volumes were calculated.

To achieve the required number of shots dictated by the test plan, a large area of concrete pavement was needed. Construction of a test section with different types of subgrades was prohibitively expensive; therefore, a survey of abandoned airfields was made to find an existing area of pavement that could be utilized for these tests. Only two sites met the requirements. One site, near Hays, Kansas, had a clay subgrade and offered a choice of two pavement thicknesses. The other site, at Fort Sumner, New Mexico, had a soil type that was predominantly a silty sand and a pavement thickness different from that of the Hays site pavement.

## SECTION II

### TEST SITES

#### 1. FORT SUMNER

The Fort Sumner test site, located in the southeastern part of New Mexico, is shown in figure 1. The test section, leased from the city of Fort Sumner, was a 75-ft-wide, 1,800-ft-long, 7-in.-thick concrete slab overlying a silty sand subgrade (fig. 2). The pavement consisted of 20-ft-long pads, 10 ft wide, except for the west-side pads which were 15 ft wide.

Before testing, the pads were numbered in sequential order as shown in figure 2.

Laboratory tests of soil samples obtained by subsoil explorations at this site were performed at CERF; concrete specimens obtained by coring some cylinders from the concrete slab were also tested at CERF. The results of these tests are given in appendix I.

#### 2. HAYS

The Hays test site, located 18 miles east of Hays, Kansas, is shown in figure 3. The test section (one of the three main runways) was 150 ft wide, 5,600 ft long, and ran in a northeast-southwest direction (fig. 4). Each pad was approximately 20 ft long and 12.5 ft wide. The Portland cement concrete slabs were 11 in. thick for the two center pads and 8 in. thick elsewhere, and rested on a 5-ft-thick organic clay layer. Beneath this layer was a 12-ft-thick silty clay layer overlying 3 ft of sand. Beneath the sand was a 5- to 6-ft-thick shale layer overlying a 6-ft-thick lime sandstone layer which was underlaid by a deep shale layer.

Before testing, the individual concrete pads were numbered in sequential order starting with the pad in the southwest corner (fig. 4). A typical number would be 5/6--the first digit describing the row, the second digit describing the column.

Soil and concrete specimens obtained by subsoil exploration and concrete coring at various points on the test section were tested in the laboratory at CERF; the results of these tests are given in appendix II.

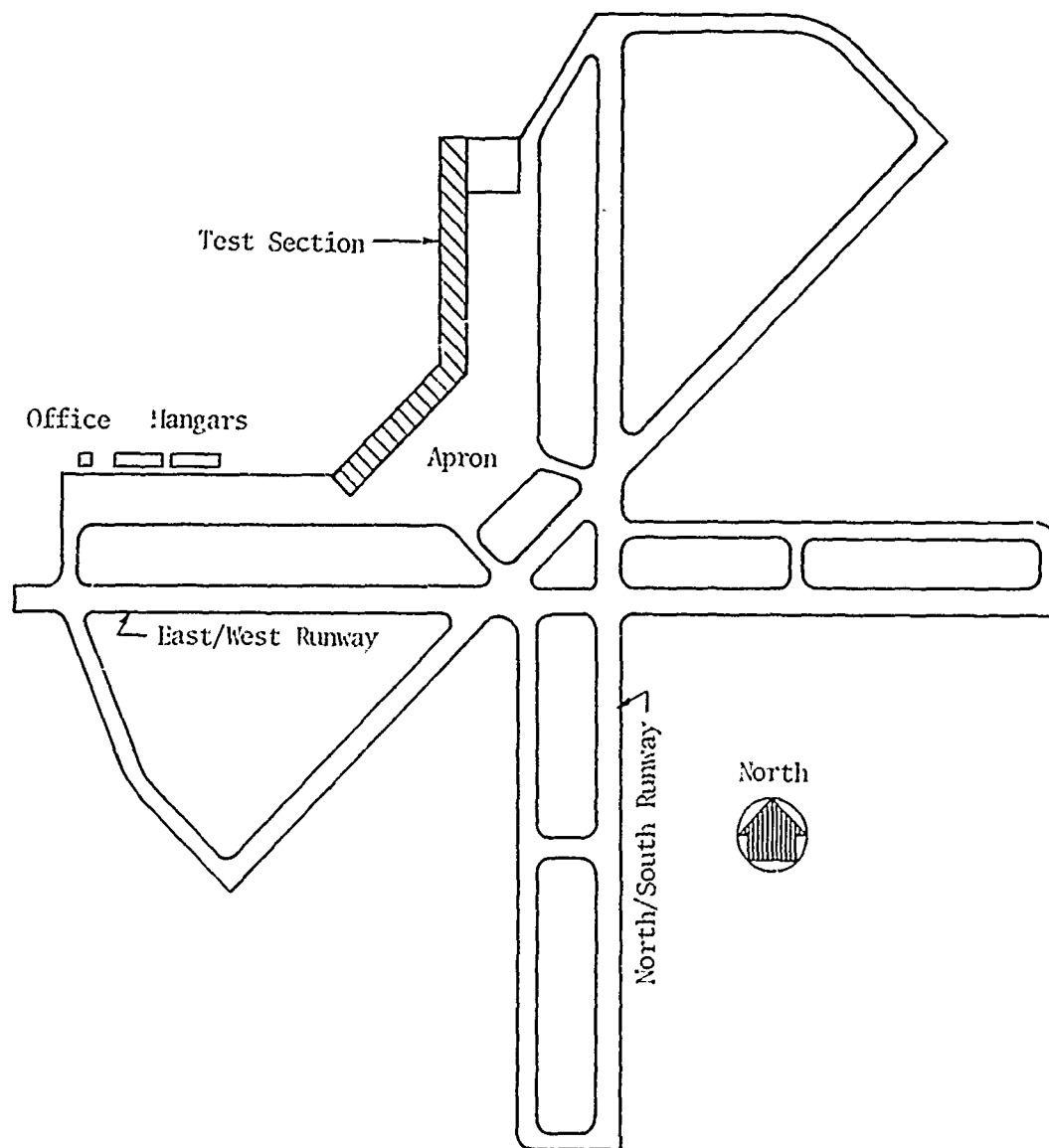


Figure 1. Fort Sumner Test Site

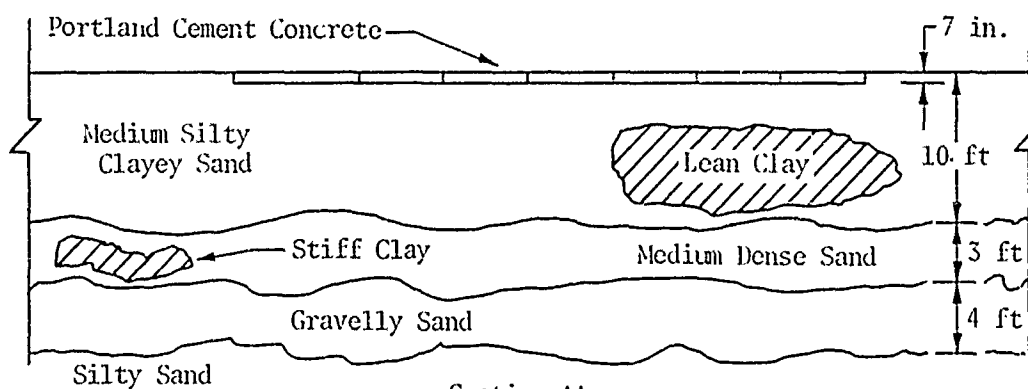
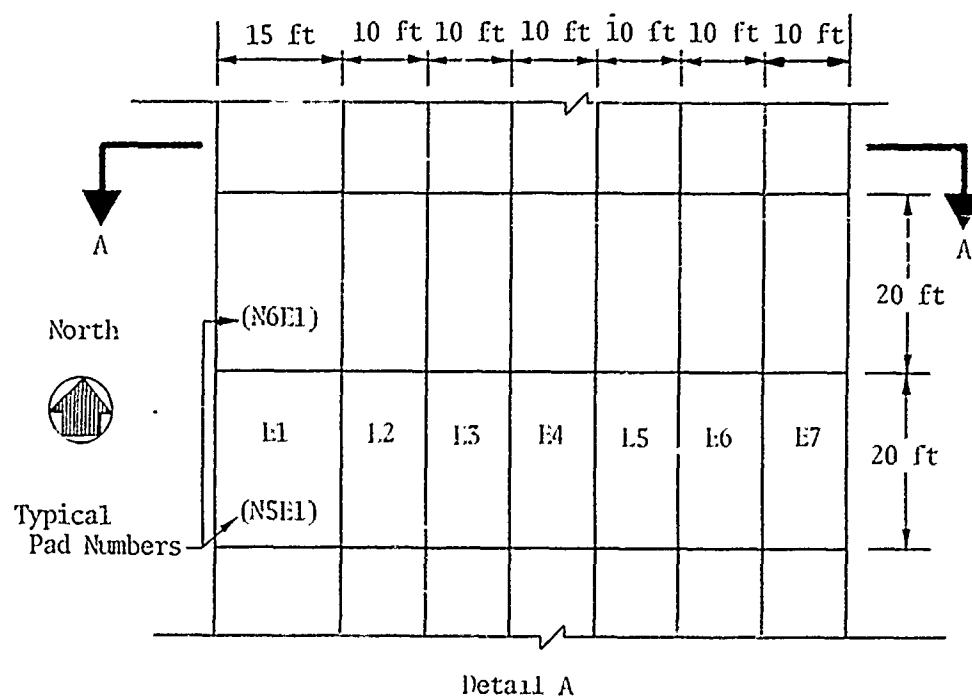
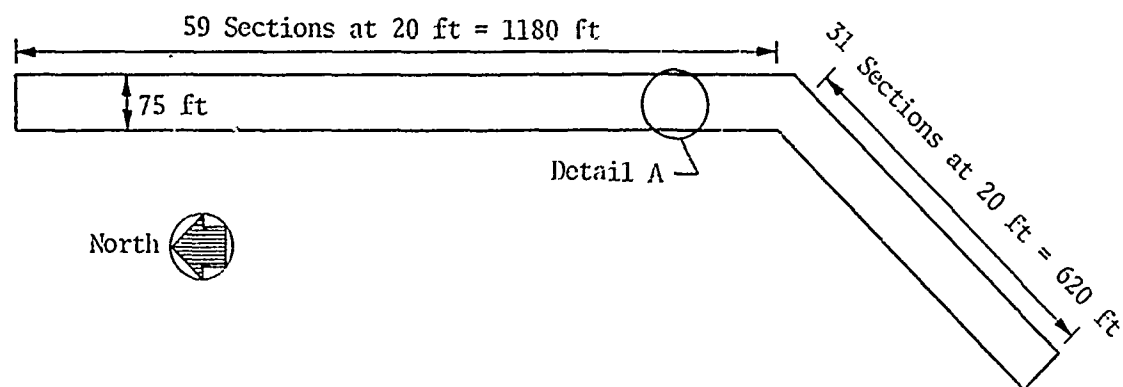


Figure 2. Fort Sumner Test Section

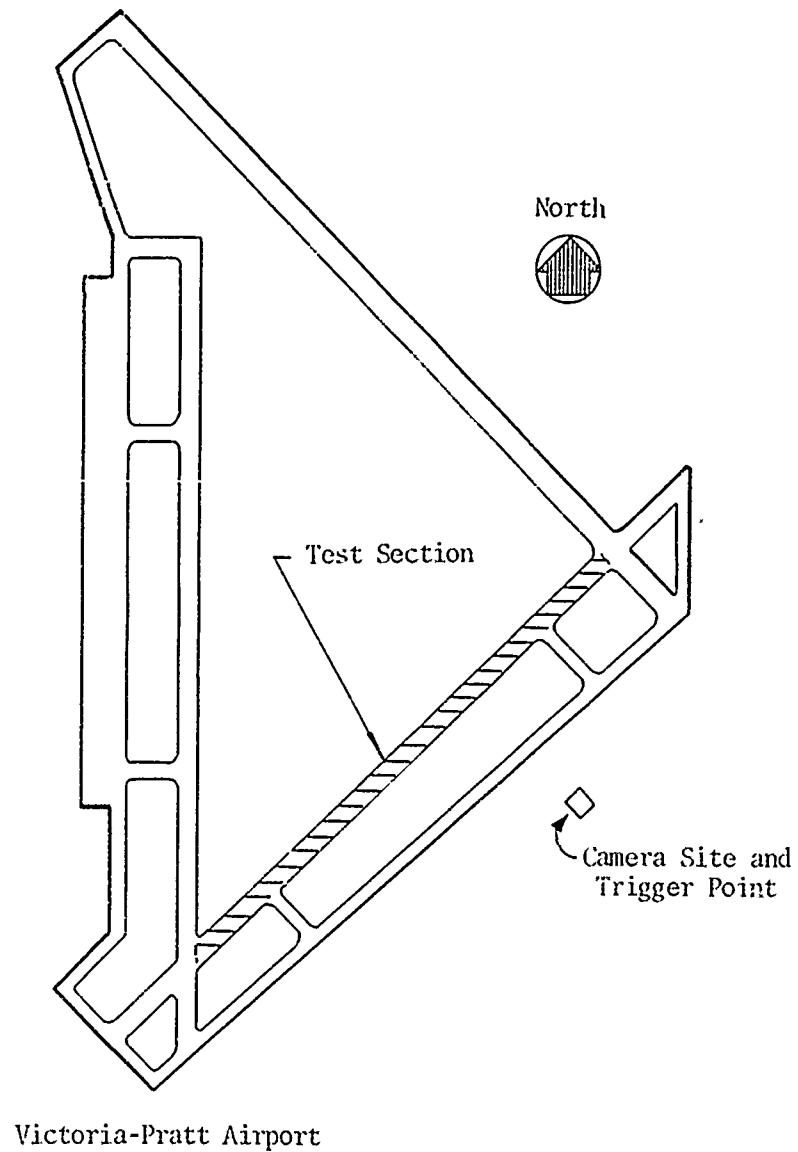


Figure 3. Hays Test Site

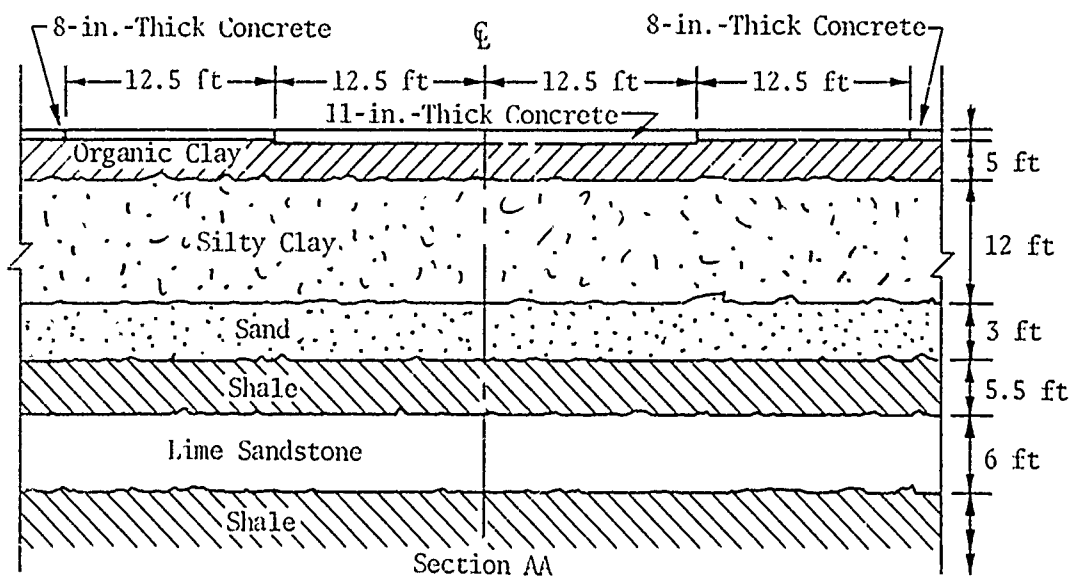
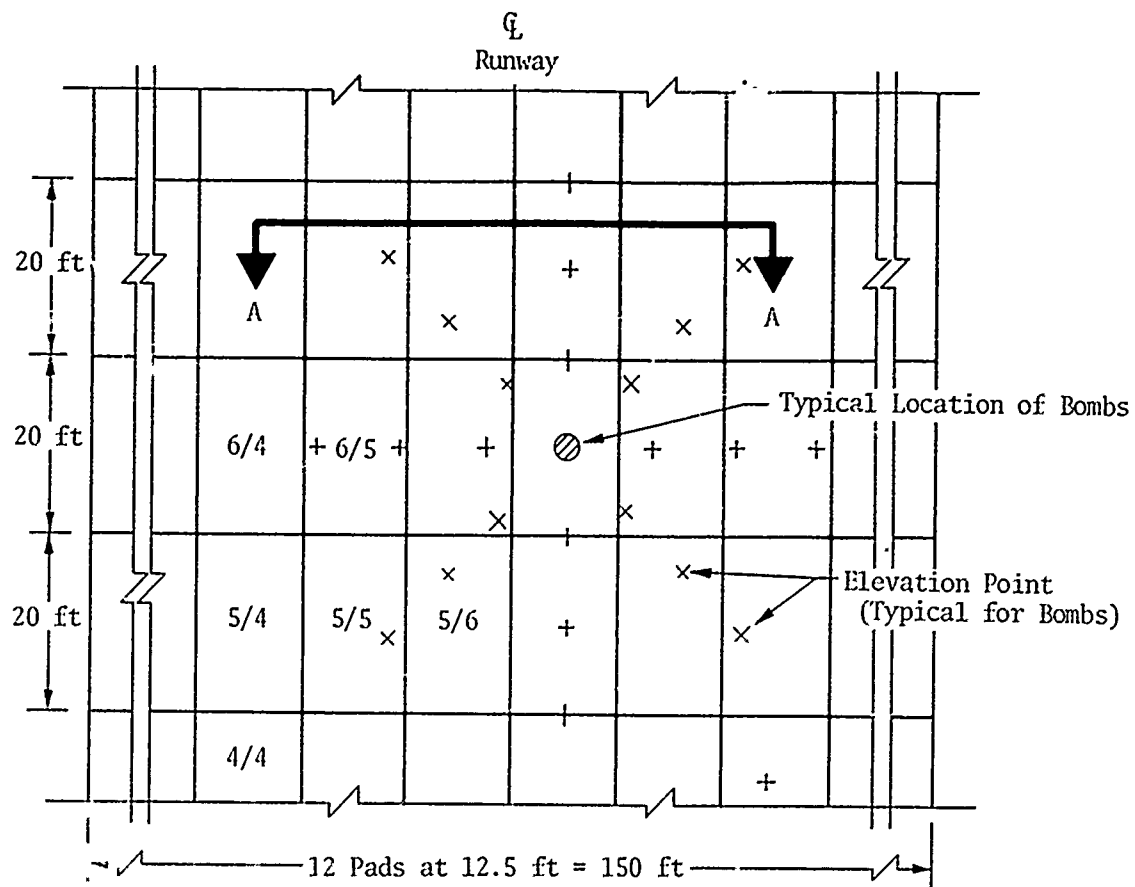


Figure 4. Hays Test Section

### SECTION III

#### EXPLOSIVES

##### 1. C-4 CHARGES

Uncased military plastic explosive (C-4) was used in various charge sizes at both Fort Sumner and Hays. This explosive, which can be manufactured easily and inexpensively, is a readily workable and stable composition with an explosive energy of approximately 1.3 times that of an equivalent weight of TNT. This explosive was formed into cylindrically shaped charges of 5, 15, and 25 lb and placed in tin cans to prevent damage during placement. Figure 5 shows the C-4 charges used.

Each charge was detonated by two booster detonation caps attached to a length of 175-grain explosive detonation cord. An electric blasting cap was taped to the detonation cord to initiate the explosion.

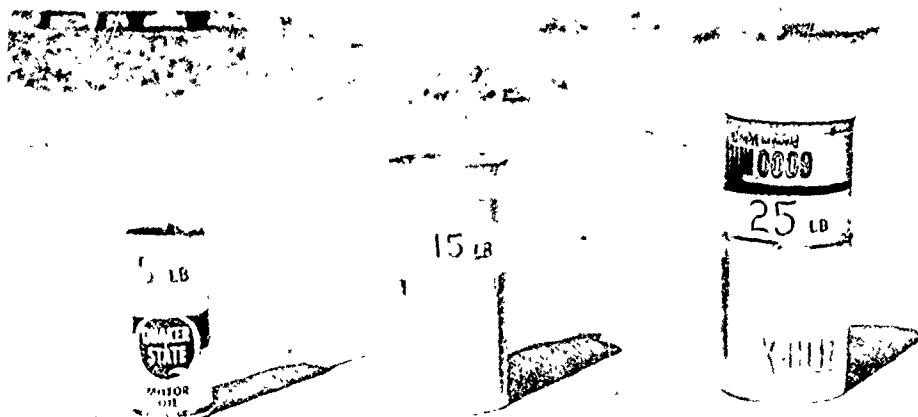
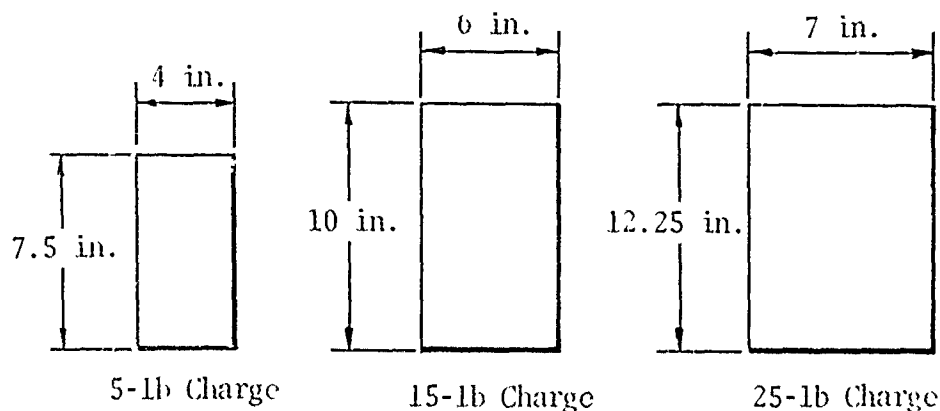


Figure 5. C-4 Charges Used at Fort Sumner and Hays

## 2. BOMBS

Three bombs were used at the Hays test site in addition to the C-4 charges. They were the MK-81 (250-lb bomb), the MK-82 (500-lb low-drag bomb), and the M-117 (750-lb general purpose bomb). Figure 6 shows these three bomb types.

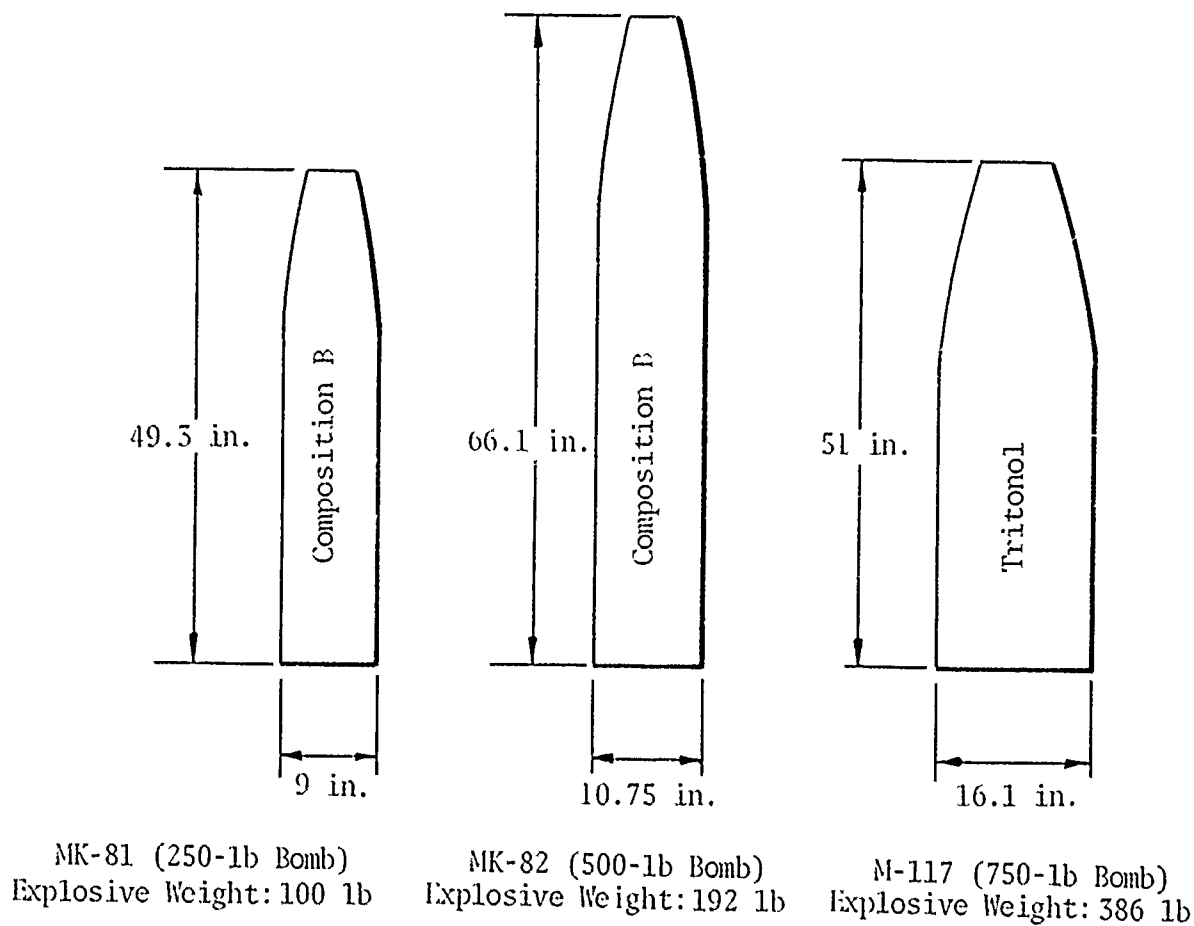


Figure 6. Bombs Used at Hays



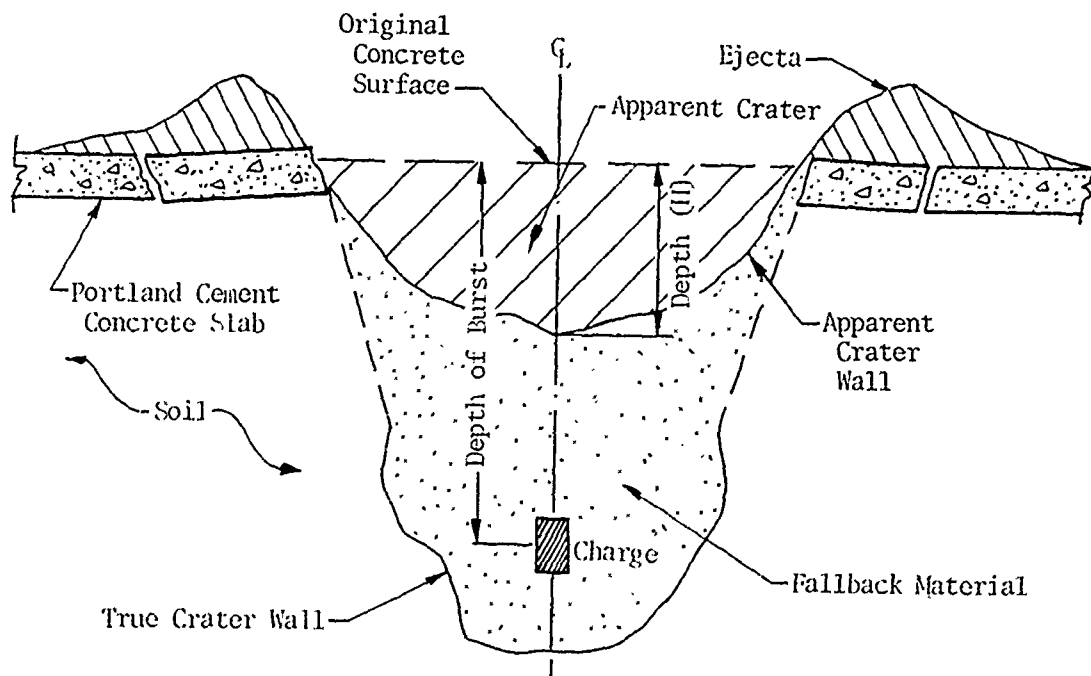
## SECTION IV

### CRATER PARAMETERS

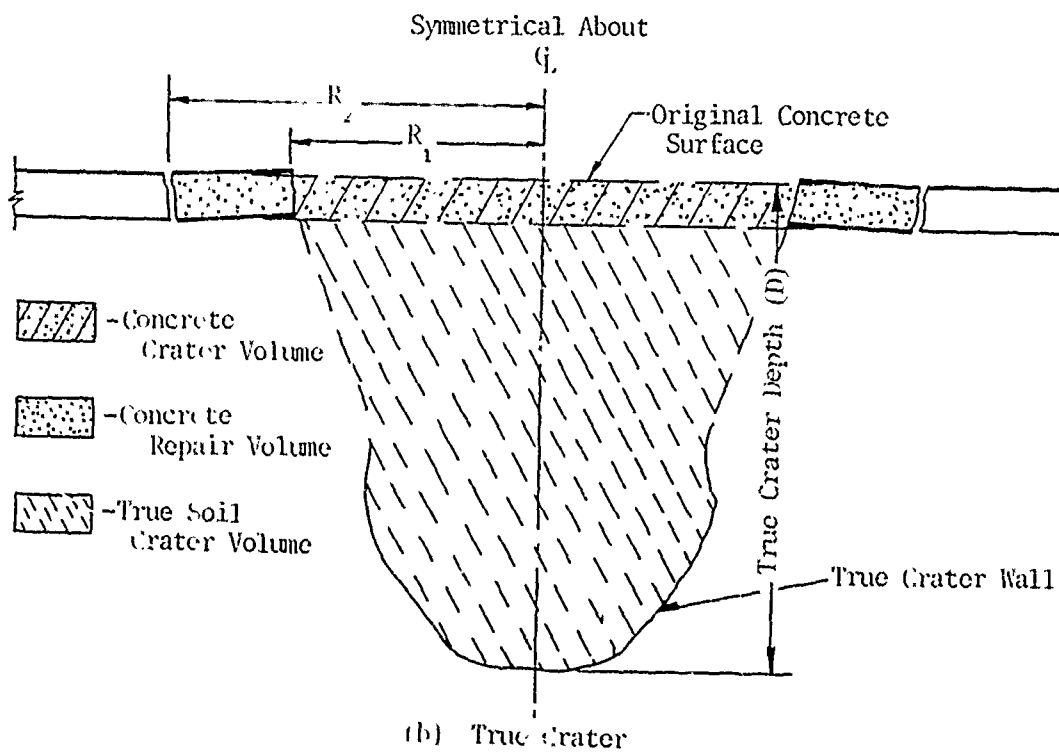
Figure 7a illustrates a typical crater caused by subsurface detonation of explosive charges in a pavement system. The crater parameters that were actually recorded in the tests conducted in this research are shown in figure 7 and are described below.

- |  |   |
|--|---|
| (1) True Crater Depth (D)                        | Depth from bottom of true crater to original concrete surface.                        |
| (2) Apparent Crater Depth (H)                    | Depth from top of fallback material at center of crater to original concrete surface. |
| (3) Depth-of-Burst (DOB)                         | Depth from original concrete surface to center of charge.                             |
| (4) Maximum Damage Depth-of-Burst (MDDOB)        | Depth-of-burst yielding a maximum damage quantity.                                    |
| (5) Ejecta                                       | All material thrown out of crater.  |
| (6) Concrete Crater Volume                       | Volume of concrete thrown out (computed from surface area of crater measured).        |
| (7) Concrete Repair Volume                       | Volume of total concrete to be repaired (calculated from crack pattern).              |
| (8) True Soil Crater Volume                      | Volume of soil crater from below the concrete slab to true crater wall.               |
| (9) Apparent Crater Volume                       | Volume of crater from original concrete surface to apparent crater wall.              |
| (10) True Soil Crater and Concrete Crater Volume | Sum of (6) and (8).   |
| (11) True Soil Crater and Concrete Repair Volume | Sum of (7) and (8).   |
| (12) Calculated Surface Crater Radius ( $R_1$ )  | An empirical number calculated from   |

$$\sqrt{\frac{\text{Concrete Crater Volume}}{\pi(\text{Concrete Thickness})}}$$



(a) Apparent Crater



(b) True Crater

Figure 7. Typical Crater

(13) Calculated Concrete Repair  
Radius ( $R_2$ )

An empirical number calculated  
from

$$\sqrt{\frac{\text{Concrete Repair Volume}}{\pi(\text{Concrete Thickness})}}$$

visualizing the utmost circum-  
ferential crack pattern in con-  
crete to be repaired.

(14)  $\pi(R_2^2 - R_1^2)$

Area of concrete to be removed  
due to heave and cracks.

(15) Maximum Radius ( $R_3$ )

Maximum radius of true crater  
at any depth.

(16) Aspect Ratio,  $D/R_1$

Ratio of true crater depth to  
surface crater radius.

Crack patterns of concrete damaged by small charges were irregular (i.e., not symmetrical) because of the effects of the joints (fig. 8). However, as the charge size increased, the effects of the joints decreased and the surface craters became symmetrical about the center of the crater. To define an average surface crater radius from the irregularly shaped crack pattern, the surface crater radius,  $R_1$ , and the concrete repair radius,  $R_2$ , were defined empirically as in items (12) and (13).

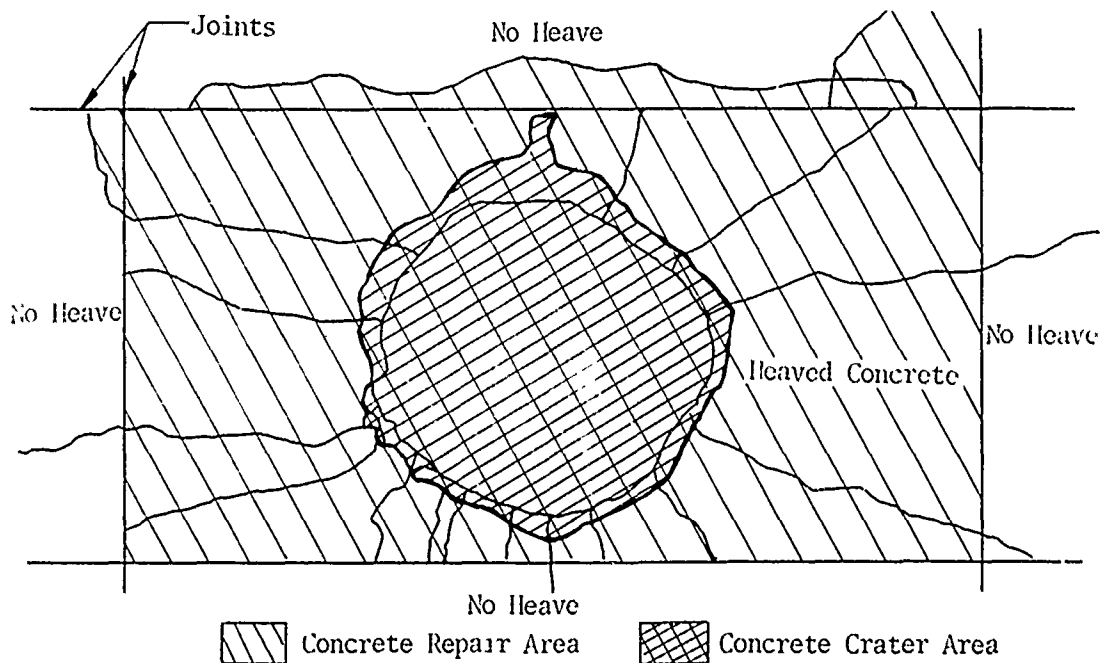


Figure 8. Typical Crack Pattern of Concrete with Joints

## SECTION V

### TEST PROCEDURES

The testing procedures were essentially the same at both test sites. The test pads were chosen on the basis of uniformity and lack of damage.

#### 1. PLACEMENT OF EXPLOSIVES

The C-4 charges and the bombs were placed at the proper depth by detonating a 2.5-lb C-4 shape charge (fig. 9) on the pavement surface to provide access to the underlying soil. An auger was then used to drill a hole the appropriate diameter of the charge or bomb being placed and to the depth desired. The charge or bomb was then lowered into the auger hole. All depths-of-burst were measured from the center of the charge to the concrete surface. Figure 10 shows the auger and a typical C-4 charge, and figure 11 shows the placement of a 500-lb bomb.

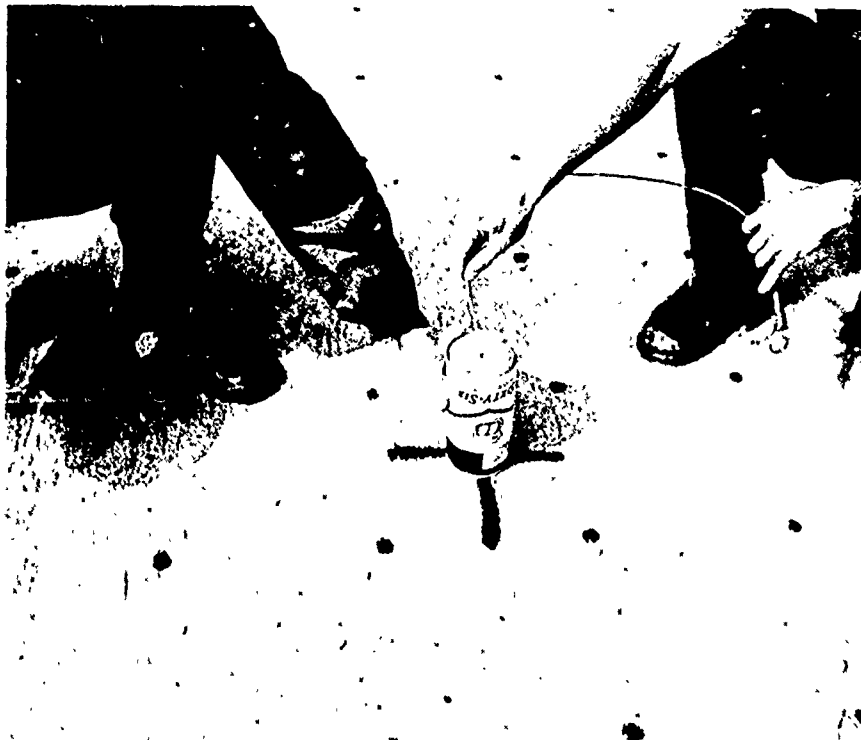


Figure 9. 2.5-lb C-4 Shape Charge

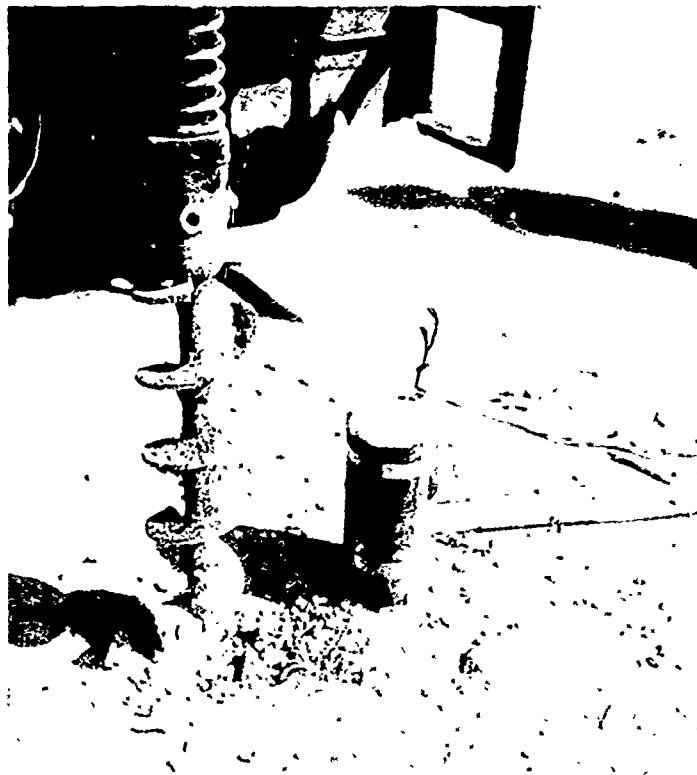


Figure 10. Auger and Typical C-4 Charge

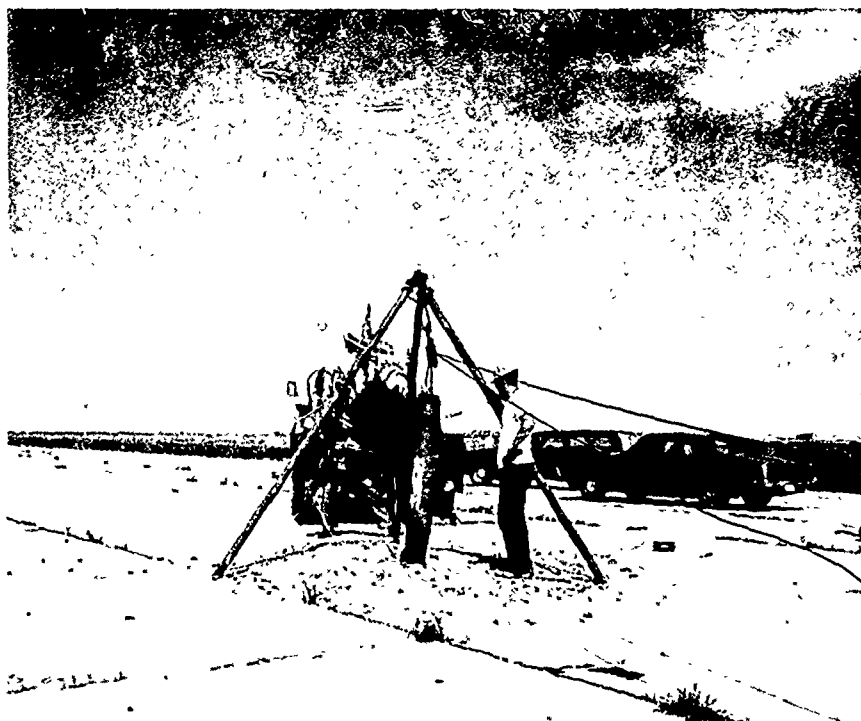


Figure 11. Placement of 500-lb Bomb

## 2. MEASUREMENTS

High-speed motion pictures at 500 and 1,500 frames per second recorded each event. Subsequent examination of the films indicates the occurrence of venting, with considerable pressure being released via the access hole through which the explosives and bombs had been placed. An initial shock-induced motion was visible on the concrete surface coincident with the initiation of venting from the access hole in all craters.

For types of craters created at shallow and intermediate depths-of-burst, pavement response to the detonation was the rapid ejection of concrete from the original surface. It was assumed that this mode of ejection resulted from a spherically shaped shock wave hitting the under-surface of the pavement. Hence, the area of concrete ejected directly above the explosive was circular in shape. As the spherically shaped shock wave expanded, the size of the ejected concentric rings was enlarged. This was accompanied by the formation of radial cracks in the surrounding slabs. The process of ejecting concentric rings of concrete continued up to a point where the shock wave was sufficiently attenuated. In most cases the last concentric ring was heaved and broken off, but not ejected, from the surrounding undamaged concrete. No visible damage to the concrete was noted beyond this point.

For types of craters created by deep depths-of-burst, which were contained within the soil medium, no concrete ejecta was visible. However, examination of the pavement after the event revealed upheaval and radial cracks.

### a. C-4 Charges

Preshot elevation measurements were taken at the center and corners of all test pads at Fort Sumner. Postshot elevation measurements were taken at those points remaining on the pads after detonation and on the crater edge in the north-south and east-west directions.

At Hays, a grid system with 1-ft squares was laid out on the pad selected for testing and on the adjoining pads. For the smaller shots, preshot elevation measurements were taken on a 2 ft-square grid to minimize the number of data points. Postshot elevation measurements were taken at 1-ft intervals on those points still remaining on the pads after detonation.

Other data collected after the initial elevation measurements were made depended on the type of crater that was formed. All craters were excavated to determine the true crater depth. True crater diameters were measured at 2-in. intervals along the vertical axis of the crater from the bottom up. Of prime importance was the accurate measurement and determination of the damaged area of concrete. The crater wall was relatively easy to find since a hard black coating existed beneath the loose fallback material. Volumes were then determined by using the elevation data. (The crater was assumed to be axisymmetric for ease of computation.)

b. Bombs

Changes in elevation were measured every 10 ft on lines emanating horizontally from the point of detonation at 45-degree intervals (fig. 4). The elevations were again recorded on points remaining after the shot to determine the amount of heave. In addition, the elevations of the fallback material were recorded in the north-south and east-west directions. Ejecta was then removed from the concrete surface and the crack pattern of the concrete was sketched. The volume of concrete thrown out was then calculated. The crater was excavated by digging a trench within the crater to the crater wall and then following the wall contour, using a hand shovel, up the sides to a height at which the wall disappeared. The crater diameters were determined in the same manner as for the C-4 charges except that vertical measurements at 6-in. intervals instead of 2-in. intervals were taken.

## SECTION VI

### FULL-SCALE FIELD TEST DATA

#### 1. CRATER TYPES

Visual observation of the craters in the field revealed that there were three types of craters caused by the C-4 charges at different depths-of-burst. These are illustrated in figure 12.

Type I craters (shallow depth-of-burst) were approximately hemispherical in shape; the pavement beyond the crater was not appreciably heaved or cracked; and the ejecta was widely scattered with small concrete pieces, some of which measured a maximum 2 ft.

In type III craters (deep depth-of-burst) no apparent crater was found; however, a cavity was found in the subgrade; the overlying concrete slab was extensively heaved with the resultant radial cracks creating huge wedge-shaped concrete pieces; and there was very little ejecta.

Type II craters (intermediate depth-of-burst) exhibited some of the characteristics of both types I and III; the apparent crater was conical in shape, while the true crater had a bulb at the bottom and the frustum of a cone at the top, and the ejecta was of intermediate size (between that of types I and III). Similar crater classifications can be seen in reference 2.

#### 2. FORT SUMNER TEST RESULTS

Appendix III lists the crater parameters of all the Fort Sumner shots and shows the cross-sectional elevations of the individual craters. Average values of the crater parameters for the three C-4 charge sizes are summarized in table I.

##### a. 5-lb Charge

Type II craters were noted for depths-of-burst of 20 in. and shallower, type III craters were noted for depths-of-burst of 40 in. and deeper, and type II and type III craters were noted at a 33-in. depth-of-burst (table I).

True soil and concrete crater volumes versus depth-of-burst are plotted in figure 13, and crater radii ( $R_1$ ,  $R_2$ , and  $R_3$ ) versus depth-of-burst are plotted in figure 14. The maximum damage depth-of-burst for all crater volumes



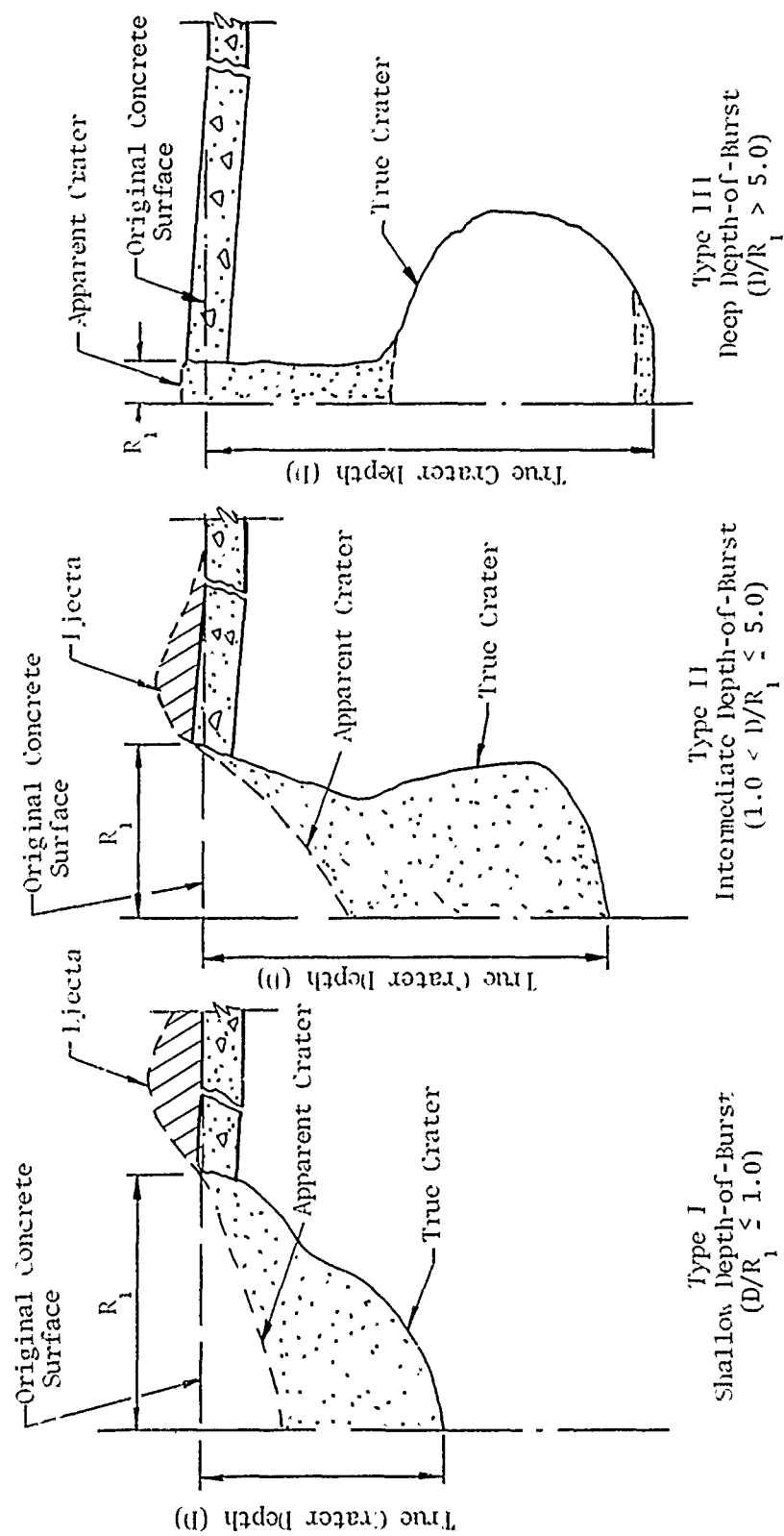


Figure 12. Crater Types

Table I  
SUMMARY OF AVERAGE DAMAGE QUANTITIES FOR C-4 CHARGES (FORT SUMNER)

Charge Size, lb	Depth of burst, in.	Volume, ft <sup>3</sup>						True Crater depth (D), ft	Radius, ft			1/R <sub>1</sub>	-(R <sub>2</sub> <sup>2</sup> - R <sub>1</sub> <sup>2</sup> )/ft <sup>2</sup>
		Concrete		True Soil Crater	Concrete and True Soil		R <sub>1</sub>		R <sub>2</sub>	R <sub>3</sub>			
		Crater	Repair		Crater	Repair							
5	17	12	11"	20	15"	52	15"	3.25	2.56	7.99	2.56	1.27	180
	20	22	11"	27	14"	49	14"	3.55	3.42	7.99	3.42	1.04	164
	33	28	11"	42	15"	70	15"	4.67	3.90	7.99	3.90	1.20	153
	33	0.55	11"	22	15"	22	15"	4.79	0.39	7.99	1.72	200	
	40	0.62	11"	19	13"	20	13"	5.00	0.58	7.99	1.58	199	
	50	0.29	11"	21	13"	21	13"	5.85	0.39	7.99	1.75	200	
60	0.46	11"	15	15"	15	15"	6.55	0.50	7.99	1.50	200		
15	10	26	150	67	15"	95	15"	3.64	3.90	8.43	3.90	0.93	175
	30	27	*	101	*	129	*	4.64	3.86	*	3.86	1.20	*
	40	50	157	84	241	154	241	4.85	3.22	9.25	5.22	0.93	185
	50	80	251	144	595	225	595	5.97	6.58	11.70	6.58	0.91	294
	70	88	188	291	473	378	473	6.50	6.85	10.13	6.85	0.96	186
	90	0.77	206	71	271	72	271	9.92	0.74	10.43	2.28	15.41	540
110	0.55	117	61	178	61	178	8.95	0.40	7.99	2.55	22.38	200	
25	34	73	212	124	356	197	356	5.58	6.27	10.71	6.27	0.89	237
	68	83	254	217	470	300	470	8.55	5.70	11.61	6.70	1.23	282
	105	64	241	**	**	**	**	**	5.86	11.52	**	**	295

\* Data lost.

\*\* Unable to excavate crater.

<sup>†</sup> Concrete thickness was 7 in. for all tests. The concrete volume of one slab, 20 ft x 10 ft, was 117 ft<sup>3</sup>.

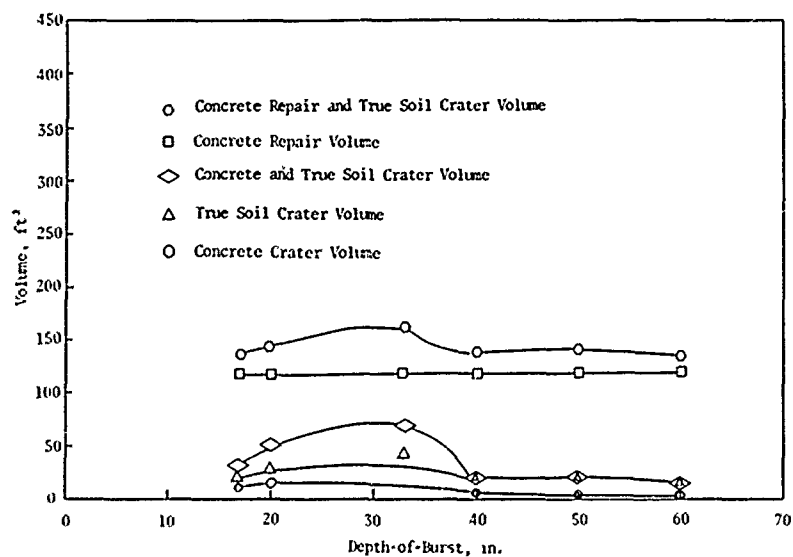


Figure 13. True Soil and Concrete Crater Volumes versus Depth-of-Burst for 5-lb Charge (Fort Sumner)

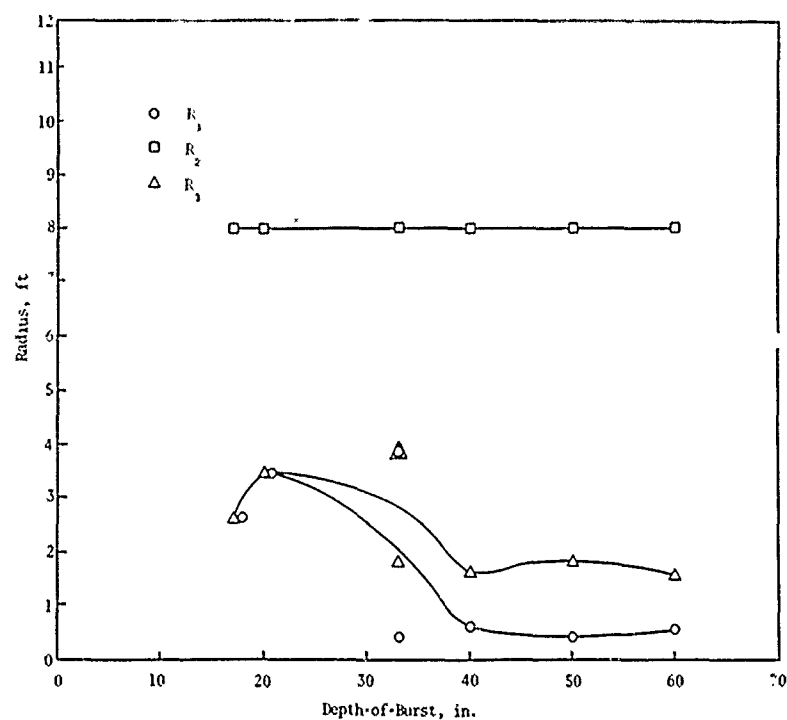


Figure 14. Crater Radii versus Depth-of-Burst for 5-lb Charge (Fort Sumner)

and crater radius  $R_3$  for the type II crater was 33 in. A crater caused by the detonation of a 5-lb charge is shown in figure 15.

Varying the depth-of-burst affected the concrete crater volumes (i.e., the concrete thrown out). However, regardless of the depth-of-burst, replacement of the entire damaged concrete pads would be necessary because of the cracking and upheaval of the concrete. Varying the depth-of-burst within the test range changed the combined concrete repair and true soil crater volume from 132 to 159 ft<sup>3</sup> (a change of only 20 percent). The average concrete repair volume was approximately 83 percent of the average combined volume and was, therefore, the more significant damage parameter.

b. 15-lb Charge

The same graphs were plotted for the 15-lb charges as for the 5-lb charges and are shown in figures 16 and 17. The maximum damage depth-of-burst was found to be 70 in. for all crater quantities except for the concrete repair volume which was 50 in. Craters caused by the detonation of a 15-lb charge are shown in figure 18.



Before Excavation

Shot 36

17-Inch Depth-of-Burst

Figure 15. Crater from Detonation of 5-lb Charge (Fort Sumner)

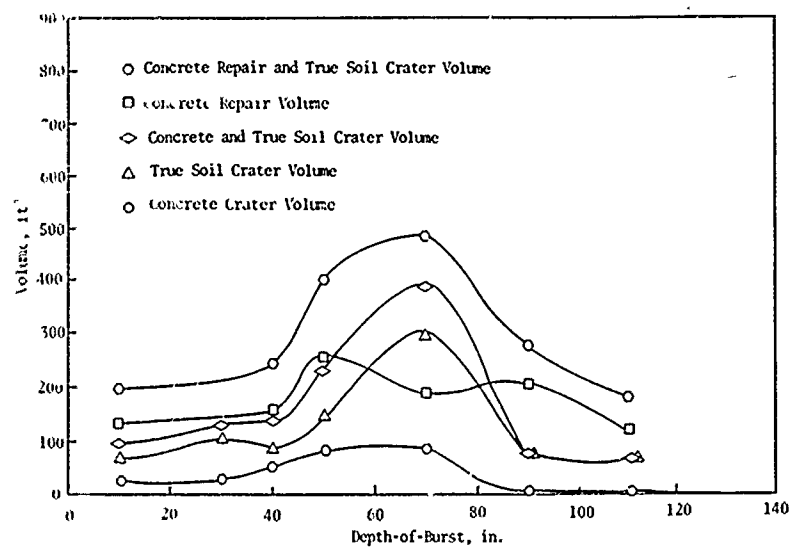


Figure 16. True Soil and Concrete Crater Volumes versus Depth-of-Burst for 15-1b Charge (Fort Sumner)

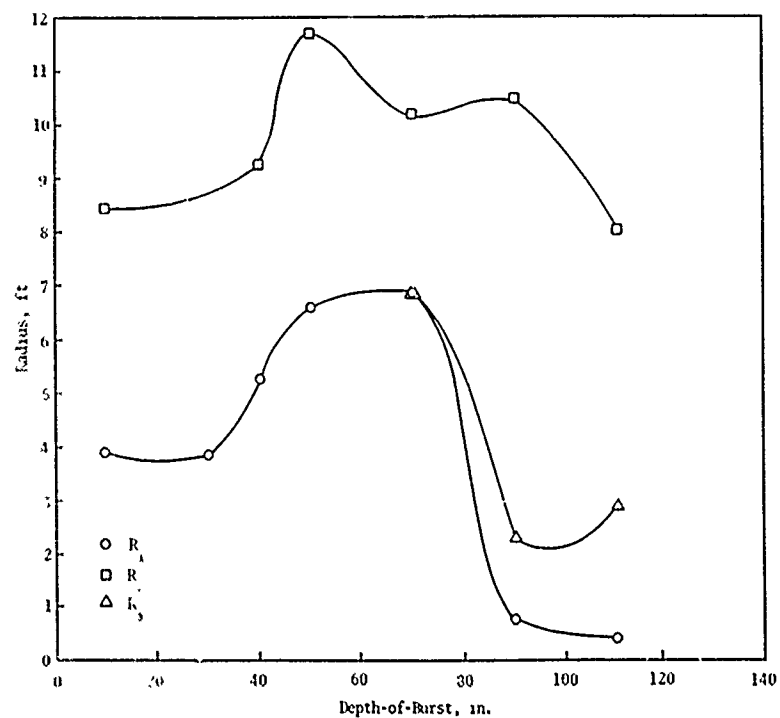


Figure 17. Crater Radii versus Depth-of-Burst for 15-1b Charge (Fort Sumner)



Before Excavation

Shot 8

10-Inch Depth-of-Burst



Before Excavation

Shot 19

40-Inch Depth-of-Burst

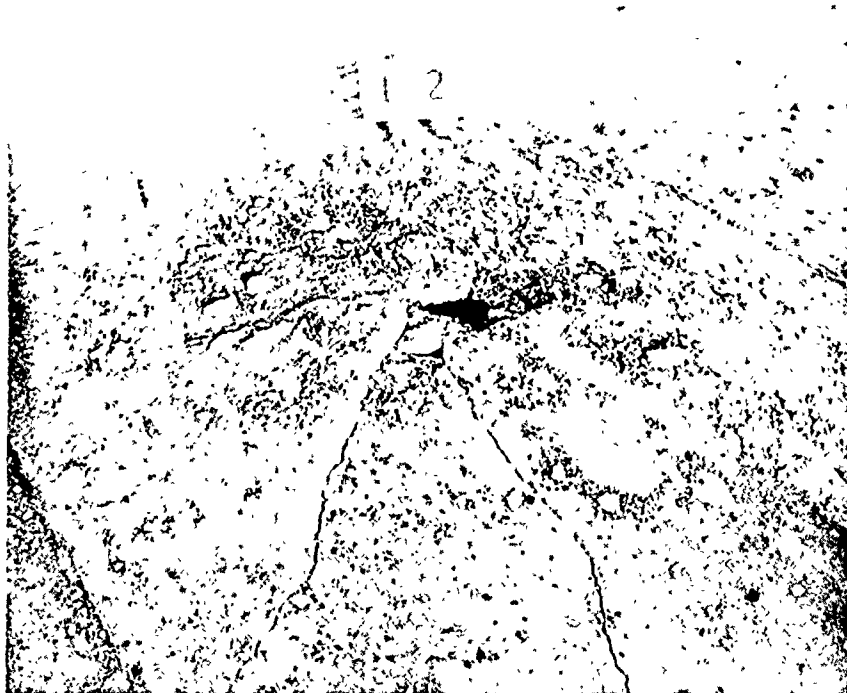
Figure 18. Craters from Detonation of 15-lb Charge (Fort Sumner)



Before Excavation

Shot 2

70-Inch Depth-of-Burst



Before Excavation

Shot 12

110-Inch Depth-of-Burst

Figure 18---Concluded

Varying the depth-of-burst from 10 to 110 in. affected both the concrete crater volume and the concrete repair volume. In this case, an average of one and one-half pads were damaged. Furthermore, by selecting the depth-of-burst so as to maximize damage to the concrete, slightly more than two pads were affected. The combined concrete repair and true soil crater volume varied from 178 to 479 ft<sup>3</sup> (an increase of about 169 percent) within the depth-of-burst range tested. The average concrete repair volume was approximately 59 percent of the average total combined volume.

c. 25-lb Charge

Figures 19 and 20 show the same graphs as previously plotted for the 5-lb and 15-lb charges. Since the subgrade at Fort Sumner consisted mostly of silty sand, the crater walls at depths-of-burst greater than 68 in. collapsed; hence, the true soil crater parameters could not be accurately measured for the 103-in. depth-of-burst. However, the maximum damage depth-of-burst for the concrete crater and the concrete repair volumes was 68 in. (fig. 19). A crater caused by the detonation of a 25-lb charge is shown in figure 21.

For the three depths-of-burst (34, 68, and 103 in.) tested, the concrete crater volumes did not vary by more than 14 percent. The average number of concrete pads damaged in this case was two. By selecting the depth-of-burst so as to maximize damage to the concrete, slightly more than two pads were affected. For the 34-in. depth-of-burst, the total repair volume was 356 ft<sup>3</sup>; for the 68-in. depth-of-burst, the total repair volume was 470 ft<sup>3</sup> (an increase of 32 percent). The average concrete repair volume was about 56 percent of the average total combined volume for these two depths-of-burst.

3. HAYS TEST RESULTS

From the recorded data, plots were made of each crater to compute the concrete crater volume, the concrete repair volume, the true soil crater volume, and the combined volumes. In addition, the true crater depth, the surface radius, and the maximum crater radius were recorded. The crater elevation data for each shot are presented in appendix IV.

a. C-4 Charges

Table II summarizes the data obtained from all shots with the 5-, 15-, and 25-lb charges beneath the 8- and 11-in.-thick concrete. These data



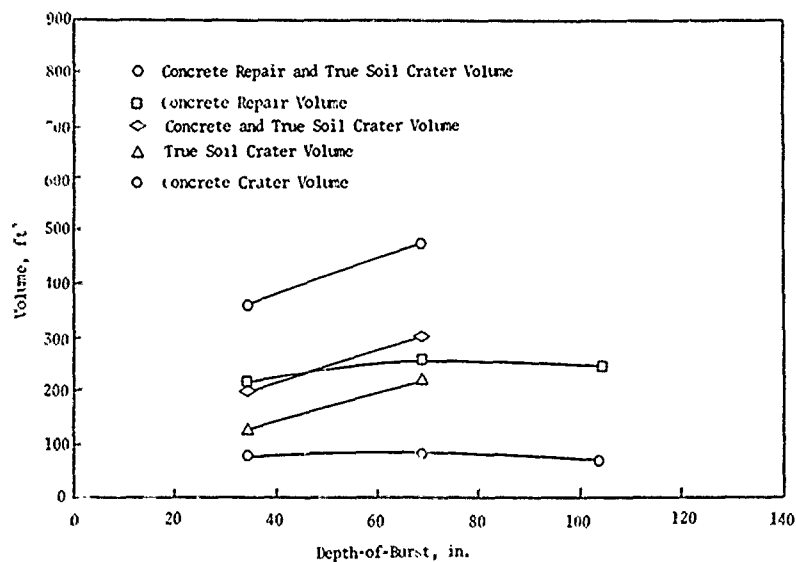


Figure 19. True Soil and Concrete Crater Volumes versus Depth-of-Burst for 25-lb Charge (Fort Sumner)

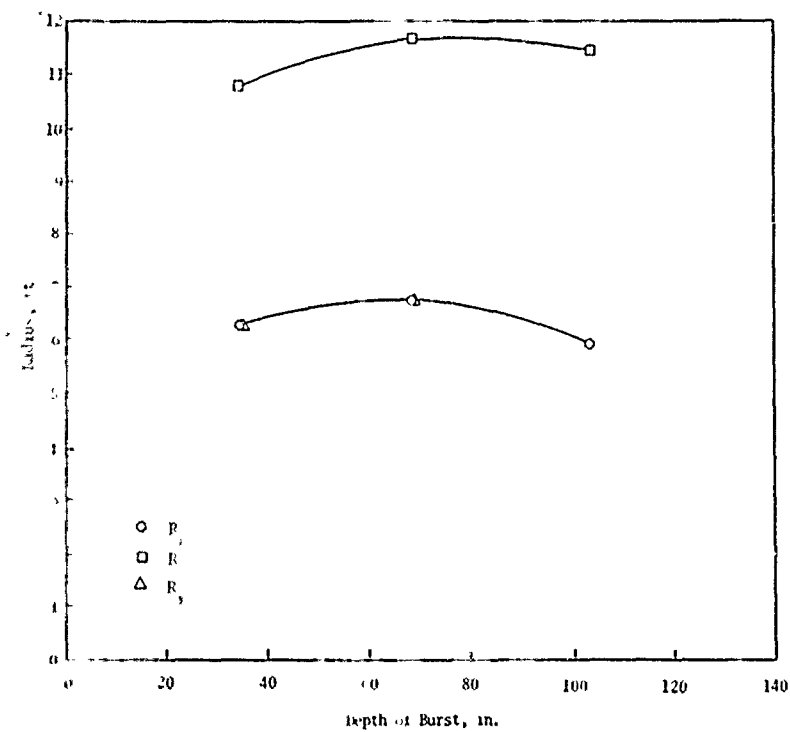


Figure 20. Crater Radii versus Depth-of-Burst for 25-lb Charge (Fort Sumner)



Before Excavation

Shot 44

68-Inch Depth-of-Burst

Figure 21. Crater from Detonation of 25-lb Charge (Fort Sumner)

were compiled using the average values of the crater damage dimensions for several shots at the same depth-of-burst.

(1) 5-lb Charge

(a) 8-Inch-Thick Concrete

Figures 22 and 23 show crater volumes and crater radii versus depth-of-burst, respectively. The maximum damage depth-of-burst was 30 in. for all parameters except the concrete repair volume for which it was 50 in. for type III craters. (See table II.) Craters caused by the detonation of a 5-lb charge on 11-in.-thick concrete are shown in figure 24.

Varying the depth-of-burst varied all damage quantities (table II). When the depth-of-burst was so selected as to maximize damage to the concrete, the damaged area increased slightly. The combined concrete repair and true soil crater volumes varied from 208 to 276 ft<sup>3</sup> (an increase of

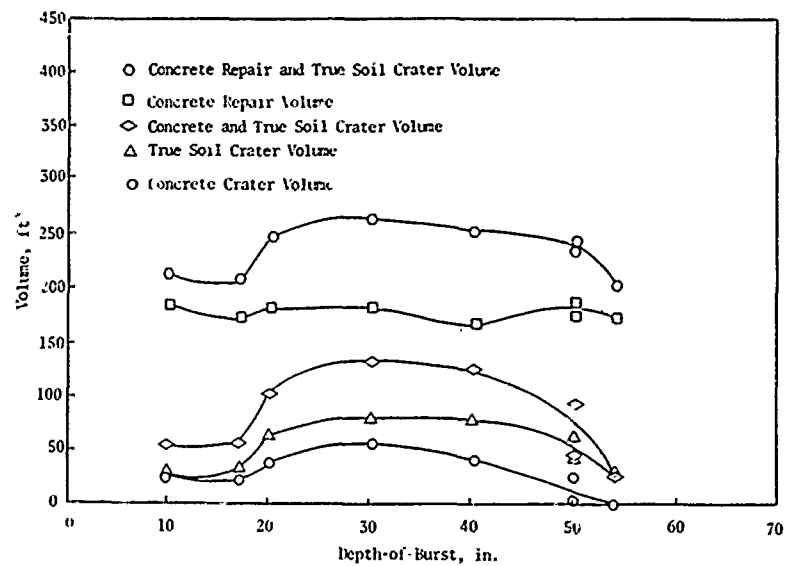


Figure 22. True Soil and Concrete Crater Volumes versus Depth-of-Burst for 5-lb Charge Under 8-Inch-Thick Concrete (11ays)

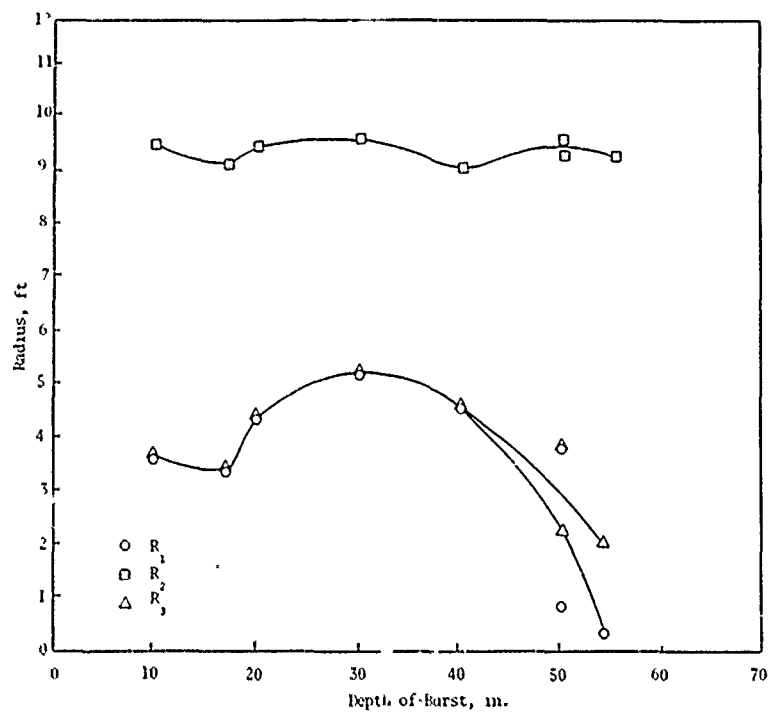


Figure 23. Crater Radii versus Depth-of-Burst for 5 lb Charge Under 8-Inch-Thick Concrete (11ays)

Table II  
SUMMARY OF AVERAGE DAMAGE QUANTITIES FOR C-4 CHARGES (HAYS)

Charge Size, lb	Concrete Thickness, in.	Depth-of- Burst, in.	Volume, ft <sup>3</sup>					True Crater Depth (D), ft	Radius, ft			D/R <sub>1</sub>	$\tau(R^2 - R^2_1)$ , ft <sup>2</sup>
			Concrete		True Soil (Crater)	Concrete and True Soil			R <sub>1</sub>	R <sub>2</sub>	R <sub>3</sub>		
			Crater	Repair*		Crater	Repair						
5	8	10	28	186	28	56	214	3.29	3.62	9.41	3.62	0.91	237
		17	24	173	35	59	208	4.17	3.38	9.08	3.38	1.23	223
		20	40	183	66	106	249	4.05	4.36	9.33	4.36	0.93	214
		30	59	184	82	136	266	4.94	5.17	9.52	5.17	0.96	201
		40	44	171	82	129	254	5.39	4.56	9.04	4.56	1.18	191
		50	51	180	68	99	248	6.34	3.85	9.27	3.85	1.65	223
		50	176	191	48	50	239	6.34	0.85	9.55	2.31	7.46	284
		54	0.24	178	50	50	208	7.33	0.34	9.21	2.00	21.56	266
15	8	20	54	229	55	109	284	3.84	4.33	8.92	4.33	0.89	191
		30	54	229	77	125	301	4.50	4.33	8.92	4.33	1.04	191
		33	57	229	53	90	282	5.00	3.58	8.92	3.58	1.40	210
		40	50	229	72	125	301	5.33	4.17	8.92	4.17	1.28	195
		10	53	171	76	129	247	4.64	5.00	9.03	5.00	0.93	178
		30	61	235	168	229	405	5.94	5.38	10.58	5.38	1.10	261
		30	68	190	149	217	314	6.76	5.61	9.50	5.61	1.20	185
		70	94	231	184	278	415	8.50	6.70	10.50	6.70	1.27	205
25	11	70	0.95	228	118	119	346	8.25	0.67	10.43	3.00	12.31	340
		90	0.95	199	106	107	305	10.52	0.67	9.71	3.00	15.70	295
		110	0.95	195	95	96	290	11.69	0.67	9.64	2.92	17.45	290
		10	46	230	83	130	313	4.58	4.01	8.94	4.01	1.14	200
		30	79	242	155	215	378	5.84	5.18	9.16	5.18	1.13	179
		50	79	243	202	281	444	7.42	5.23	9.19	5.23	1.46	184
		70	1.01	276	104	105	381	9.05	0.58	9.81	2.76	15.60	301
		90	1.29	236	131	132	368	10.05	0.67	9.06	3.13	15.00	256
25	8	110	1.29	239	116	117	356	11.71	0.67	9.12	2.71	17.48	260
		50	99	225	262	361	487	7.60	6.87	10.36	6.87	1.11	189
		71	101	264	486	587	750	9.19	6.92	11.20	6.92	1.53	244
25	8	95	0.33	353	153	154	509	10.94	0.39	12.98	3.61	28.05	529
		119	0.33	336	126	114	463	12.75	0.39	12.56	3.22	32.69	495

\*The concrete volume of one slab was 167 ft<sup>3</sup> for the 8-in.-thick slab and 229 ft<sup>3</sup> for the 11-in.-thick slab.



After Excavation

Shot 59

50-Inch Depth-of-Burst



Before Excavation

Shot 55

50-Inch Depth-of-Burst

Figure 24. Craters from Detonation of 5-lb Charge Under 8-Inch-Thick Concrete (11ays)

about 28 percent) within the depth-of-burst range. The average concrete repair volume was about 77 percent of the average combined repair volume.

(b) 11-Inch-Thick Concrete

Figures 25 and 26 show crater volumes and crater radii versus depth-of-burst, respectively. The maximum damage depth-of-burst for the concrete crater volume and crater radii  $R_1$  and  $R_3$  was 30 in. Although the concrete crater volume for all depths-of-burst was less than the concrete volume of one pad, damage to the concrete was such that one entire pad would have to be replaced (repaired). The combined concrete repair and true soil crater volume varied from 282 to 301 ft<sup>3</sup> (an increase of about 7 percent) within the depth-of-burst range. The average concrete repair volume was about the same as that for the 8-in.-thick concrete (about 82 percent of the combined volume).

(2) 15-lb Charge

(a) 8-Inch-Thick Concrete

Figures 27 and 28 show crater volumes and crater radii versus depth-of-burst, respectively. It can be noted from these figures that two peaks occurred--one at a 30-in. and the other at a 70-in. depth-of-burst. The maximum damage depth-of-burst for the concrete repair volume and true soil crater volume was 30 in.; it was 70 in. for all other crater damage. Both type II and type III craters occurred at the 70-in. depth-of-burst, but the maximum damage depth-of-burst noted was for type III craters. Craters caused by the detonation of a 15-lb charge on 8-in.-thick concrete are shown in figure 29.

Table II shows that about one and one-quarter pads were damaged with the depth-of-burst having little influence. When the depth-of-burst was so selected as to maximize damage to the concrete, about one and one-half pads were affected. The combined concrete repair and true soil crater volume varied from 247 to 415 ft<sup>3</sup> (an increase of about 68 percent) within the depth-of-burst range. The average concrete repair volume was about 63 percent of the average combined repair volume.

(b) 11-Inch-Thick Concrete

Figures 30 and 31 show crater volumes and crater radii versus depth-of-burst, respectively. The maximum damage depth-of-burst for all

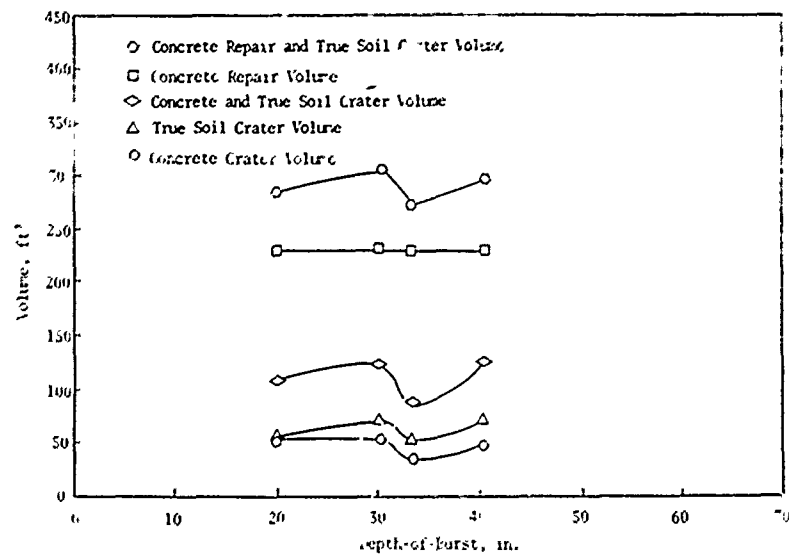


Figure 25. True Soil and Concrete Crater Volumes versus Depth-of-Burst for 5-lb Charge Under 11-Inch-Thick Concrete (11ays)

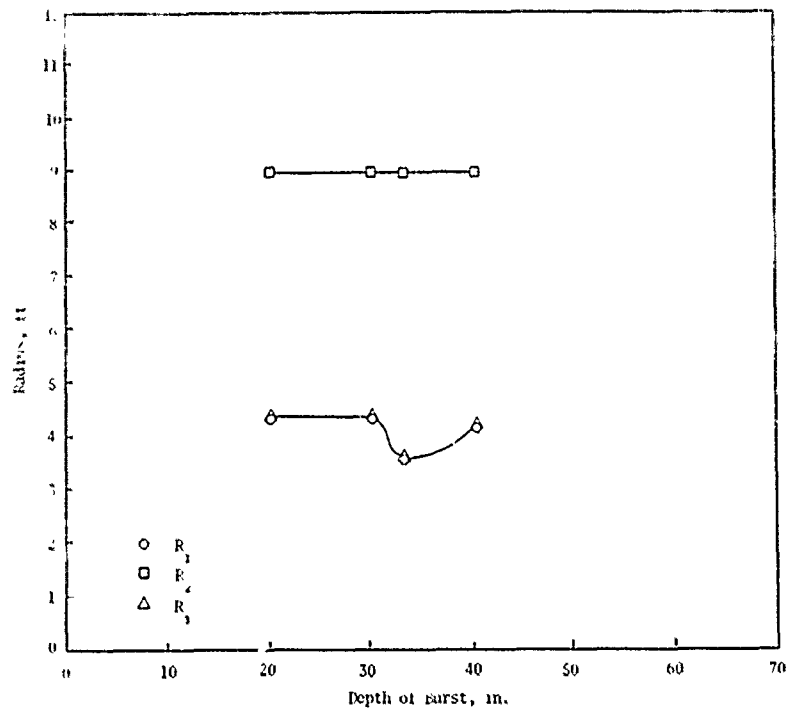


Figure 26. Crater Radii versus Depth-of-Burst for 5-lb Charge Under 11 Inch-Thick Concrete (11ays)

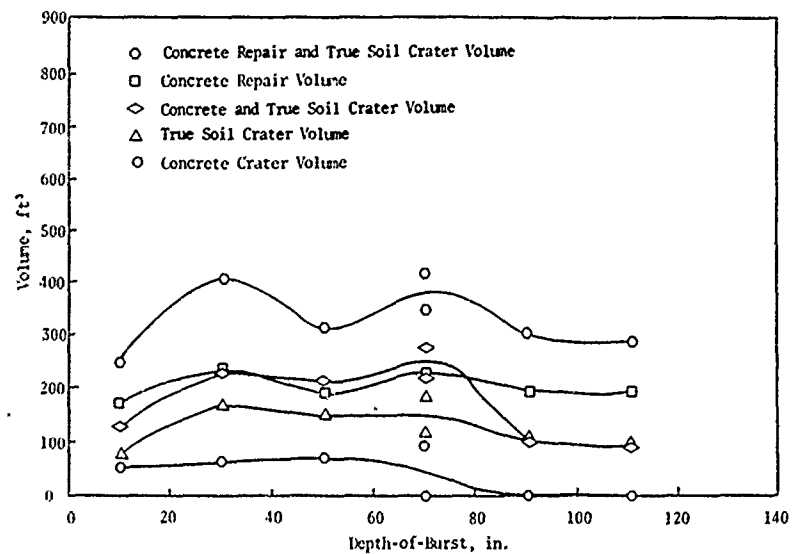


Figure 27. True Soil and Concrete Crater Volumes versus Depth-of-Burst for 15-lb Charge Under 8-Inch-Thick Concrete (Hays)

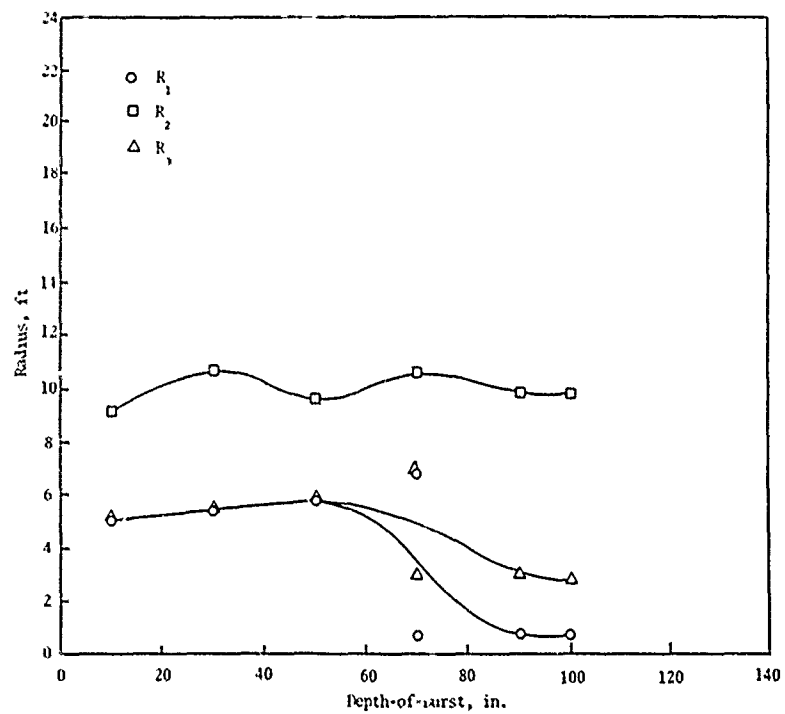
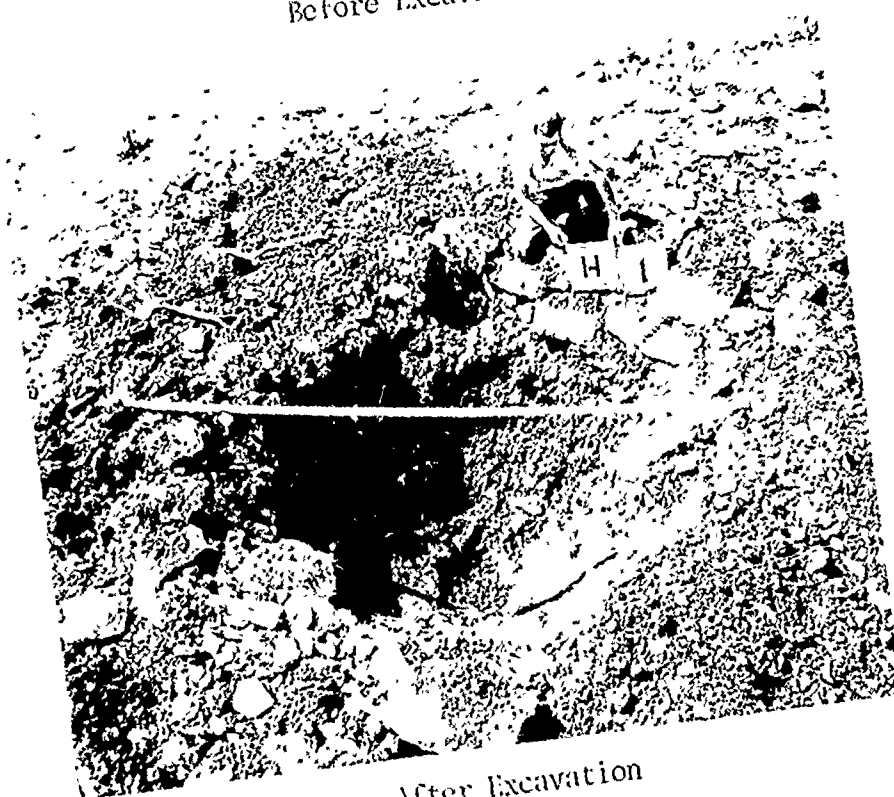


Figure 28. Crater Radii versus Depth-of-Burst for 15-lb Charge Under 8-Inch-Thick Concrete (Hays)





Before Excavation



After Excavation

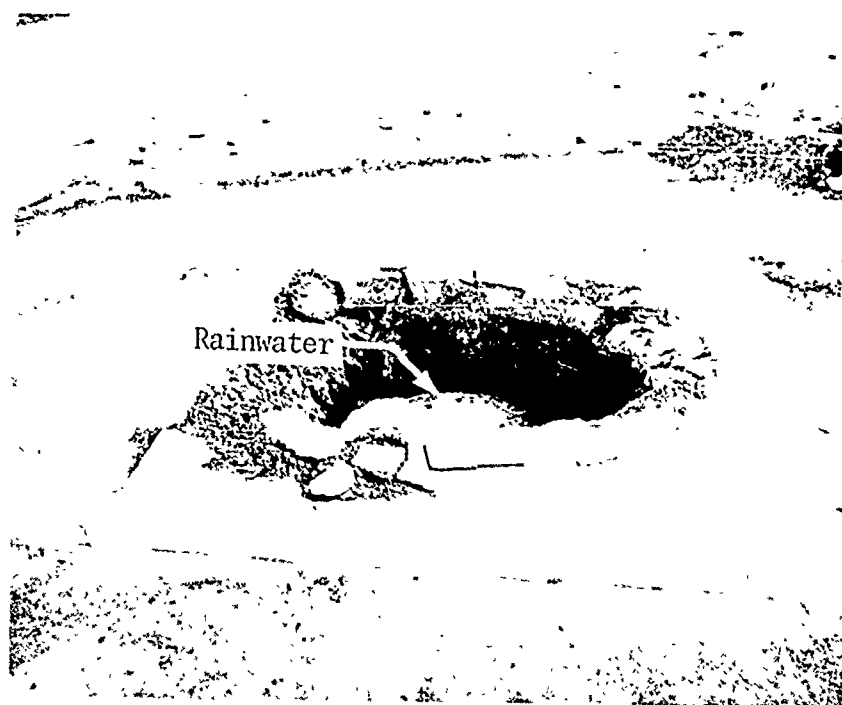
10-Inch Depth-of-Burst

Shot 1

Figure 29. Craters from Detonation of 15-lb Charge Under 8-Inch-Thick Concrete (11ays)



Before Excavation



After Excavation

Shot 5

30-Inch Depth-of-Burst

Figure 29---Continued



Before Excavation

Shot 20

50-Inch Depth-of-Burst



Before Excavation

Shot 11

70-Inch Depth-of-Burst

Figure 29---Concluded

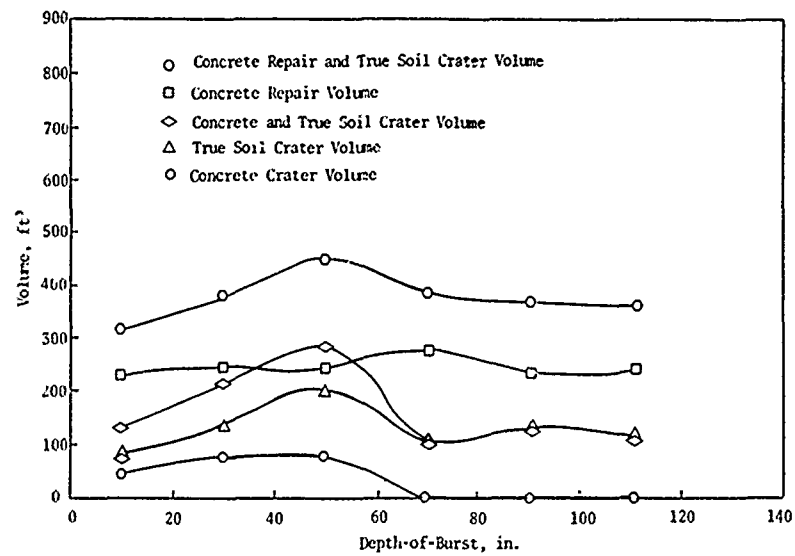


Figure 30. True Soil and Concrete Crater Volumes versus Depth-of-Burst for 15-lb Charge Under 11-Inch-Thick Concrete (Hays)

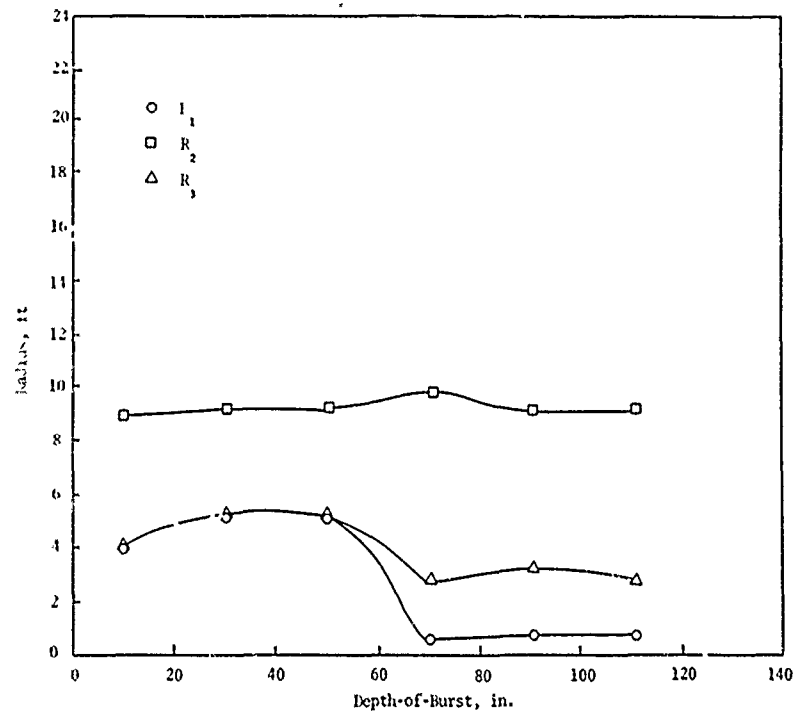


Figure 31. Crater Radii versus Depth-of-Burst for 15-lb Charge Under 11-Inch-Thick Concrete (Hays)

damage conditions except the concrete repair volume was 50 in.; it was 70 in. for the concrete repair volume. The maximum true crater radius,  $R_3$ , was observed for shallow depths-of-burst (mainly type I craters); however, a second smaller peak was noticeable at a deeper depth where types II and III craters are formed. Craters caused by the detonation of a 15-lb charge on 11-in.-thick concrete are shown in figure 32.

Table II shows that slightly more than one pad on the average was damaged with the depth-of-burst having little influence. The combined concrete repair and true soil crater volume varied from 313 to 444 ft<sup>3</sup> (an increase of about 42 percent) within the depth-of-burst range. The average concrete repair volume was about 65 percent of the average combined repair volume.

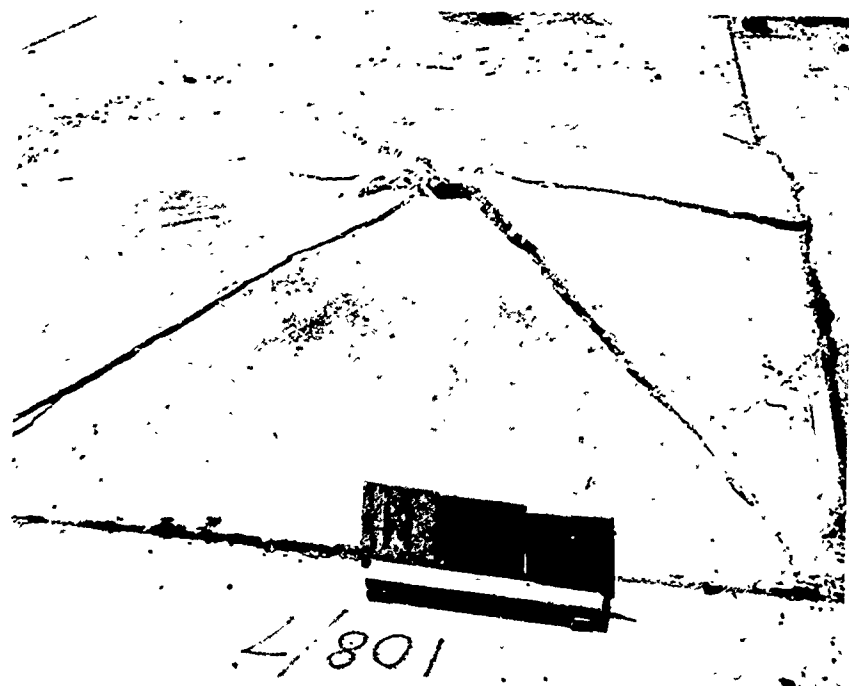
### (3) 25-lb Charge, 8-Inch-Thick Concrete

Figures 33 and 34 show crater volumes and crater radii versus depth-of-burst, respectively. The maximum damage depth-of-burst for all damage conditions except the concrete repair volume was 71 in. (type II crater). The maximum damage depth-of-burst for the concrete repair volume was 95 in. (type III crater). The maximum true crater radius,  $R_3$ , was found at the surface. (See table II.) Craters caused by the detonation of a 25-lb charge on 8-in.-thick concrete are shown in figure 35.

Table II shows that about one and three-fourths pads on the average were damaged with the depth-of-burst having little influence. When the depth-of-burst was so selected as to maximize damage to the concrete, slightly more than two pads were affected. The combined concrete repair and true soil crater volume varied from 463 to 750 ft<sup>3</sup> (an increase of about 62 percent) within the depth-of-burst range. The average concrete repair volume was about 53 percent of the average combined repair volume.

### b. Bombs

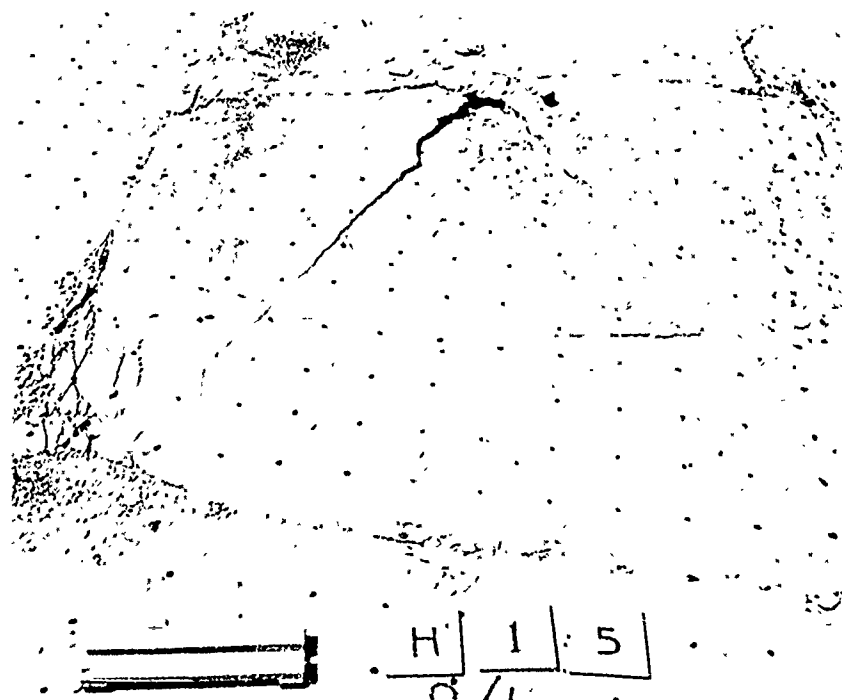
After completion of the tests using smaller charges, tests were conducted using the MK-81 (250-lb), the MK-82 (500-lb), and the M-117 (750-lb) bombs. Data taken were similar to those taken in the C-4 charge shots. In addition, the apparent crater depth was measured and the ejecta and the apparent crater volume were recorded. All bomb shots were conducted at the midsection of the pavement where the average concrete thickness was approximately 11 in. Table III summarizes the results of the eighteen bomb shots.



Before Excavation

Shot 3A

70-Inch Depth-of-Burst



Before Excavation

Shot 15

90-Inch Depth-of-Burst

Figure 32. Craters from Detonation of 15-1b Charge  
Under 11-Inch-Thick Concrete (11ays)

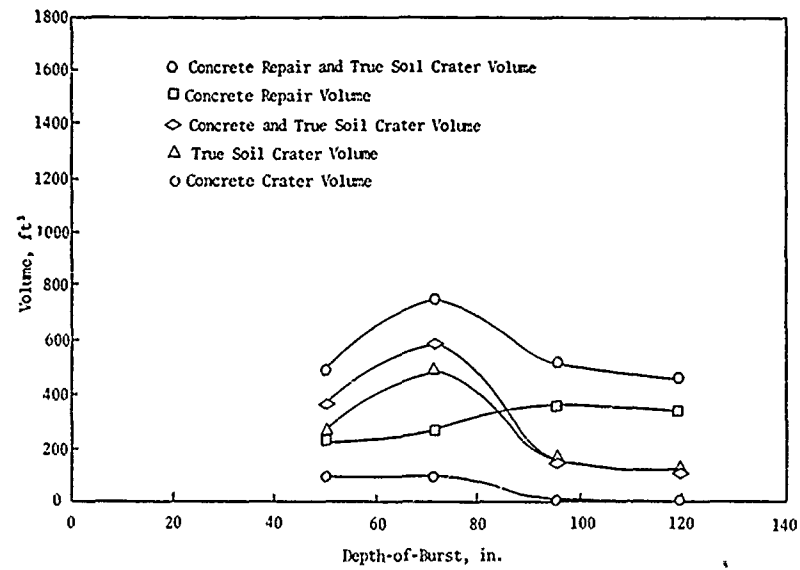


Figure 33. True Soil and Concrete Crater Volumes versus Depth-of-Burst for 25-lb Charge Under 8-Inch-Thick Concrete (11ays)

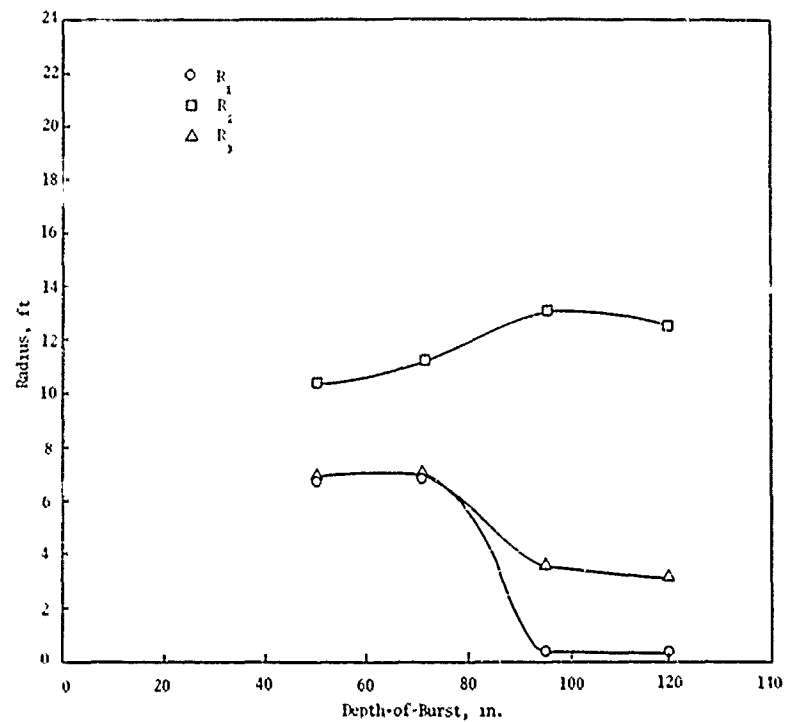


Figure 34. Crater Radii versus Depth-of-Burst for 25-lb Charge Under 8-Inch-Thick Concrete (11ays)



Before Excavation

Shot 62

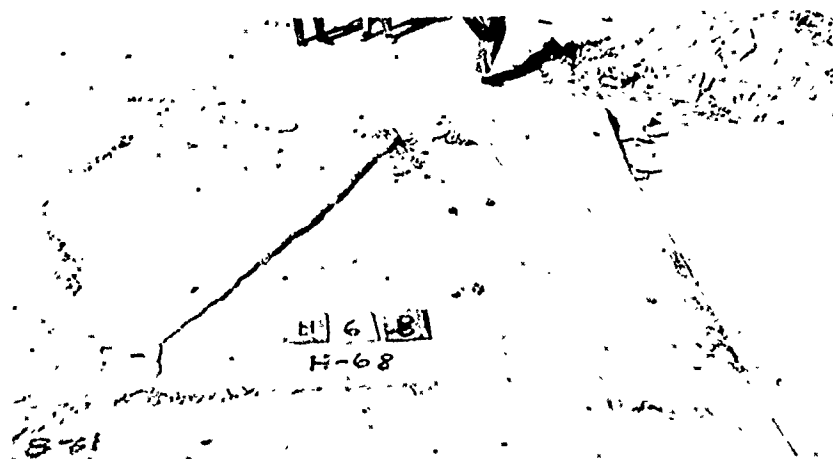
71-Inch Depth-of-Burst



Before Excavation

Shot 64

95-Inch Depth-of-Burst



Before Excavation

Shot 68

119-Inch Depth-of-Burst

Figure 35. Craters from Detonation of 25-lb Charge Under 8-Inch-Thick Concrete (Hays)



Table III

## SUMMARY OF AVERAGE DAMAGE QUANTITIES FOR BCMBs (HAYS)

Bomb Size, lb	Shot	Depth-of-Burst, ft	True Crater										Apparent Crater				
			Volume, ft <sup>3</sup>					Crater Depth (D), ft	Crater Radius, ft			$\pi(R_1^2 + R_2^2) \cdot D$ , ft <sup>2</sup>	Ljct.	Volume, ft <sup>3</sup>		Crater Depth (D), ft	
			Concrete		Soil Crater	Crater	Concrete and Soil		Repair	R <sub>1</sub>	R <sub>2</sub>			R <sub>3</sub>	Crater		Approximate Crater†
			Crater	Repair**													
250 (6K-81)	71	8	541	1180	2,45*	2,998	3,63*	13.10	13.70	20.24	637	221	693	830	5.65		
	70	10	621	1176	2,215	2,836	3,391	13.40	14.68	20.20	605	217	713	719	3.90		
	75	10	486	1490	3,064	3,350	4,554	15.00	12.99	22.71	1094	593	779	734	3.45		
	70 and 75*	10	554	1353	2,640	3,195	3,973	14.20	13.83	21.4*	849	420	746	757	4.68		
	72	13	470	1095	2,395	2,875	3,488	17.40	12.7*	19.50	782	274	42	17	3.20		
500 (N3-82)	73	15	583	2208	4,000	4,583	6,208	19.30	14.25	27.68	1770	216	4*	++	-0.40		
	74	17	439	2095	**	**	**	**	12.34	21.9*	1806	639	++	++	-0.50		
	85	9	800	2100	2,950	3,750	5,050	13.10	16.66	27.00	1418	652	1864	1220	6.20		
	80	12	1140	2242	5,771	6,911	8,010	17.00	19.89	27.90	1202	524	1212	1190	7.55		
	84*	12	852	1624	**	**	**	**	17.00	25.74	862	781	1383	1342	6.10		
750 (N-117)	82	12	984	1953	**	**	**	**	18.44	25.82	1032	653	1308	1266	6.83		
	81	15	831	1788	3,50*	6,72*	7,685	19.00	16.98	24.71	1043	1008	681	735	5.55		
	88	18	486	2177	**	**	**	**	13.00	27.49	1342	407	33	40	0.40		
	83	21	151	2021	**	**	**	**	7.24	26.49	2037	554	108	87	2.50		
	91	12	2137	2534	**	**	**	**	27.24	29.66	423	1275	4370	4000	10.60		
950 (N-117)	90	15	1325	2900	12,834	14,152	15,734	22.00	21.44	31.75	1718	1516	3924	4020	9.40		
	92	15	1243	3862	**	**	**	**	20.7*	36.61	2854	1495	3225	3114	8.60		
	92 and 92*	15	1284	3381	**	**	**	**	21.10	31.1*	2286	1506	3575	3567	9.00		
	93	18	1415	4045	12,527	13,942	16,572	21.00	22.16	37.4*	3367	1357	2540	1900	7.20		
	94	18	1537	3334	9,103	11,139	12,956	23.62	25.10	31.02	1959	808	1260	1320	6.00		
	95 and 94*	18	1476	3690	11,665	12,541	14,754	23.81	22.63	35.75	2113	1083	1900	1610	6.60		
	95	20.5	802	2700	**	**	**	**	16.08	30.16	1983	383	35	35	0.80		

\* Average values at same depth-of-burst.

\*\* Crater not excavated.

† Core shape =  $\pi r^2 (H/3)$ ,  $r$  = apparent crater radius,  $H$  = apparent crater depth.

‡ No apparent crater (all heave).

+++ The concrete volume of one slab, 11 in. thick and 20 ft x 12.5 ft, was 229 ft<sup>3</sup>.

(1) MK-81 (250-lb Bomb)

Five of the six craters were excavated. Figures 36 and 37 show true crater volumes and crater radii versus depth-of-burst, respectively. Figure 36 shows that the maximum damage depth-of-burst for the concrete crater and the concrete repair volume occurred at a 15-ft depth-of-burst. However, the maximum damage depth-of-burst for the other damage conditions could not be determined since the crater for the shot at the 17-ft depth-of-burst was not excavated. Craters caused by the detonation of an MK-81 bomb are shown in figure 38.

Table III shows that about six and three-fourths pads on the average were damaged by varying the depth-of-burst from 8 to 17 ft. However, the maximum damage to the concrete was about nine and three-fourths pads at a depth-of-burst of 15 ft. The combined concrete repair and true soil crater volume varied from 3,391 to 6,208 ft<sup>3</sup> (an increase of about 83 percent) for the five craters excavated. The average concrete repair volume was about 36 percent of the average combined repair volume.

(2) MK-82 (500-lb Bomb)

Three of the six craters were excavated. Figures 39 and 40 show true crater volumes and crater radii versus depth-of-burst, respectively. The maximum damage depth-of-burst for the concrete crater volume was 12 ft; it was 18 ft for the concrete repair volume. (This was based on the data obtained by averaging the damage for two shots at a 12-ft depth-of-burst. However, one of these two shots produced greater damage to the concrete than the shot at the 18-ft depth-of-burst.) The apparent crater depth was largest at the 12-ft depth-of-burst. Craters caused by the detonation of an MK-82 bomb are shown in figure 41.

Table III shows that about eight and three-fourths pads on the average were damaged by varying the depth-of-burst from 9 to 21 ft. However, the maximum damage to the concrete was slightly more than nine and three-fourths pads at a depth-of-burst of 12 ft (slightly larger than that for the MK-81 bomb). The combined concrete repair and true soil crater volume varied from 5,050 to 8,010 ft<sup>3</sup> (an increase of 59 percent) for the three craters excavated. The average concrete repair volume was about 29.5 percent of the average combined repair volume for the three shots excavated.

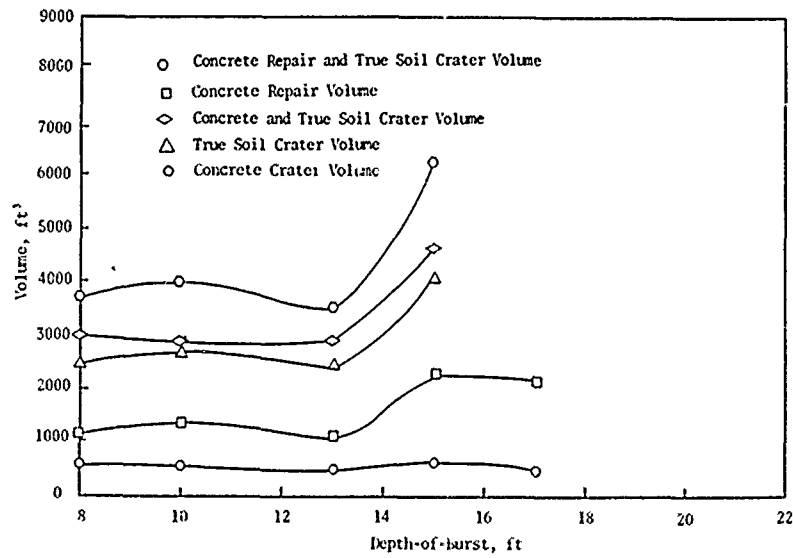


Figure 36. True Soil and Concrete Crater Volumes versus Depth-of-Burst for MK-81 Bomb (Hays)

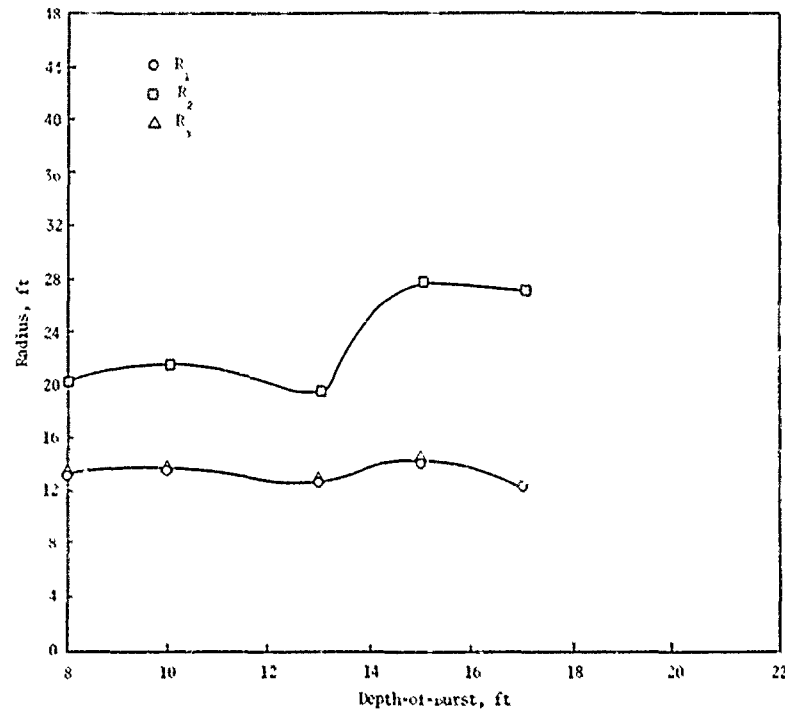


Figure 37. Crater Radii versus Depth-of-Burst for MK-81 Bomb (Hays)



After Excavation

Shot 71

8-Foot Depth-of-Burst



Before Excavation



After Excavation

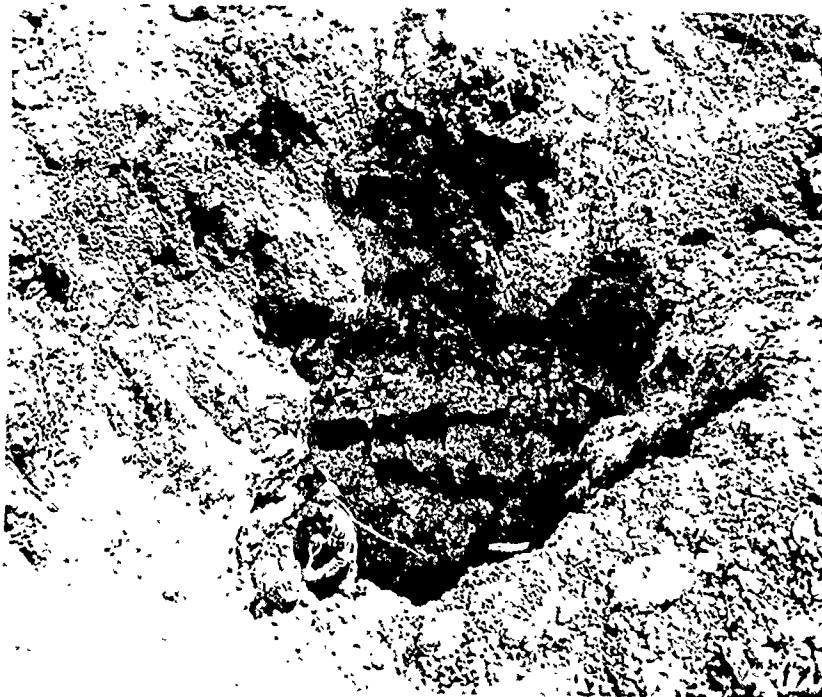
Shot 70

10-Foot Depth-of-Burst

Figure 38. Craters from Detonation of MK-81 Bomb (Ilays)



Before Excavation



After Excavation

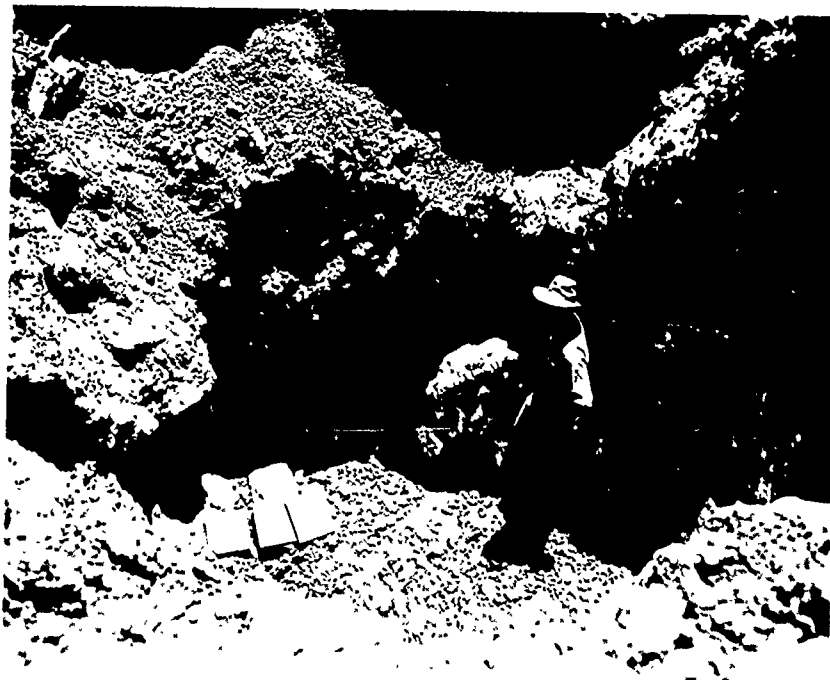
Shot 72

13-Foot Depth-of-Burst

Figure 38---Continued



Before Excavation



After Excavation

Shot 73

15-Foot Depth-of-Burst

Figure 38---Concluded

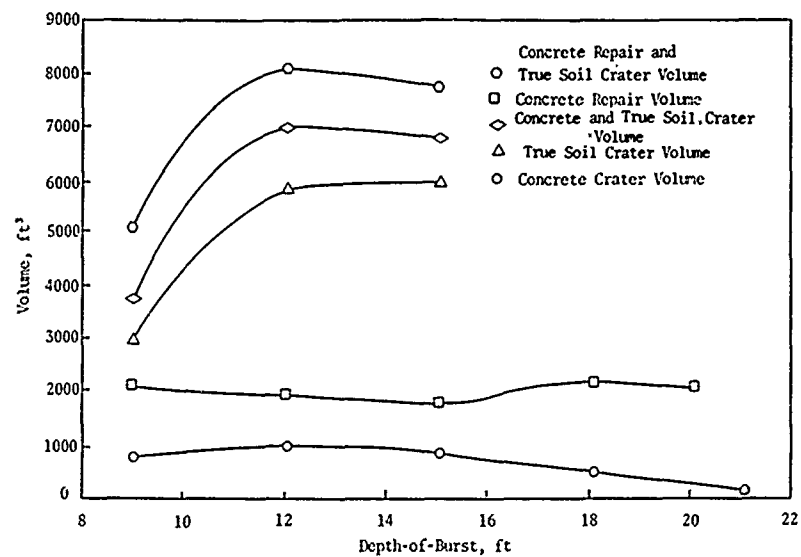


Figure 39. True Soil and Concrete Crater Volumes versus Depth-of-Burst for MK-82 Bomb (Hays)

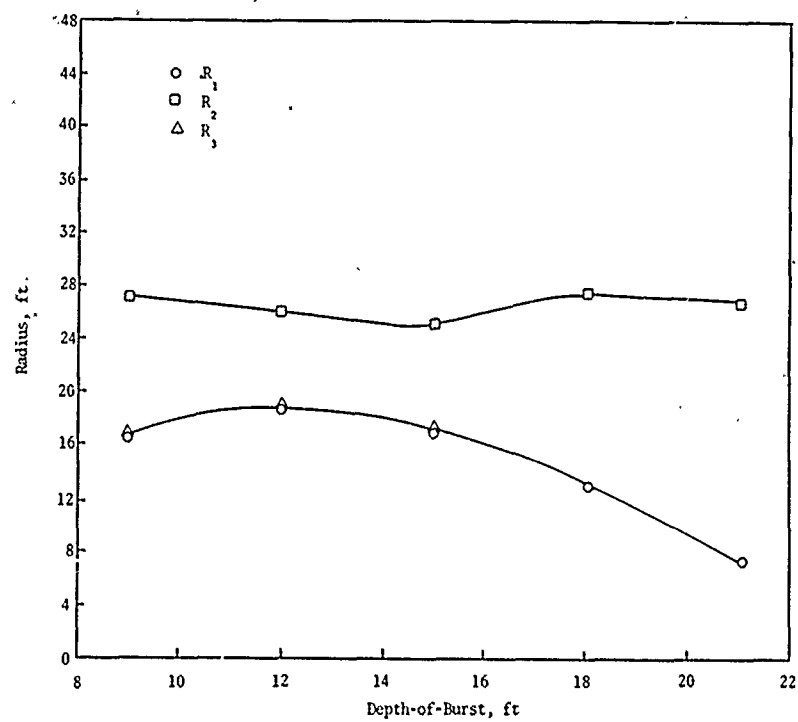


Figure 40. Crater Radii versus Depth-of-Burst for MK-82 Bomb (Hays)



Before Excavation

Shot 85

9-Foot Depth-of-Burst



Before Excavation

Shot 80

12-Foot Depth-of-Burst

Figure 41. Craters from Detonation of MK-82 Bomb (Ilays)





Before Excavation



After Excavation

Shot 82

15-Foot Depth-of-Burst

Figure 41---Continued



Crater Not Excavated

Shot 81

18-Foot Depth-of-Burst



Crater Not Excavated

Shot 83

21-Foot Depth-of-Burst

Figure 41---Concluded

(3) M-117 (750-lb Bomb)

Three of the six craters were excavated. Figures 42 and 43 show true crater volumes and crater radii versus depth-of-burst, respectively. The maximum damage depth-of-burst for the concrete repair volume was 18 ft. Craters caused by the detonation of an M-117 bomb are shown in figure 44.

Table III shows that about fourteen pads on the average were damaged by varying the depth-of-burst from 12 to 20.5 ft. However, the maximum damage to the concrete was nearly eighteen pads at a depth-of-burst of 18 ft. The combined concrete repair and true soil crater volume for the three shots varied from 12,936 to 16,572 ft<sup>3</sup> (an increase of 28 percent). The average concrete repair volume was about 22.7 percent of the average combined repair volume for the three shots excavated.

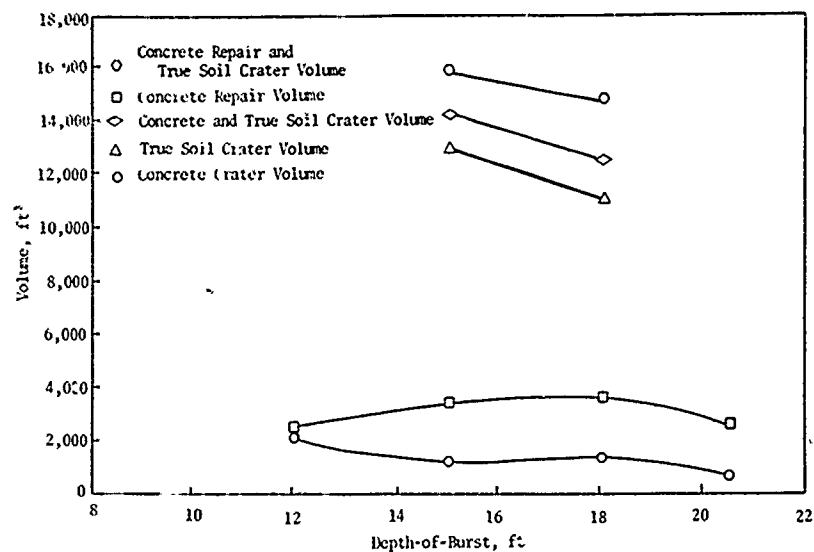


Figure 42. True Soil and Concrete Crater Volumes versus Depth-of-Burst for M-117 Bomb (Hays)

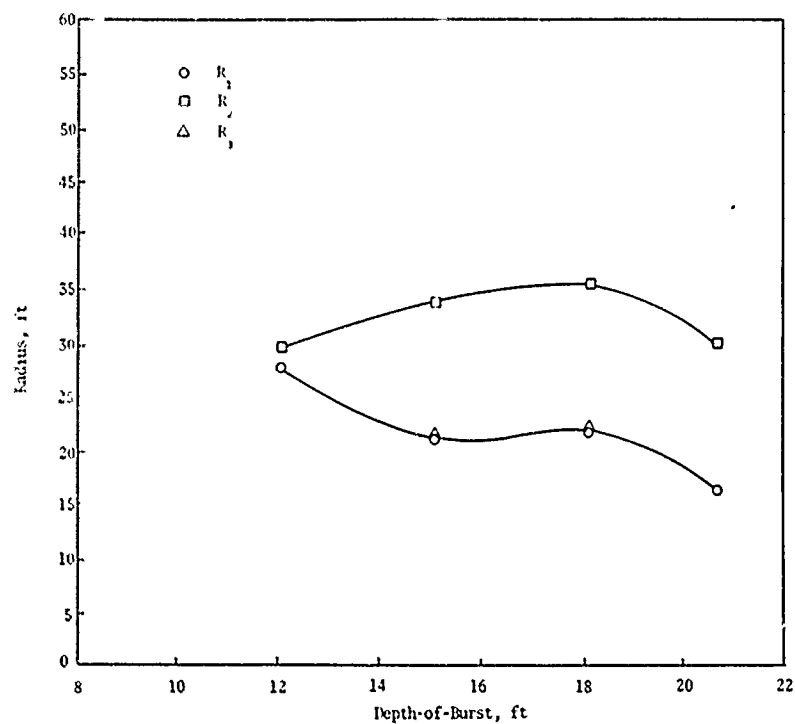


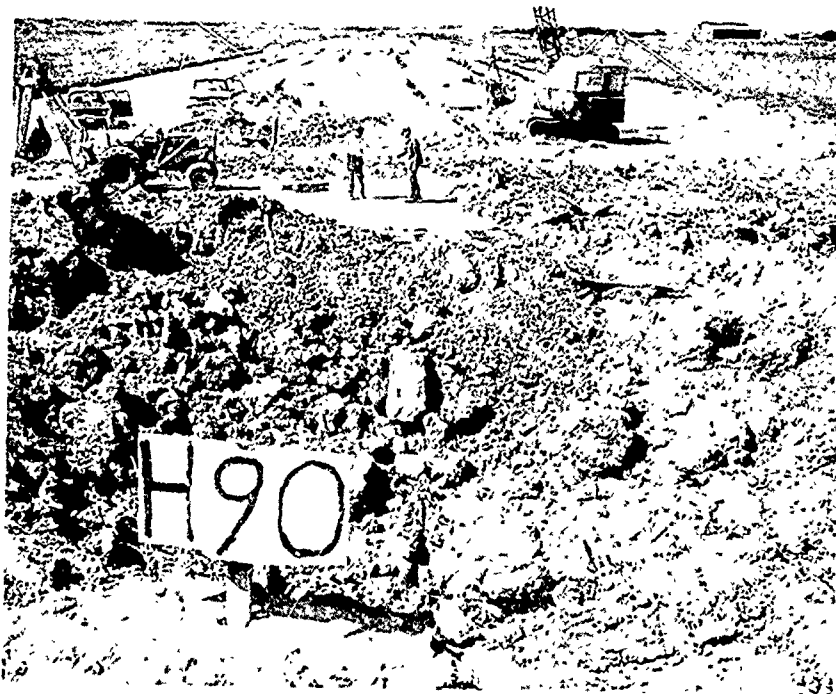
Figure 43. Crater Radii versus Depth-of-Burst for M-117 Bomb (Hays)



Crater Not Excavated

Shot 91

12-Foot Depth-of-Burst



Before Excavation

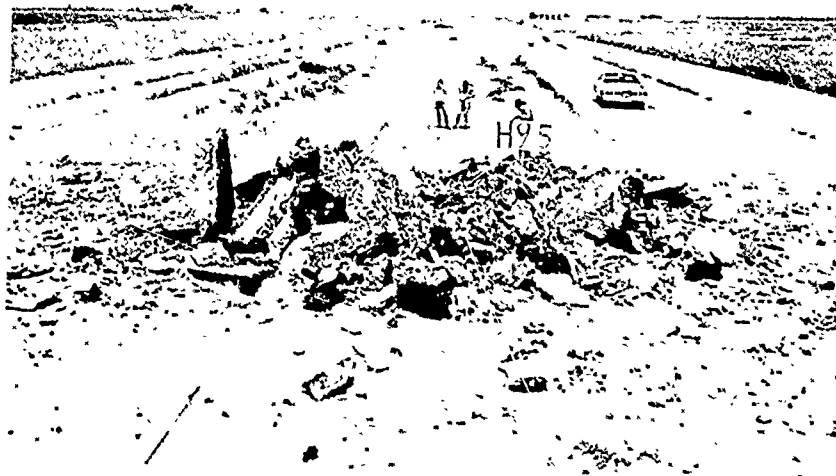
Shot 90

15-Foot Depth-of-Burst

Figure 44. Craters from Detonation of M-117 Bomb (Ilays)



Shot 95                      Before Excavation                      18-Foot Depth-of-Burst



Crater Not Excavated

Shot 95                      20.5-Foot Depth-of-Burst

Figure 44---Concluded

# SECTION VII

## DATA ANALYSIS

In the previous section, the crater data obtained from each of the charges and bombs at the Fort Sumner and Hays test sites were presented. In this section, an attempt is made to analyze some of the pertinent crater damage data as a function of charge size and depth-of-burst.

### 1. FORT SUMNER DATA

Table IV shows crater damage for the shallowest depth-of-burst and the maximum damage depth-of-burst. Figure 45, which shows crater damage for the three C-4 charge sizes, reveals the following:

(1) The damage increases with increasing charge size at the shallowest depth-of-burst.

(2) At the maximum damage depth-of-burst, the damage caused by the 15-lb charge is higher than expected since it is about the same as that caused by the 25-lb charge. It may be noted from table IV that the shallowest depth-of-burst as well as the maximum damage depth-of-burst varies for each charge size.

Table IV  
SHALLOWEST AND MAXIMUM DAMAGE DEPTH-OF-BURST DATA FOR  
C-4 CHARGES (FORT SUMNER)

Charge Size, lb	Depth-of- Burst, in.	Average Volume, ft <sup>3</sup>					Surface Crater Radius (R <sub>1</sub> ), ft
		Concrete		True Soil Crater	Concrete and Soil		
		Crater	Repair		Crater	Repair	
5	17	12	117	20	32	137	2.56
	33	28	117	42	70	159	3.90
15	10	28	130	67	95	197	3.90
	50 70	88	251	291	379	479	6.85
25	34	73	212	124	197	356	6.27
	68	83	254	217	300	470	6.70

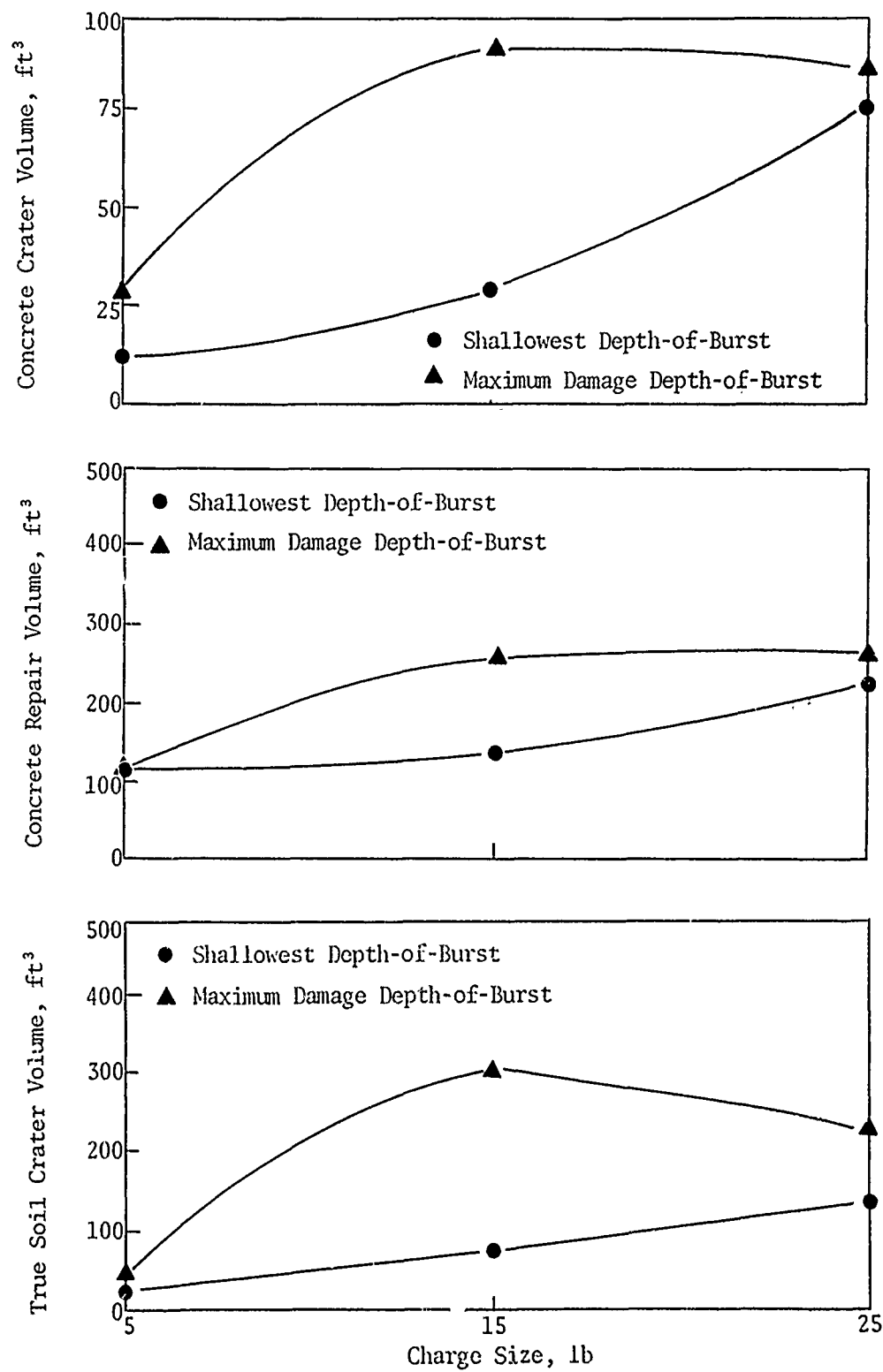


Figure 45. Crater Damage versus Charge Size (Fort Sumner)



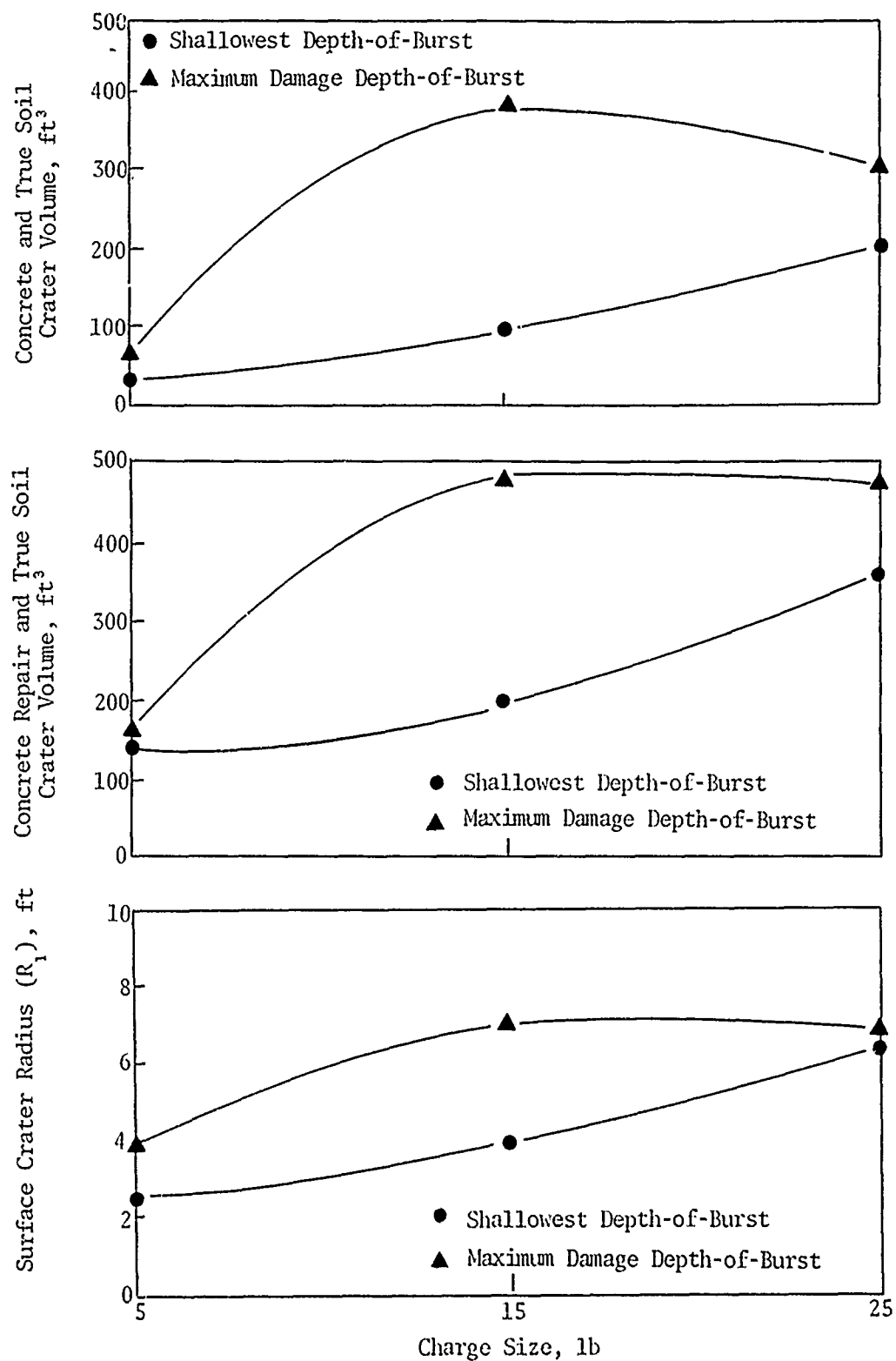


Figure 45---Concluded

Figure 46 shows the ratio of average concrete repair volume to the average combined repair volume as a function of the C-4 charge size. This figure indicates that the concrete repair volume decreases as the charge size is increased; however, the concrete repair volume is more than 50 percent of the combined repair volume. Figure 47 shows the area of concrete to be removed (because of heaves and cracks) versus depth-of-burst for all the craters and all the C-4 charge sizes. In general, the area of concrete to be removed increases with increasing depth. However, for the 5-lb charge, this increase is very small; for the 15-lb charge, the concrete area to be removed increases up to a depth-of-burst of 90 in. and then decreases. Figure 48 shows the true crater depth versus depth-of-burst for all charges. These data were fitted with the straight line  $y = A + Bx$ . It might be expected that, for a given depth-of-burst, the larger the charge the greater the true crater depth. This trend is seen in figure 48.

Based on the data given in table I, the following limits of aspect ratios ( $D/R_1$ ) can be specified for the three types of craters:

Crater Type	$D/R_1$
I	$\leq 1.0$
II	$> 1.0$ to $\leq 5.0$
III	$> 5.0$

Figure 49 shows the aspect ratios for different depths-of-burst for the three crater types. The data in this figure were taken from appendix III. Although one would expect type I craters to occur at shallow depths-of-burst and type II craters at intermediate depths-of-burst, it is seen that both crater types occurred in these depth-of-burst ranges (fig. 49). However, type III craters occurred only at the deeper depths-of-burst.

## 2. HAYS DATA

### a. C-4 Charges

The thickness of the concrete slab at Fort Sumner was uniform throughout, but at Hays there were concrete slabs of two thicknesses (8 and 11 in.). This should help evaluate the effect of the concrete thickness on the crater damage. However, it appears from table II that, although the thickness does

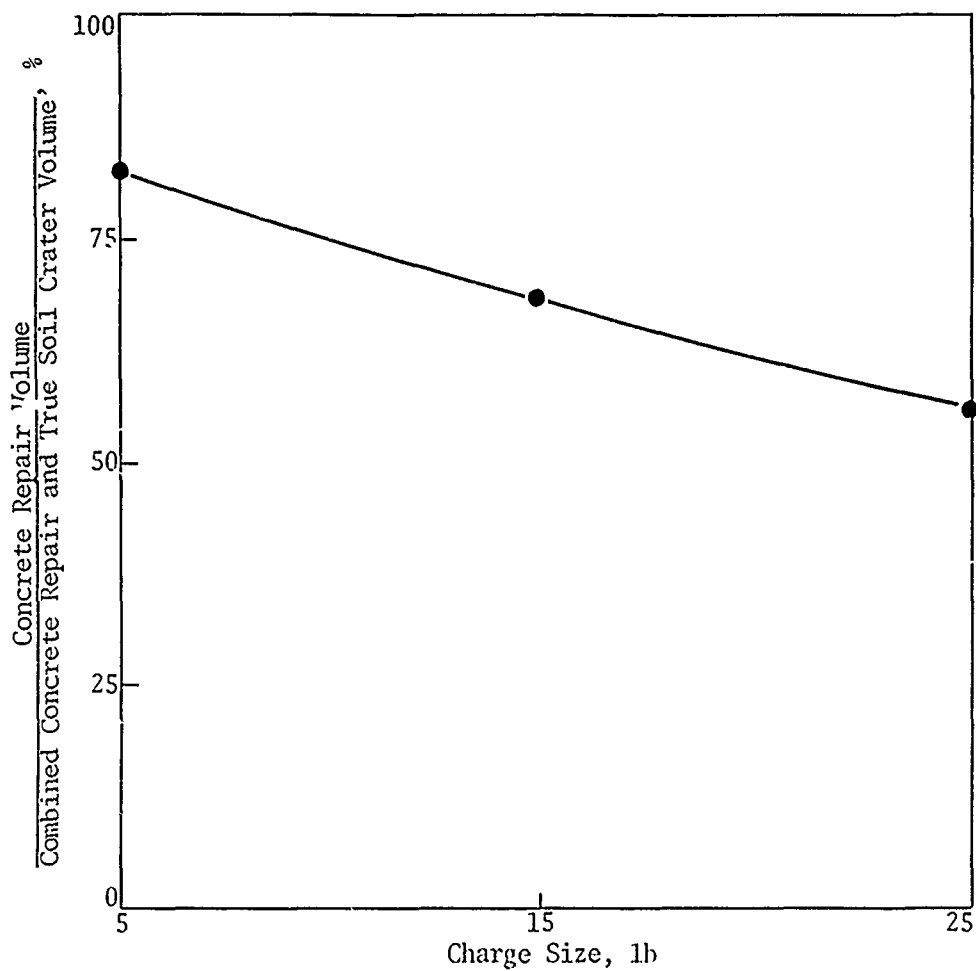


Figure 46. Ratio of Average Concrete Repair Volume to Average Combined Repair Volume versus C-4 Charge Size (Fort Sumner)

have some influence on the crater damage, the differences in concrete repair volumes, etc., are not very significant. For the 5-lb charge at 20-, 30-, and 40-in. depths-of-burst (with the maximum damage depth-of-burst assumed to be 30 in.), the average concrete area to be repaired in the 8-in.-thick concrete was about 9 percent larger than that in the 11-in.-thick concrete. For the 15-lb charge at 30-, 50-, and 70-in. depths-of-burst (with the maximum damage depths-of-burst assumed to be 30 in. for the 8-in.-thick concrete area and 70 in. for the 11-in.-thick concrete area), the average concrete area to be repaired in the 8-in.-thick concrete was about 17.5 percent larger than that in the 11-in.-thick concrete.

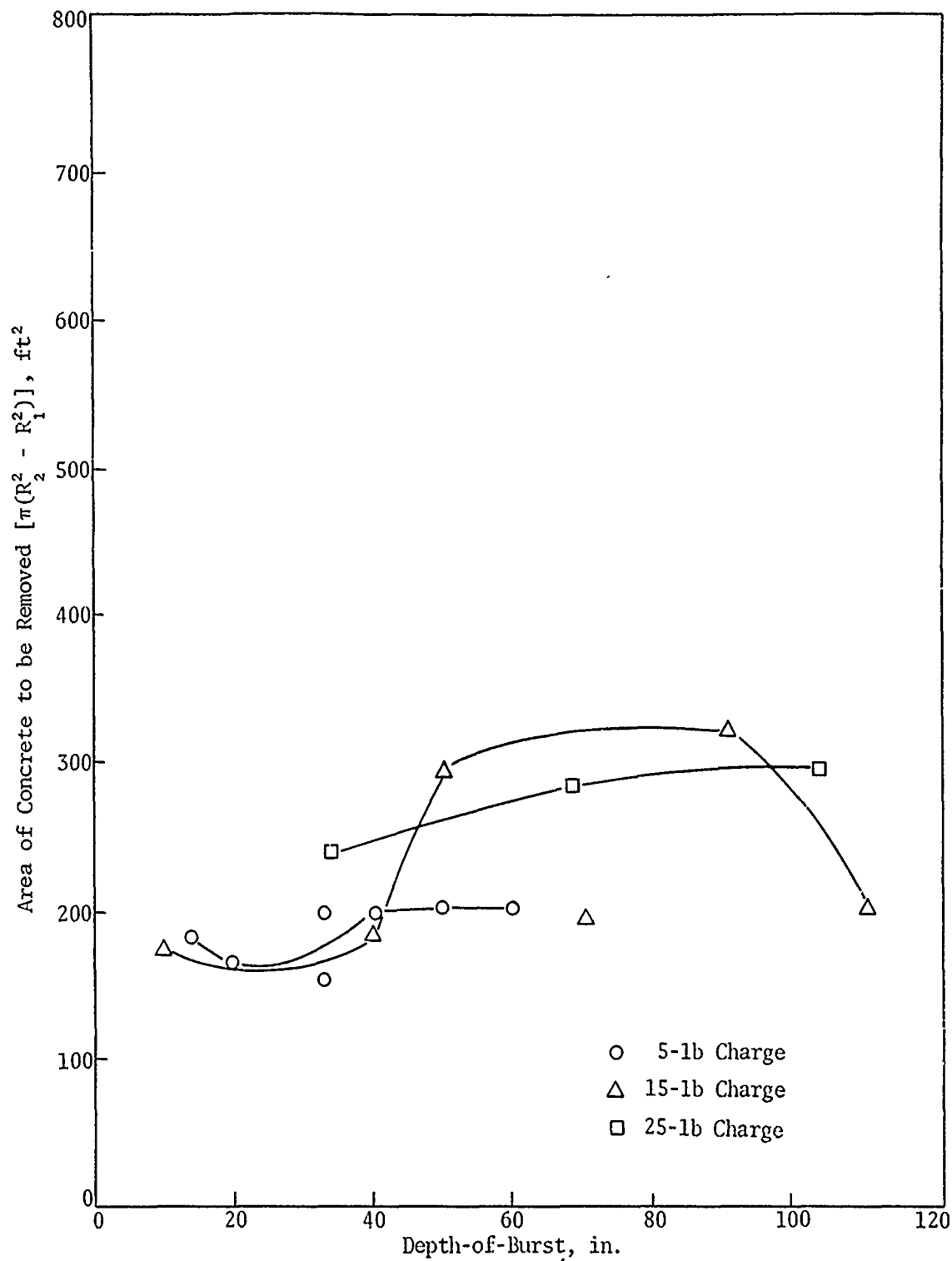


Figure 47. Area of Concrete to be Removed versus Depth-of-Burst for C-4 Charges (Fort Sumner)

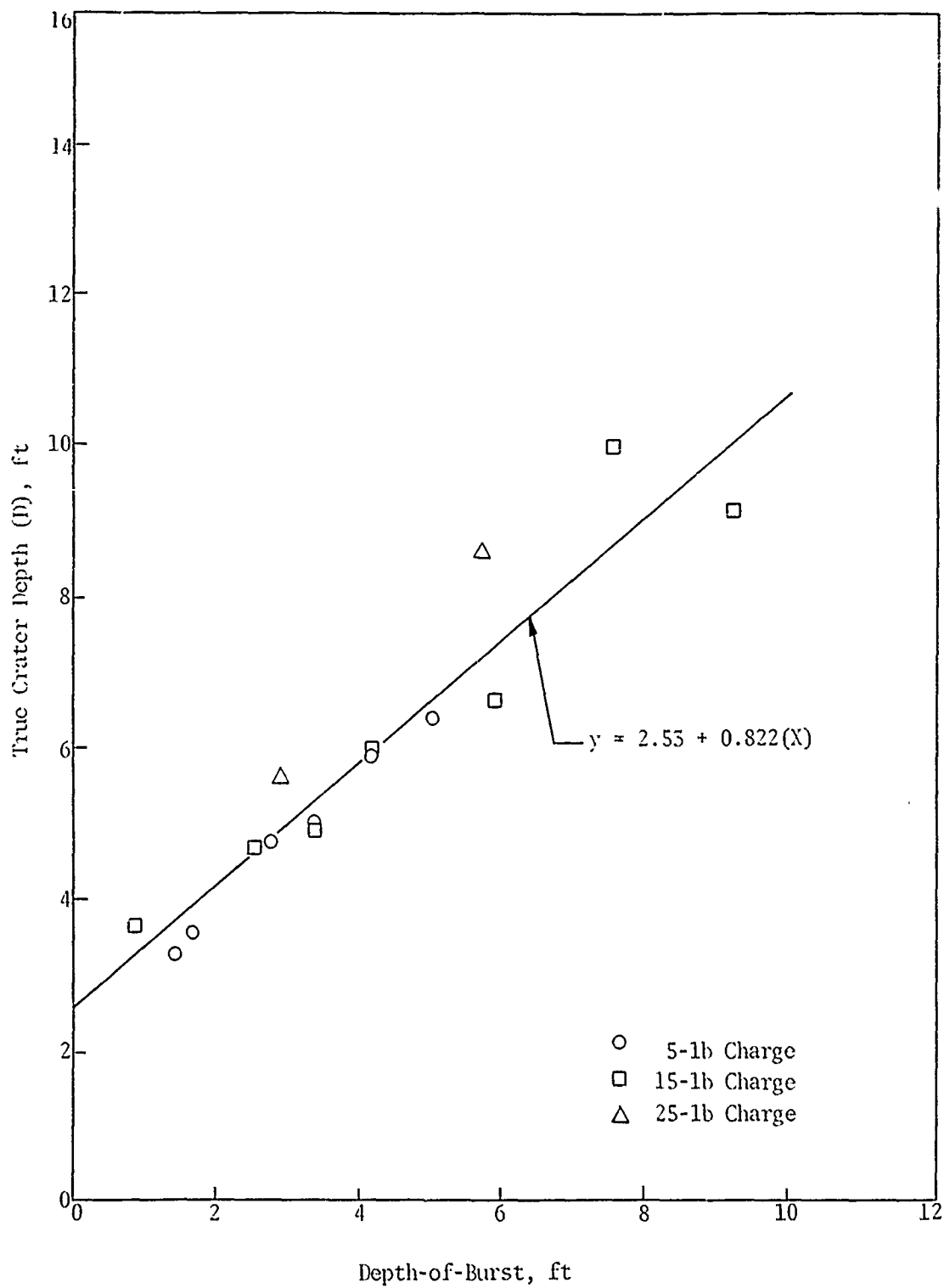


Figure 48. True Crater Depth versus Depth-of-Burst (Fort Sumner)

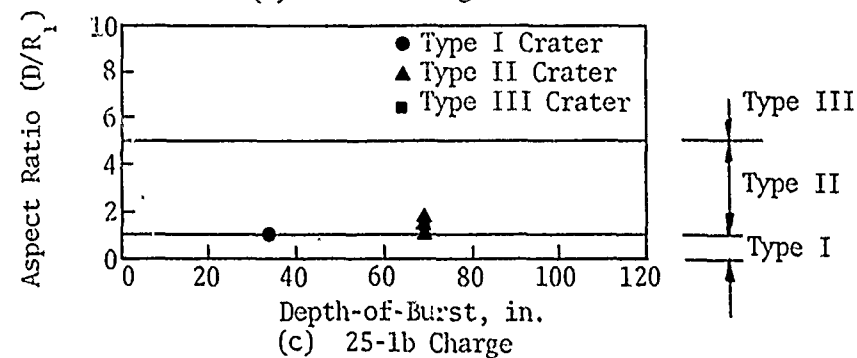
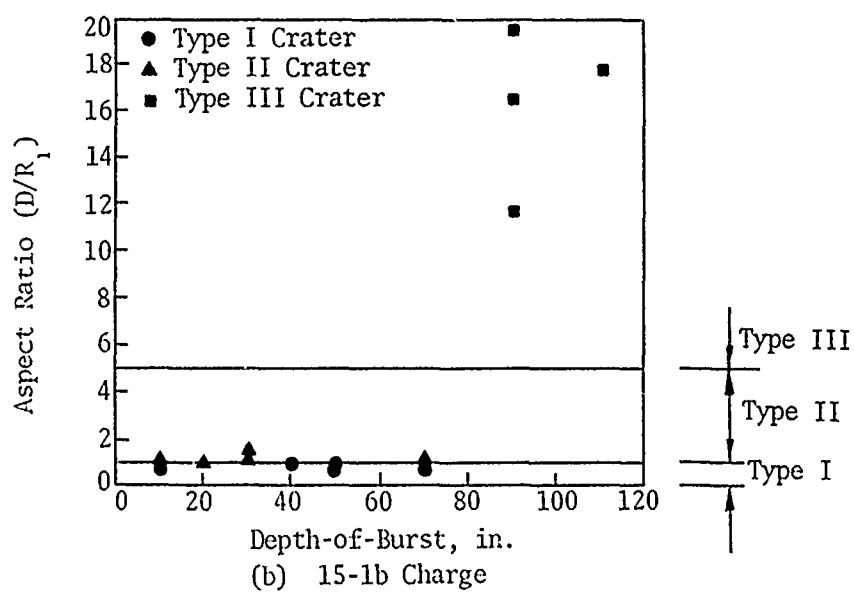
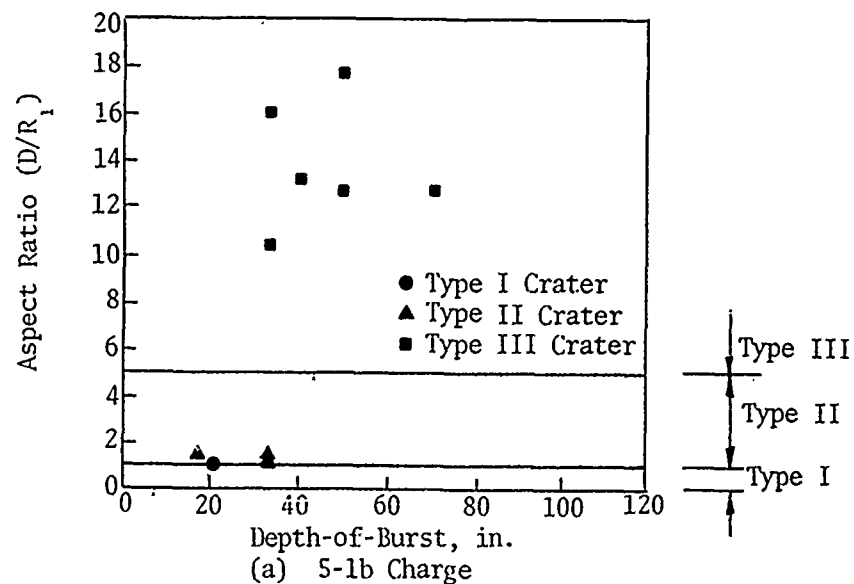


Figure 49. Aspect Ratio versus Depth-of-Burst for C-4 Charges (Fort Sumner)

Table V shows the crater damage for the shallowest depth-of-burst and the maximum damage depth-of-burst. Figure 50 shows crater damage for the three C-4 charge sizes and the two concrete thicknesses. For the 8-in.-thick concrete, the damage in general increased with increasing charge sizes for both the shallowest depth-of-burst and the maximum damage depth-of-burst. No tests were conducted with the 25-lb charge under the 11-in.-thick concrete.

Figure 51 shows the ratio of average concrete repair volume to the average combined repair volume as a function of the C-4 charge size. This figure indicates that the concrete repair volume decreases as the charge size is increased; however, the concrete repair volume is still slightly more than 50 percent of the combined repair volume for the three C-4 charges tested.

Table V  
SHALLOWEST AND MAXIMUM DAMAGE DEPTH-OF-BURST DATA FOR  
C-4 CHARGES (HAYS)

Charge Size, lb	Concrete Thickness, in.	Depth-of-burst, in.	Average Volume, ft <sup>3</sup>					Surface Crater Radius (R <sub>1</sub> ), ft
			Concrete		True Soil Crater	Concrete and Soil		
			Crater	Repair		Crater	Repair	
5	8	10	28	186	28	56	214	5.62
		30	59		82	136	266	5.17
		50		191				
	11	20	54	229	55	109	284	4.53
		30	54	229	72	125	301	4.53
15	8	10	53	171	76	129	247	5.00
		30		235				
		70	94		184	278	415	6.70
	11	10	46	230	83	130	313	4.01
50		79		202	281	444	5.23	
70			276					
25	8	50	99	225	262	361	487	6.87
		71	101		486	587	750	6.92
		95		355				

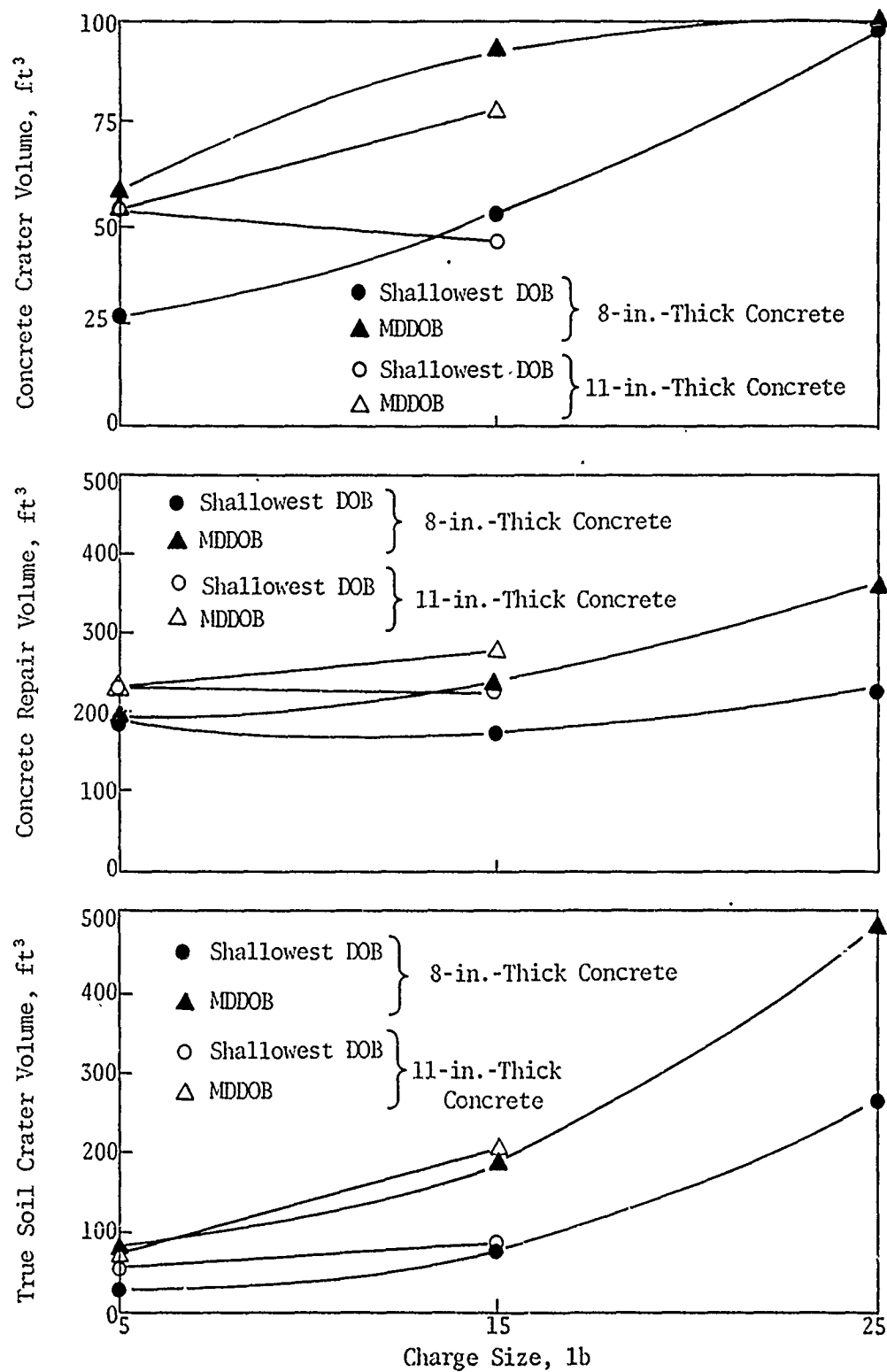


Figure 50. Crater Damage versus Charge Size (Hays)



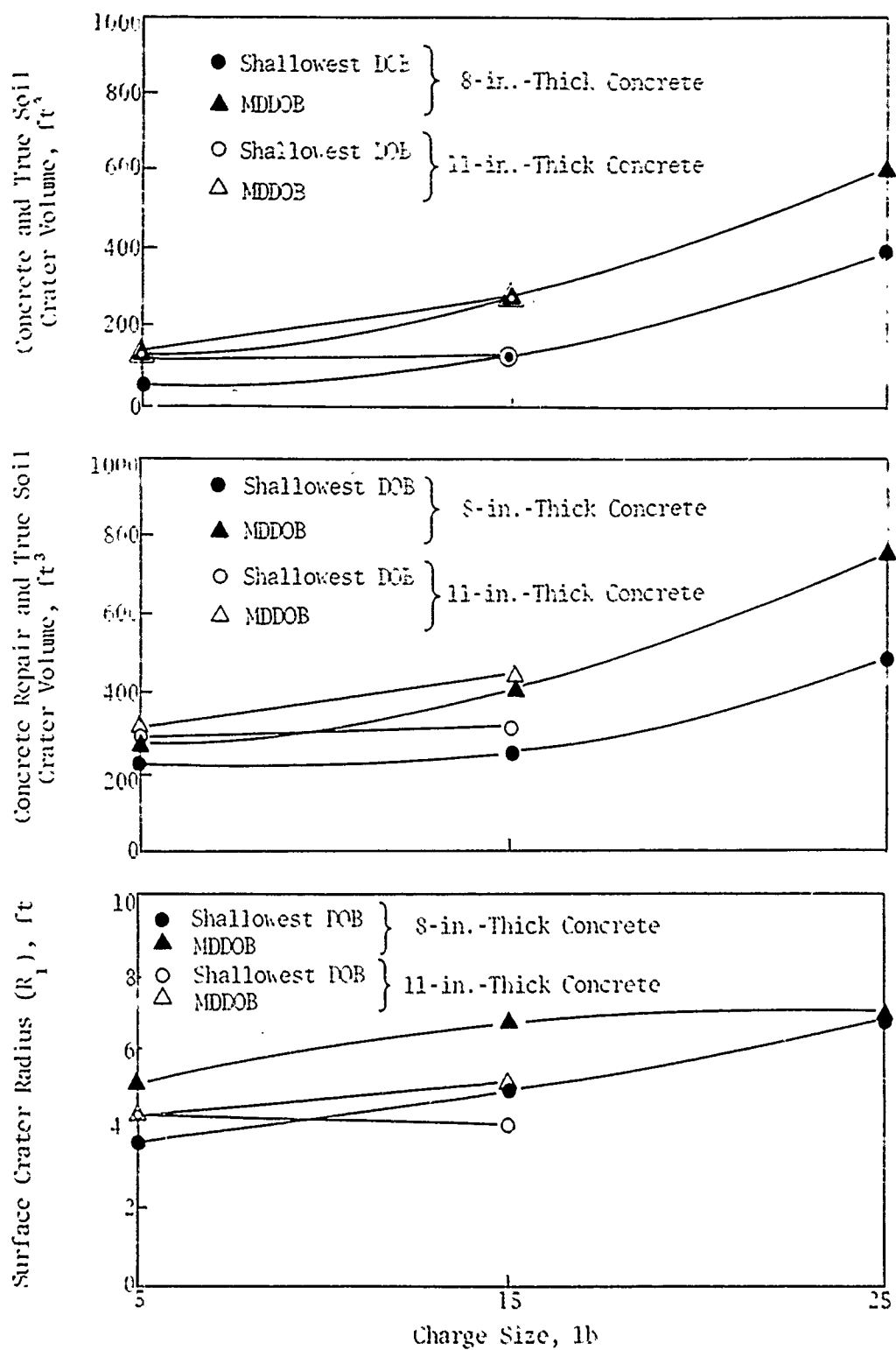


Figure 50---Concluded

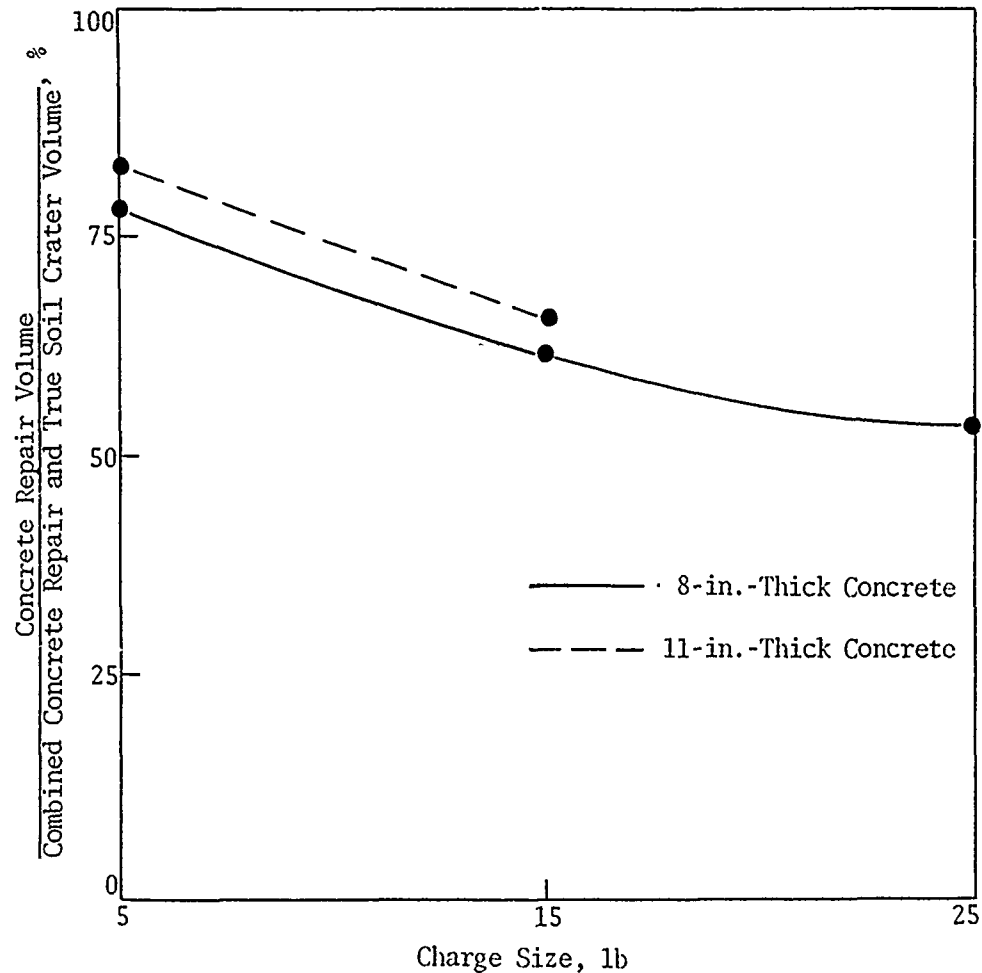
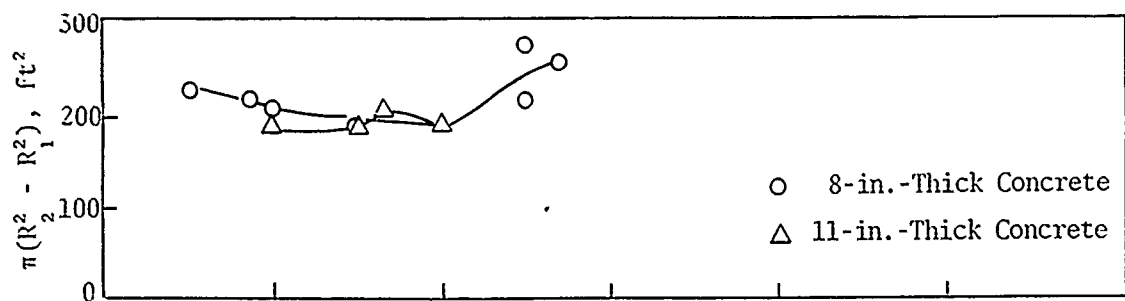
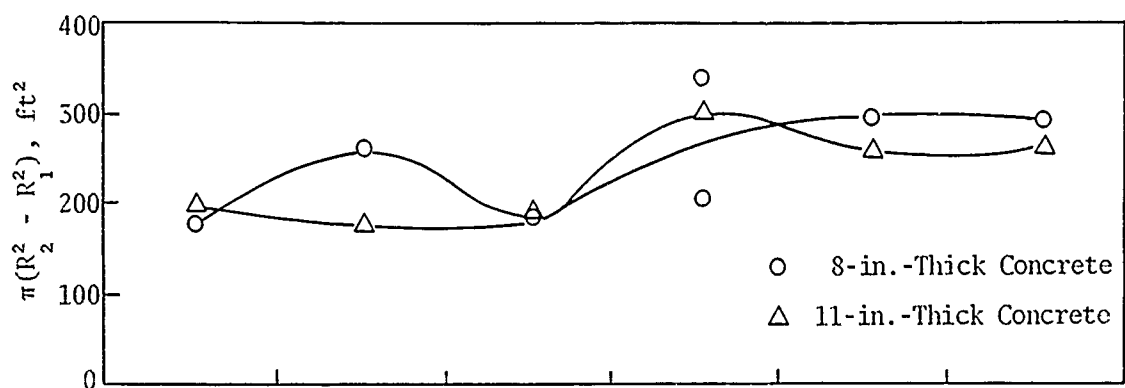


Figure 51. Ratio of Average Concrete Repair Volume to Average Combined Repair Volume versus C-4 Charge Size (Hays)

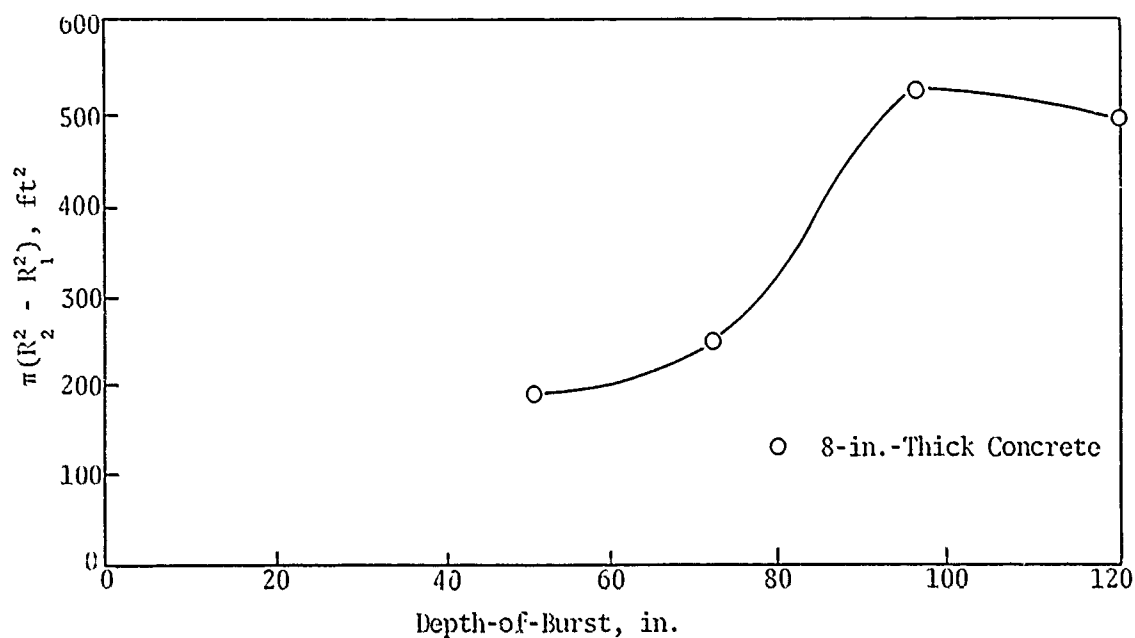
Figure 52 shows the area of concrete to be removed versus depth-of-burst for the three C-4 charge sizes. For the 5- and 15-lb charges, the area of concrete to be removed increased by 25 to 50 percent with increasing depths of-burst; however, for the 25-lb charge, the damaged area increased by 150 percent (i.e., from about 200 ft<sup>3</sup> at 50 in. to about 500 ft<sup>3</sup> at 119 in. over the range of depth-of-burst tested). An examination of the data in table II reveals a general trend indicating that the concrete area to be removed is a major part of the total concrete repair area. For instance, the concrete area to be removed is about 80 percent of the total concrete area to be repaired for the 5-lb charge.



(a) 5-lb Charge



(b) 15-lb Charge



(c) 25-lb Charge

Figure 52. Area of Concrete to be Removed versus Depth-of-Burst for C-4 Charges (11ays)

The limits of aspect ratios observed at Fort Sumner were similar to those calculated from the data at Hays (fig. 53). These data were taken from appendix IV.

The data pertaining to the C-4 charges were assumed to be quite reliable since several tests were performed with each charge at the same depth-of-burst. Therefore, an attempt was made to analyze these data by similitude relationships to verify the scaling factor and the distortion factor.

Similitude analysis of the crater phenomenon gives the following relationship based on mass scaling by neglecting gravity (ref. 3):

$$(W_1/W_2)^{1/n} = (C_1/C_2) \quad (1)$$

where

$n$  = scaling factor

$W_{1,2}$  = weight of explosive in prototype and model, respectively

$C_{1,2}$  = linear parameters in prototype and model, respectively.

Table VI shows the scaling factors obtained by scaling the maximum damage depth-of-burst and the true surface crater radius,  $R_1$ . The values of  $n$  varied from 1.40 to 2.50 for the maximum damage depth-of-burst and from 1.82 to 5.50 for  $R_1$ , excluding the data from the 15-lb charge under the 8-in.-thick concrete. For the 15-lb charge under the 8-in.-thick concrete, either a low value of  $n$  (i.e., 0.44) or very large values of  $n$  (viz., 34.07 and 15.82) were obtained. A constant scaling factor could not be obtained from the given relationship because the pavement system was not geometrically scaled for different charges.

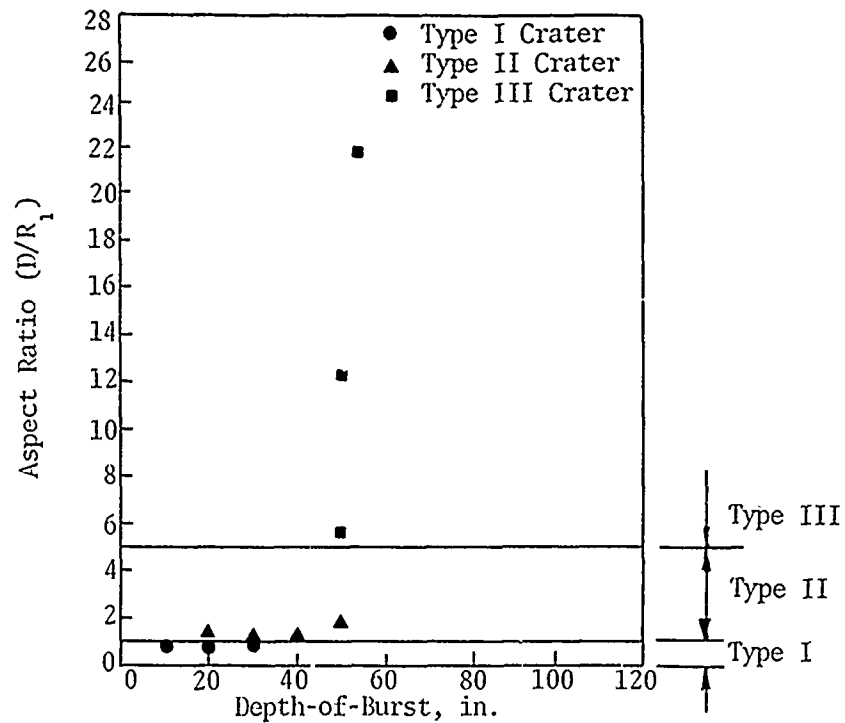
Furthermore, similitude analysis gives the relationship between the weights of the charges,  $W_1$  and  $W_2$ , and the crater volumes,  $V_1$  and  $V_2$ .

$$(W_1/W_2) = (V_1/V_2) \quad (2)$$

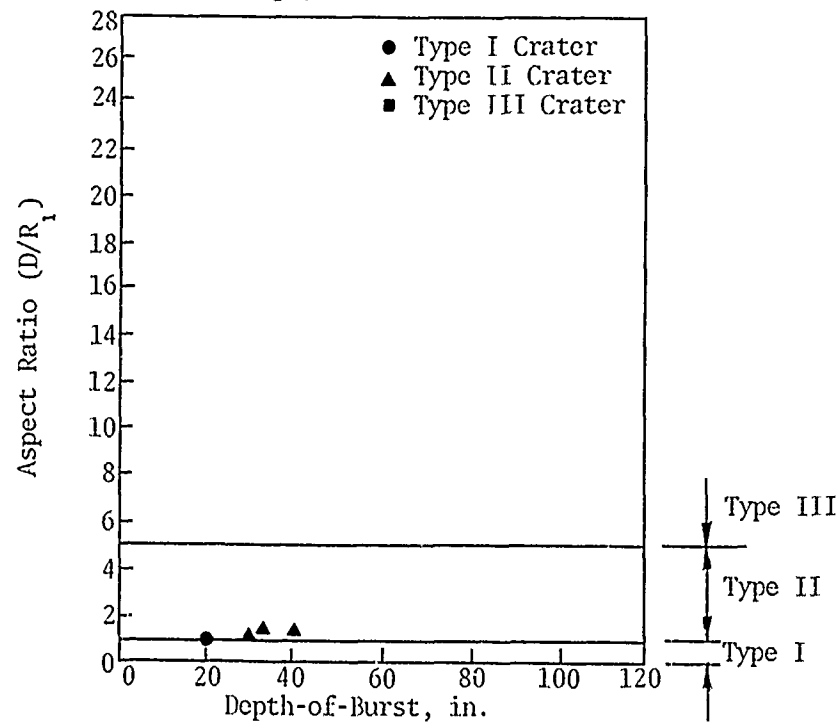
If this relationship is not satisfied exactly for distorted models, a distortion factor,  $m$ , may be determined to give the following identity:

$$(W_1/W_2) = m(V_1/V_2) \quad (3)$$

Table VI shows the computed distortion factors for all maximum crater volumes. For the concrete repair volume, it varied from 1.10 to 2.69; for the true soil

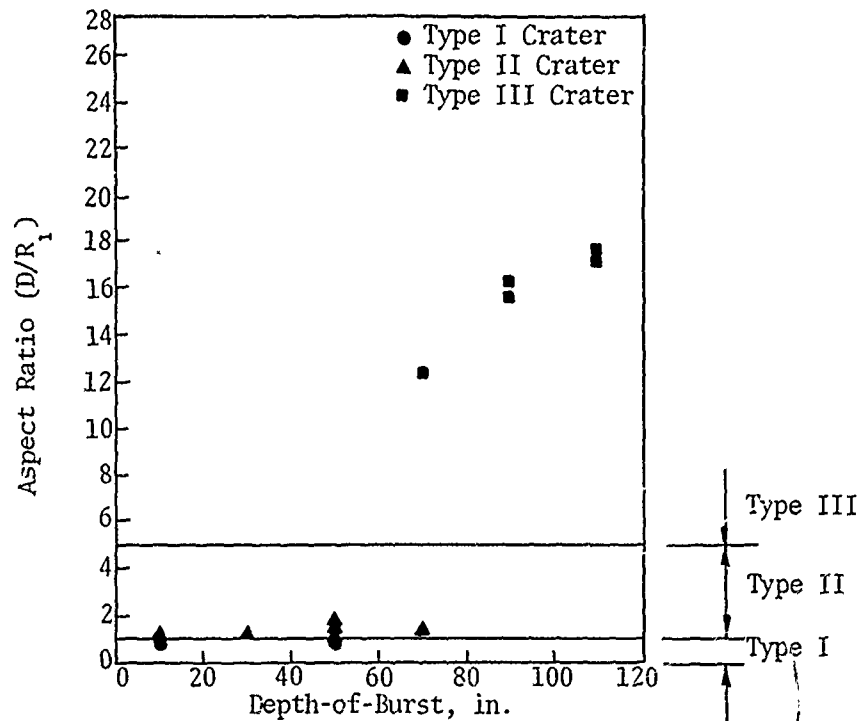


(a) 5-lb Charge, 8-Inch-Thick Concrete

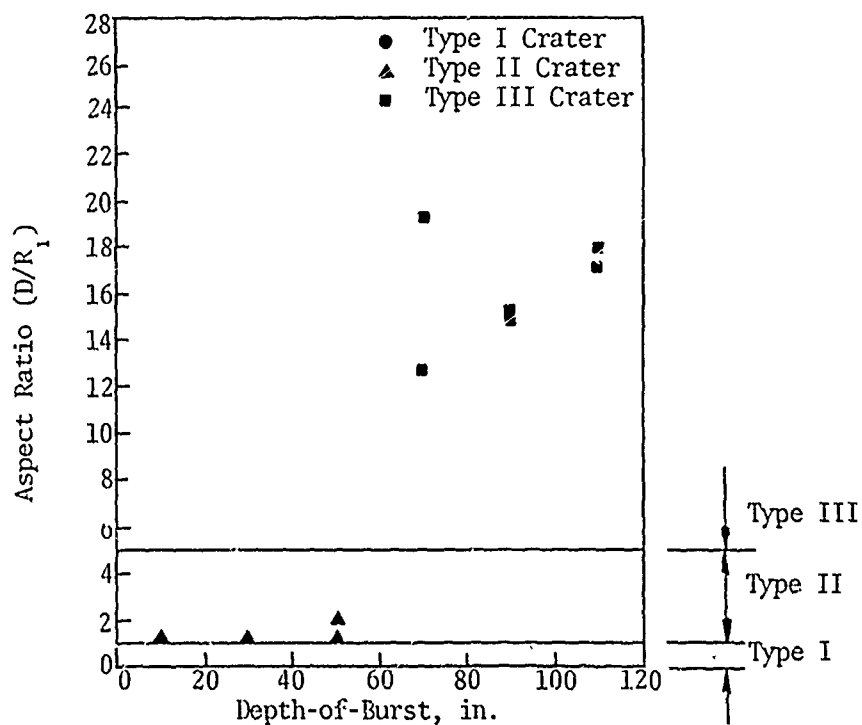


(b) 5-lb Charge, 11-Inch-Thick Concrete

Figure 53. Aspect Ratio versus Depth-of-Burst for C-4 Charges (11ays)

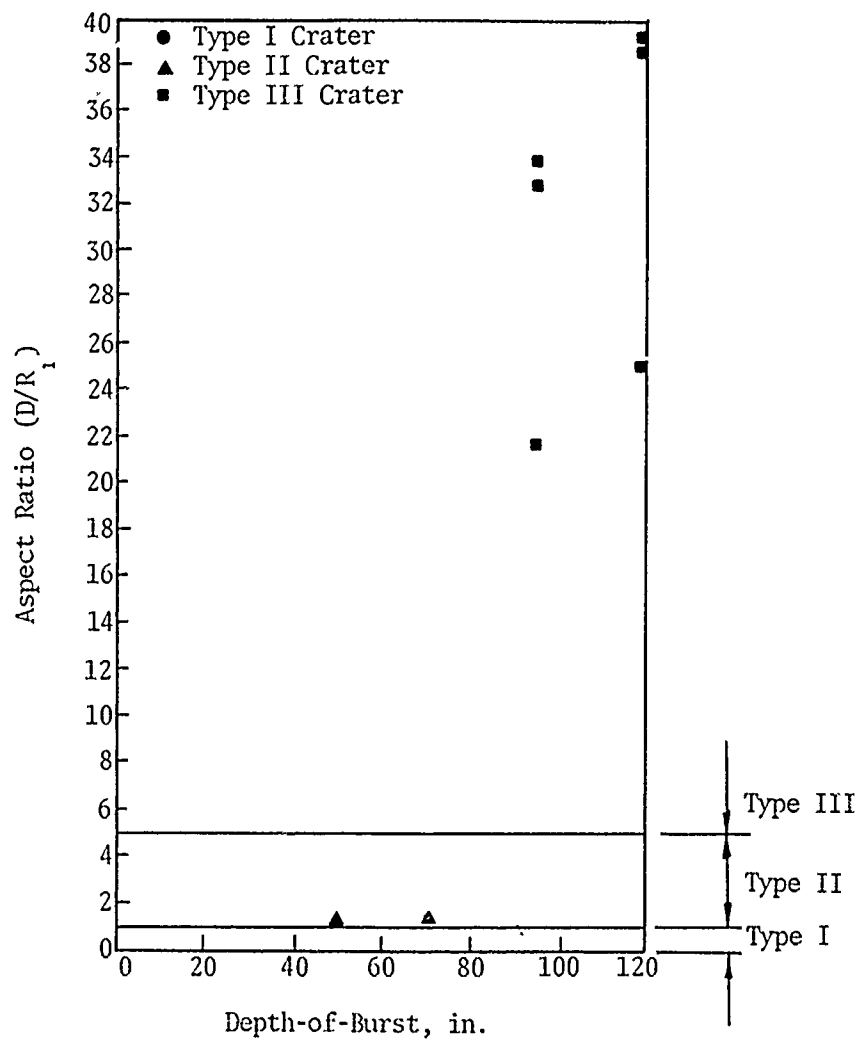


(c) 15-lb Charge, 8-Inch-Thick Concrete



(d) 15-lb Charge, 11-Inch-Thick Concrete

Figure 53---Continued



(e) 25-lb Charge, 8-Inch-Thick Concrete

Figure 53---Concluded

Table VI

## SCALING AND DISTORTION FACTORS FOR C-4 CHARGES (HAYS)

Charge Size, lb	Concrete Thickness, in.	Maximum Damage Depth-of-Burst		Crater Radius		Concrete Crater		Concrete Repair		True Soil Crater		Concrete and True Soil Crater		Concrete and True Soil Repair Crater	
		Depth, ft	n*	R <sub>1</sub> , ft	n*	Volume, ft <sup>3</sup>	m**	Volume, ft <sup>3</sup>	m**	Volume, ft <sup>3</sup>	m**	Volume, ft <sup>3</sup>	m**	Volume, ft <sup>3</sup>	m**
5	8	2.50	1.87 (1) <sup>†</sup>	5.17	5.50	59	2.92	191	2.69	82	0.84	136	1.16	266	1.77
	11	4.17	2.50 (2)												
15	8	2.50	1.40 (1)	4.53	3.42	54	2.67	229	3.23	72	0.74	125	1.06	301	2.01
	11	2.50	0.44 (2)					235	1.10						
25	8	5.83	34.07 (1)	6.70	15.82	94	1.55			184	0.65	278	0.79	415	0.92
	11	4.17	1.46 (1)	5.23	1.82	79	1.30	276	1.50	202	0.69	281	0.80	444	0.99
25	8	5.92	1.00 (1)	6.92	1.00	101	1.00	355	1.00	486	1.00	587	1.00	750	1.00
		7.92	1.00 (2)												

\* Scaling factor (n) =  $\log(W_1/W_2)/\log(C_1/C_2)$ , where  $W_1$  = 25-lb charge,  $W_2$  = 5-lb or 15-lb charge, and  $C_{1,2}$  = maximum damage depth-of-burst or  $R_1$ .

\*\* Distortion factor (m) =  $(W_1/W_2)/(V_1/V_2)$ , where  $W_1$  = 25-lb charge,  $W_2$  = 5-lb or 15-lb charge, and  $V_{1,2}$  = concrete or soil volumes.

† (1) Using maximum damage depth-of-burst for 25-lb charge = 5.92 ft.

(2) Using maximum damage depth-of-burst for 25-lb charge = 7.92 ft.



crater volume, it varied from 0.63 to 0.84. A larger distortion, which increases as the ratio of the explosive weights increases, is apparent when the concrete volumes are compared. Again, this distortion is expected since the pavement system was not scaled. For the combined crater volume, the distortion factor approaches unity mainly because the concrete crater volumes for the smaller charges are larger than the predicted values, while the true soil crater volumes are less than the predicted values.

b. Bombs

Table VII shows the crater damage for the shallowest depth-of-burst and the maximum damage depth-of-burst. Figure 54 shows the crater damage for the bombs. It is seen from this figure that, in general, the damage increases with increasing bomb sizes both for the shallowest depth-of-burst and the maximum damage depth-of-burst.

Table VII  
SHALLOWEST AND MAXIMUM DAMAGE DEPTH-OF-BURST DATA  
FOR BOMBS (HAYS)

Bomb Size, lb	Depth-of- Burst, ft	Average Volume, ft <sup>3</sup>					Surface Crater Radius (R <sub>1</sub> ), ft
		Concrete		True Soil Crater	Concrete and Soil		
		Crater	Repair		Crater	Repair	
250 (MK-81)	8	541	1180	2,457	2,998	3,637	13.70
	15	583	2208	4,000	4,583	6,208	14.23
500 (MK-82)	9	800	2100	2,950	3,750	5,050	16.66
	12	986			6,911	9,010	18.44
	15			5,897			
	18		2177				
750 (M-117)	12	2137	2534				27.24
	15			12,834	14,152	15,734	
	18		3690				

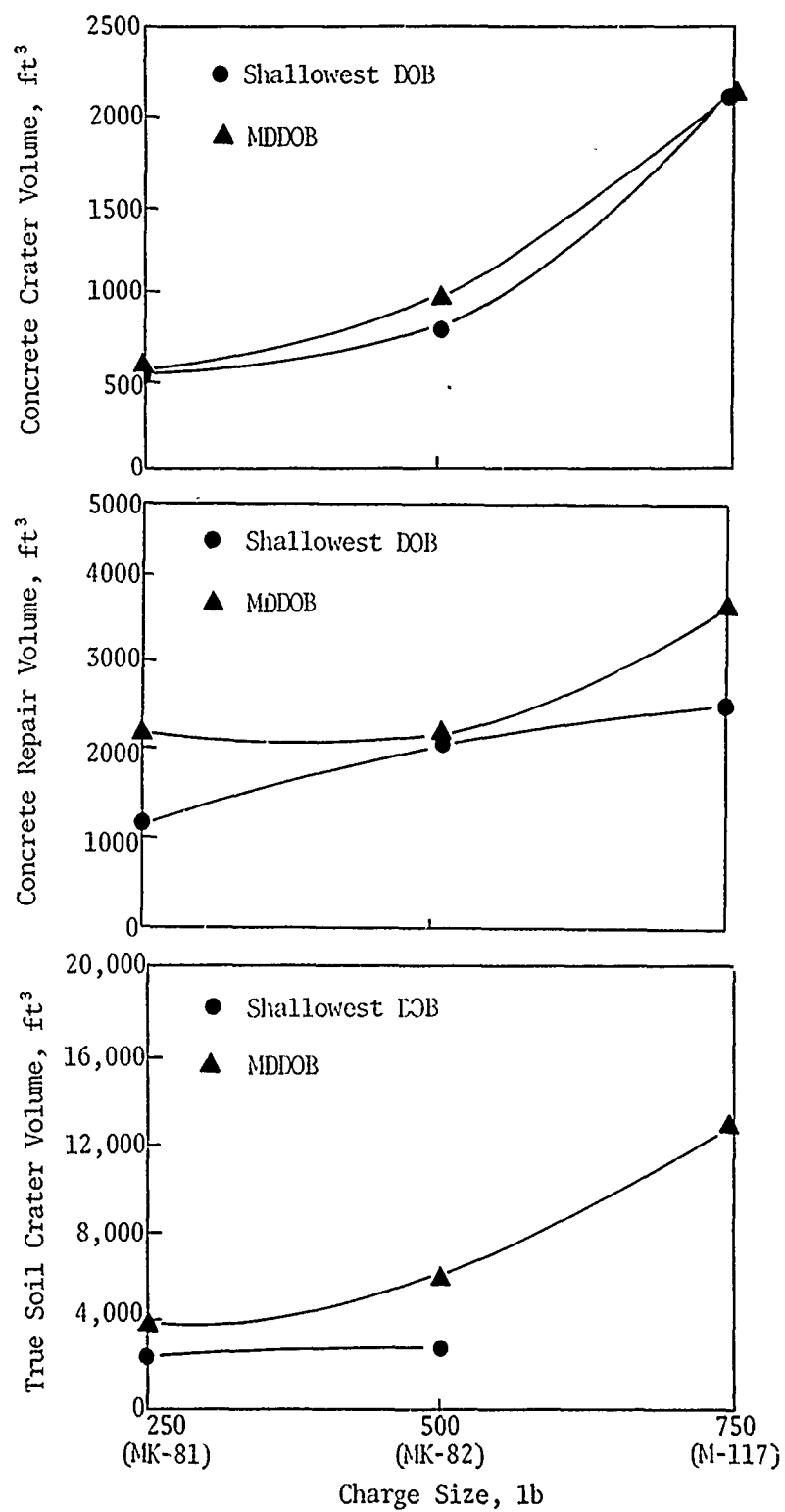


Figure 54. Crater Damage versus Bomb Size (Hays)

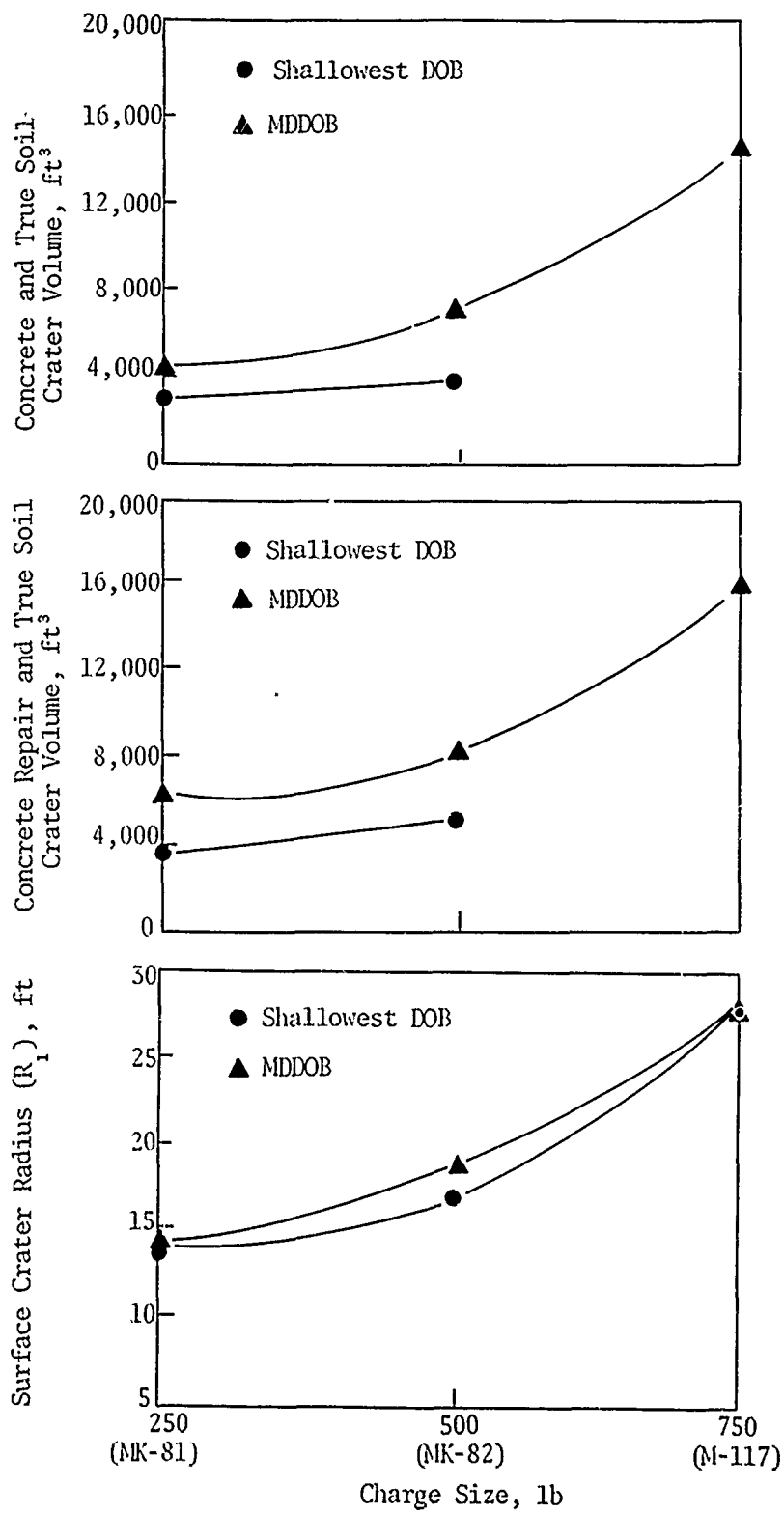


Figure 54---Concluded

Figure 55 shows the area of damaged concrete to be removed versus depth-of-burst for the three bomb sizes. There appears to be no consistent trend for the different bombs with increasing depth-of-burst. A comparison of the volume of concrete to be removed and the concrete repair volume for the bombs (table III) indicates the general trend that the concrete area to be removed is a major part of the total concrete repair area. For the three bomb sizes tested, the concrete area to be removed was about 60 percent of the total concrete repair area.

Figures 56 and 57 show the apparent crater depth, and the ejecta versus depth-of-burst, respectively, for the three bomb sizes. Figure 56 indicates that the apparent crater depth generally decreases with increasing depths-of-burst. This indicates that a camouflet will occur with greater depths-of-burst. Figure 57 shows that, for the MK-82 and the M-117 bombs, the ejecta volume increases with increasing depths-of-burst up to a 15-ft depth-of-burst and then it decreases with greater depths-of-burst. This trend was not found for the MK-81 bomb. The apparent crater volume versus depth-of-burst for the three bomb sizes is plotted in figure 58. Here again, the occurrence of a camouflet at deeper depths-of-burst is indicated by the fact that the apparent crater volume approaches zero with deeper depths-of-burst for each of the bombs tested. In figure 58, the volumes were computed by two different methods--the cone formula which assumes that the apparent crater can be approximated by a cone, and a more accurate method based on actual elevation measurements. As this figure indicates, the apparent crater volumes can be computed very well using the cone formula.

Table VIII summarizes the apparent crater data for the bombs tested. As the table shows, the volume of available material on the surface (i.e., ejecta and concrete repair volume less concrete crater volume) is, in general, much larger than the apparent crater volume and, hence, can possibly be used as backfill for repair purposes. Appendix II lists the in-place densities taken on the ejecta, the fallback material, and the crater wall. These densities were either determined by sand cone tests or by balloon density tests. As these data indicate, the ejecta and the fallback material are less dense than the material in the crater wall.

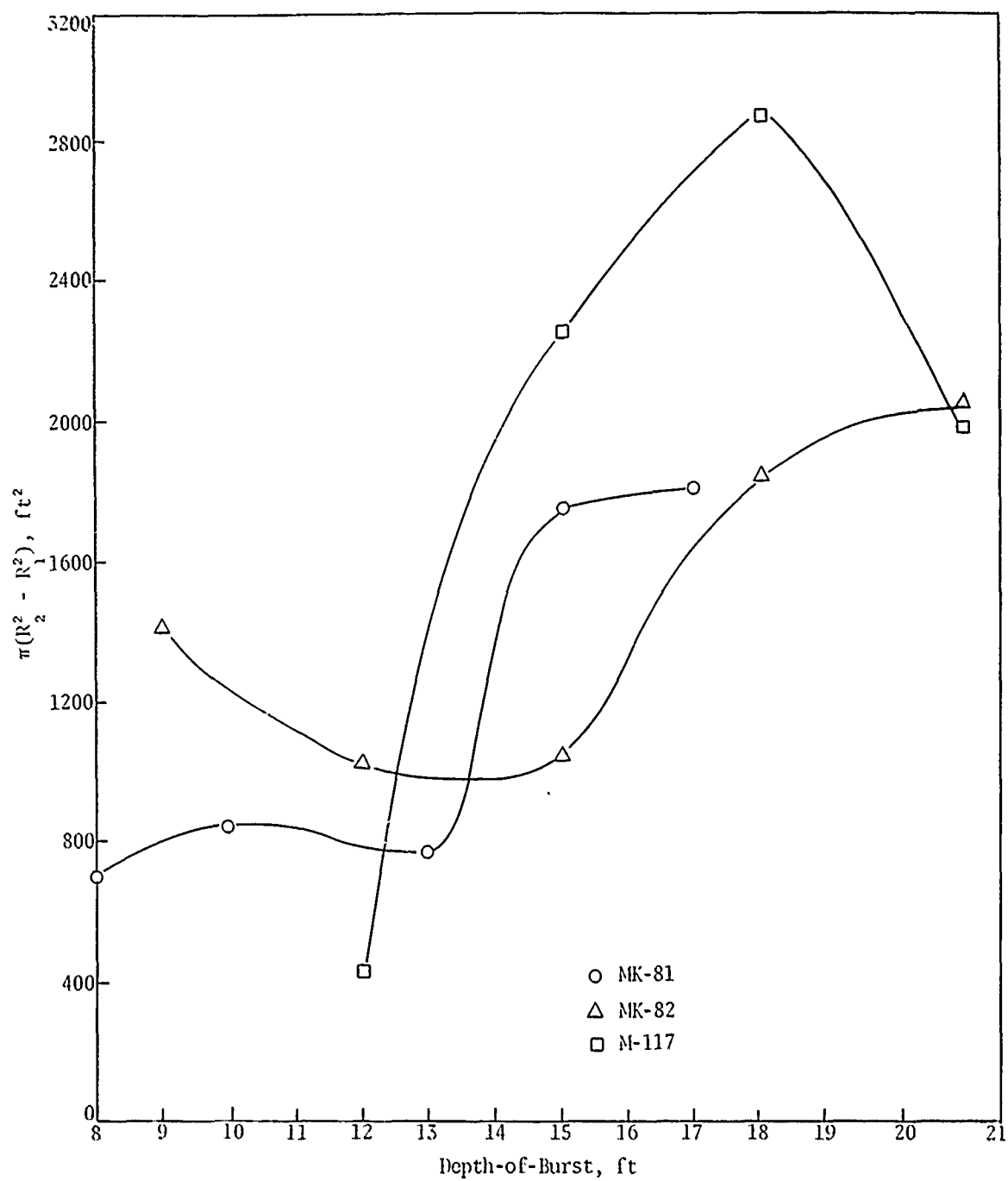


Figure 55. Area of Concrete to be Removed versus Depth-of-Burst for Bombs (Ilays)

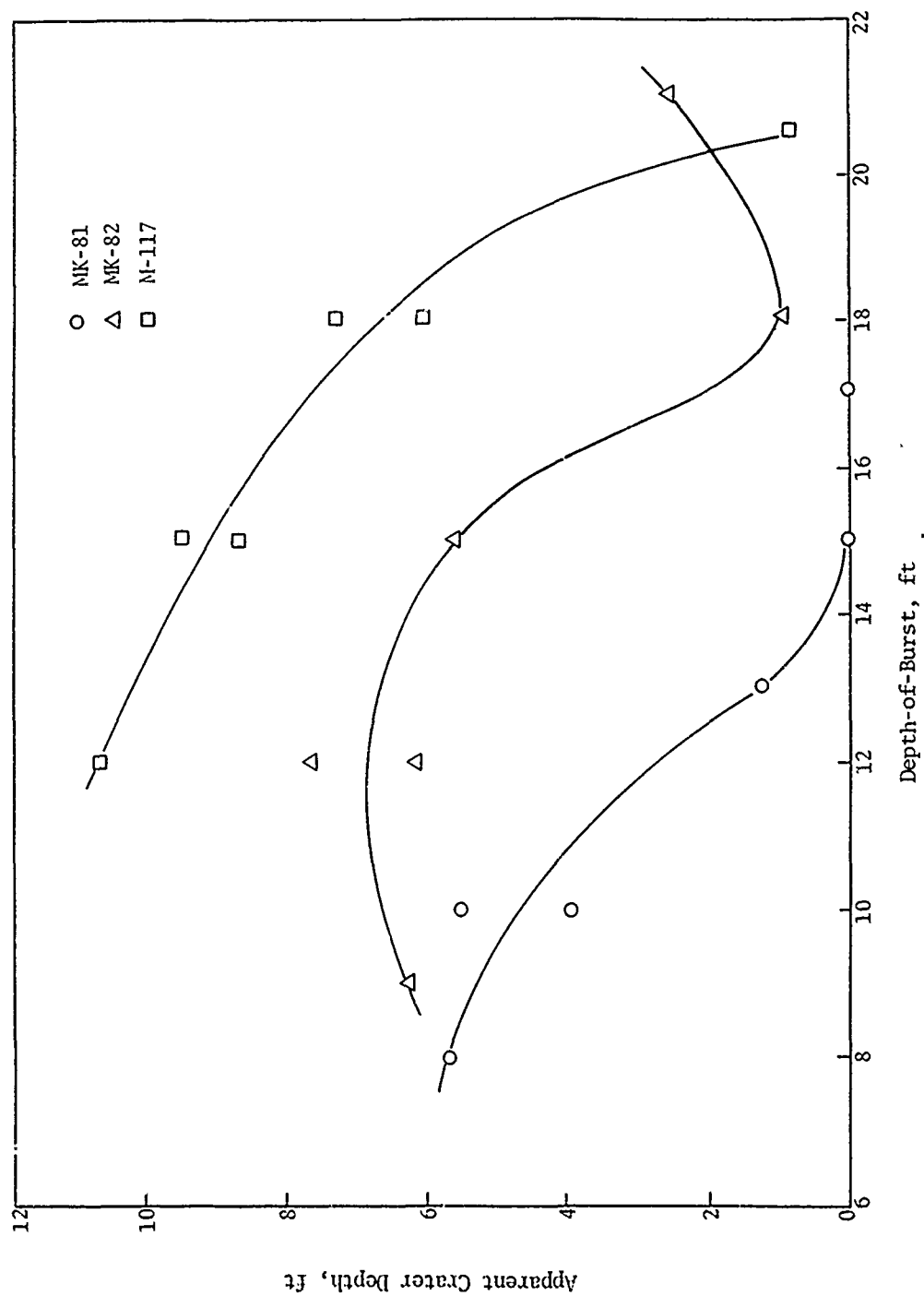


Figure 56. Apparent Crater Depth versus Depth-of-Burst for Bombs (Hays)

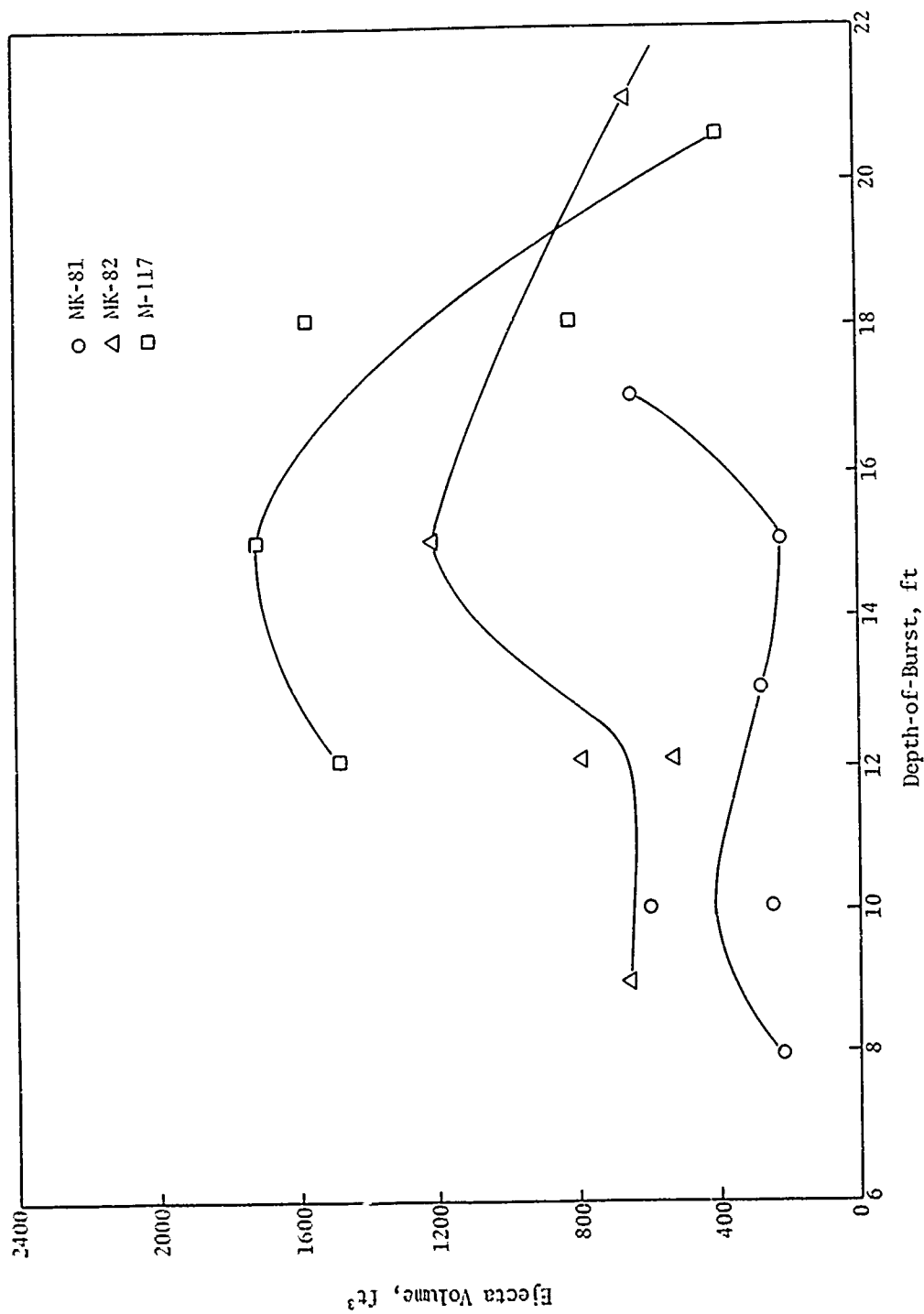


Figure 57. Ejecta versus Depth-of-Burst for Bombs (Ilays)

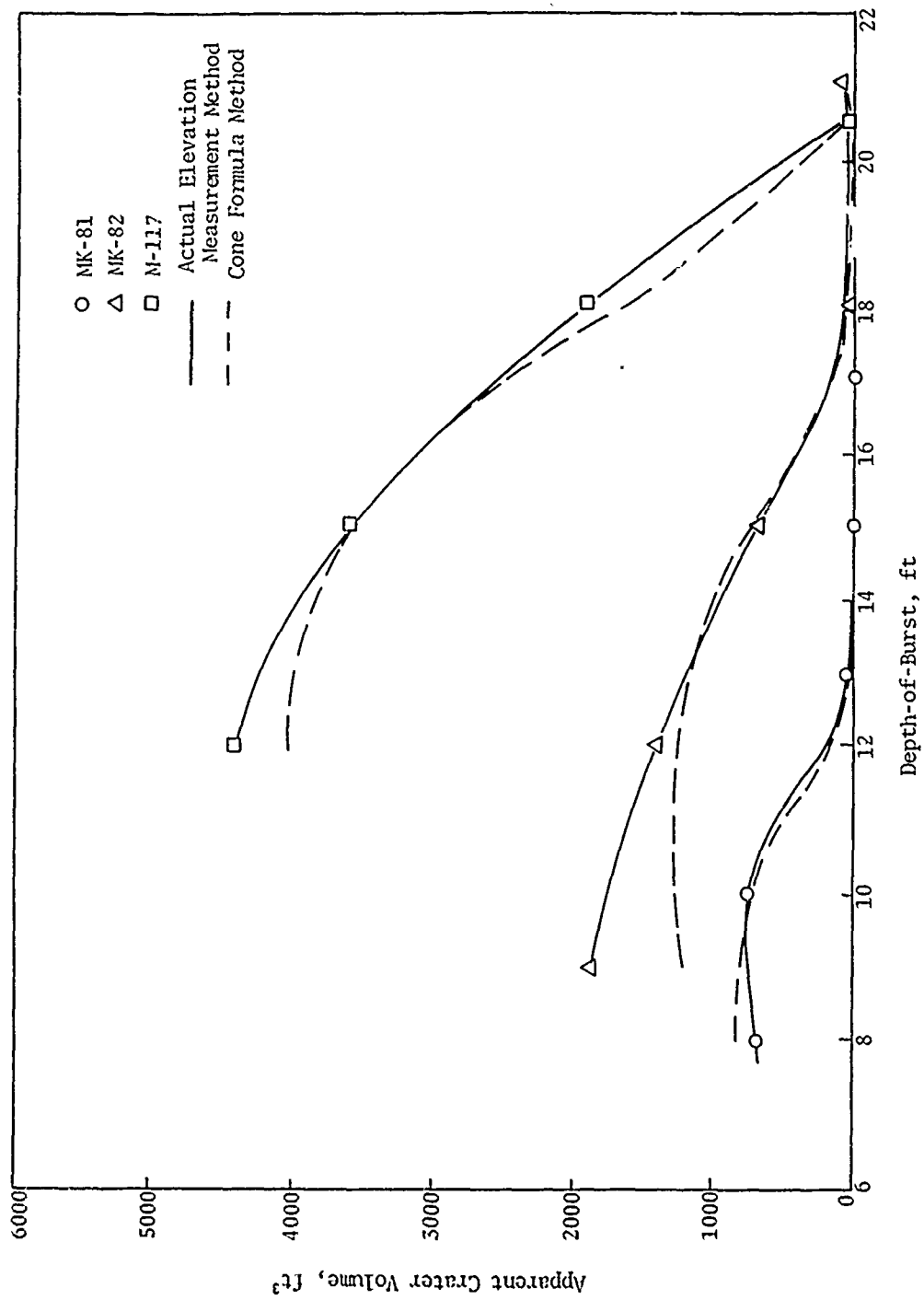


Figure 58. Apparent Crater Volume versus Depth-of-Burst for Bombs (ftays)



Table VIII

## SUMMARY OF APPARENT CRATER DAMAGE FOR BOMBS (HAYS)

Bomb Size, lb	Depth-of-Burst, ft	Concrete Volume, ft <sup>3</sup>			Ejecta Volume, ft <sup>3</sup> (4)	Material Available, ft <sup>3</sup> (3)+(4)	Apparent Crater Volume, ft <sup>3</sup>
		Crater (1)	Repair (2)	(2)-(1) (3)			
250 (MK-81)	8*	541	1180	639	221	860	693
	10	554	1383	779	420	1199	746
	13	470	1095	625	274	899	42
	15	583	2208	1625	216	1841	None
	17	439	2095	1656	639	2295	None
500 (MK-82)	9*	800	2100	1300	652	1952	1864
	12*	986	1933	947	653	1600	1398
	15	831	1788	957	1008	1965	681
	18	486	2177	1691	407	2098	33
	21	151	2021	1870	554	2424	108
750 (M-117)	12*	2137	2534	397	1275	1672	4370
	15	1283	3381	2098	1506	3604	3575
	18*	1476	3690	2214	1083	3297	1900
	20.5	802	2700	1898	383	2281	35

\* Average of two shots.

c. C-4 Charges and Bombs

Figure 59 shows true crater depth versus depth-of-burst for all C-4 charges and bombs. These data, which seem to fall within a narrow band, were approximated by the linear equation  $y = A + Bx$  as shown in the figure.

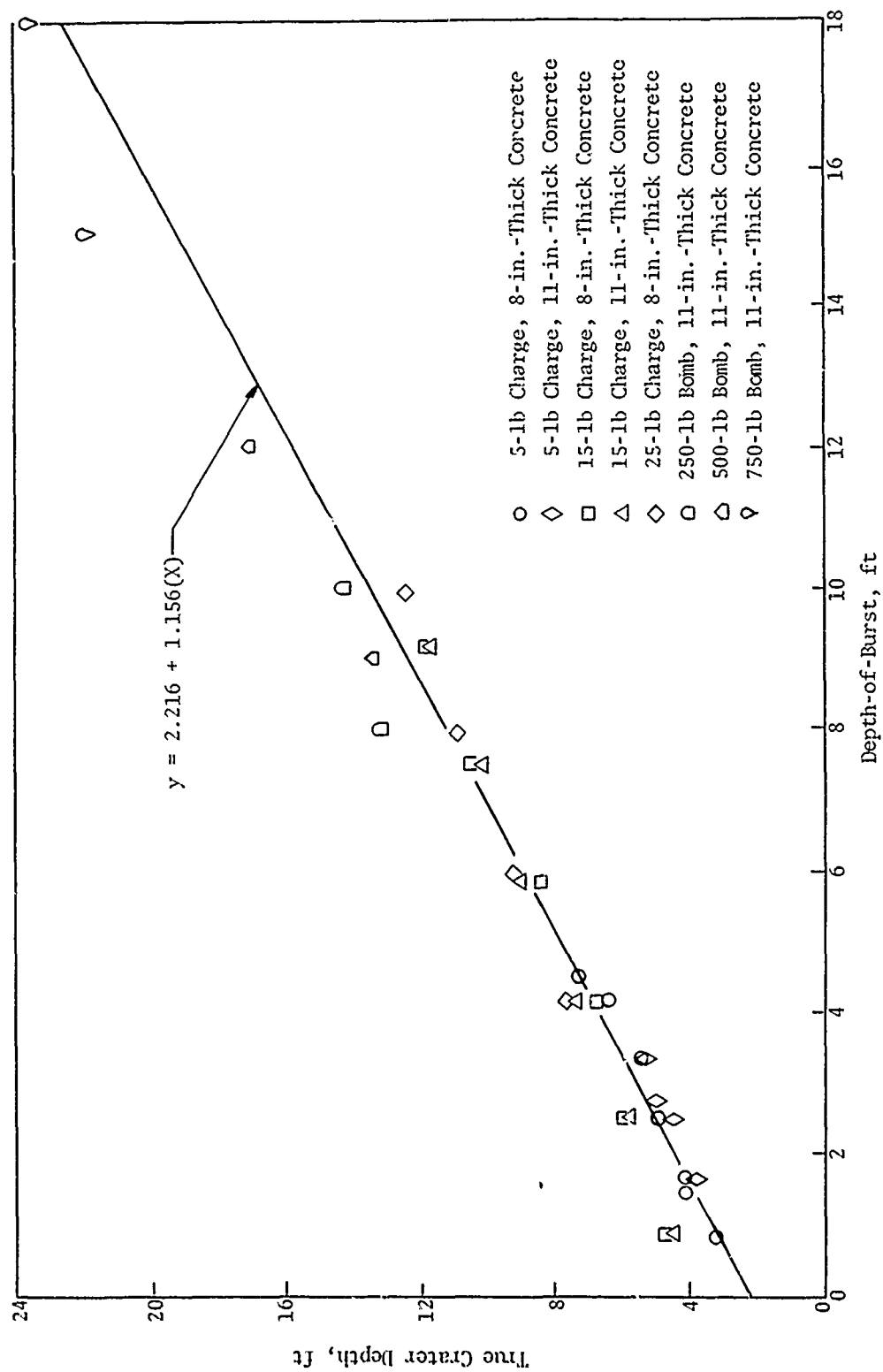


Figure 59. True Crater Depth versus Depth-of-Burst for C-4 Charges and Bombs (Hays)

## SECTION VIII

### SMALL-SCALE MODEL FEASIBILITY STUDY

The objectives of this feasibility study were to review pertinent available literature and to conduct small-scale field tests to determine if pavement systems and cratering charges can be modeled using similitude relationships derived for cratering problems in earth media; however, the field tests conducted at Fort Sumner and Hays were not modeled. The full-scale pavement tests conducted at CERF were modeled in this feasibility study.

#### 1. LITERATURE SURVEY

A limited literature survey was conducted to review the progress made in the field of cratering in general and to study past accomplishments in the area of pavement cratering.

Johnson and Fischer (ref. 4) reported on a laboratory study of the effects of mechanical properties of material on crater dimensions which was conducted by the Bureau of Mines. They found that the static tensile strength was related to the maximum scaled crater dimensions obtained by blasting. However, the nature of this relationship was such that it was useless for cratering predictions. Field data were found to be consistent with laboratory tests for both synthetic material and rock. More scatter occurred between other physical properties and maximum crater dimensions; however, some trend relationships existed. They concluded that the maximum charge depth at which cratering would occur was not determined by the strength of the material but by the pulse attenuation in the material, and that the maximum crater depths tended to be more or less constant between scaled charge depths of 0.5 and 2.

Vesić (ref. 2) has given an extensive review of the work accomplished up to 1963 on theoretical studies of the mechanics of explosive cratering in an earth medium. Depending on the relative depth of the explosive charge, three different crater types were identified: (1) camouflet and subsidence crater; (2) deep crater; and (3) shallow or surface crater. A camouflet (the type III crater described in this report is similar to a camouflet) is formed by expansion of the gas sphere. If the cavity roof collapses, a subsidence crater appears at the ground surface. A deep crater (similar to the type II craters in this report) is formed by expansion and breakthrough of the gas sphere,

followed by slope failures. The reflected tension waves may be significant during the formation of this type of crater in some media. Shallow or surface craters are formed by different mechanisms. Depending on the characteristics of the medium, plastic deformation or fracturing by the stress or shock waves is of the greatest importance. Vesić presented a theory which enabled rational analysis of camouflets and subsidence craters and deep craters that are of primary interest to the engineer. The consequences of the proposed theory were examined by Vesić and found to be in general agreement with experience. Considering the strength and deformation properties of the medium, he derived a modified scaling law for crater dimensions and found that the conventional scaling exponent was not a constant, but varied with the properties of the earth media and the actual depth-of-burst.

Moraski and Teal (ref. 5) reported on an investigation of the effects of gravity on explosive crater formation in a cohesionless medium. They concluded that crater diameters and depths varied inversely with gravity. It is very interesting to note that they conducted tests at 1.0 g in the laboratory and at 0.17, 0.38, and 2.5 g on a C-131B aircraft.

Chabai (ref. 3) conducted a similitude study on the scaling dimensions of craters produced by buried explosives. Using the principles of dimensional analysis, he determined that linear crater dimensions were proportional to the cube root of the charge weight, whether the explosion was represented in energy or mass dimensions, when gravitational effects were neglected. When gravity was included in the dimensional analysis, the cube-root scaling was valid when a mass dimension was used for the explosive charge; however, when the charge was expressed in energy dimensions, crater dimensions were proportional to the fourth root of the charge weight. Divoky (ref. 6) in his discussion of Chabai's paper indicated that if similarity was achieved between two experiments, both the mass gravity scaling law and the energy scaling law, each correctly derived, should be consistent. He concluded that mass requires the scaling of the energy release per unit mass of explosive and this, in turn, should reduce the mass law to the corresponding energy law.

Saxe and DelManzo (ref. 7) conducted research on scaling conventional high explosive and nuclear craters. They found that the linear relationships of the dimensionless parameters developed by them were useful for crater predictions. Furthermore, these relationships provided a capability of scaling from high

explosive to nuclear events not only for a particular radius or depth, but for shape as well, i.e., maintenance of a specific radius-to-depth ratio.

Galbraith (ref. 8) conducted an experimental study on motion analysis of small explosive cratering events in dry Ottawa sand by use of the cube-root scaling of the explosive charge. The scaling of time was unsuccessful.

Bessert (ref. 9), in his experimental study on the effects of charge size and depth-of-burst variations in laboratory-scale cratering experiments in sand, found that the empirically derived scaling exponent of  $1/3.4$  provides a better scaling relationship for crater dimensions than either the cube-root or fourth-root scaling rules. Furthermore, this scaling provided a better correlation with high-energy explosion data than either the cube-root or fourth-root scaling. Bessert recommended computer techniques to determine exact scaling exponents and analysis of volume variation to determine scaling relationship.

Carlson and Newell (ref. 10) reported on an experimental study to verify the relationship between soil crater ejecta distribution and its origin for single high-explosive charges of various weights detonated at various depths-of-burst. Using cube-root scaling Carlson and Newell concluded that crater radius, depth, and volume are proportional to charge weight.

D'Andrea, et al., (ref. 11) reported on experiments in a homogeneous granite to test scaling laws for various charge weights. They found that agreement among the data was best when empirical scaling exponents greater than one-third were assumed.

No definite conclusions can be drawn about the scaling exponent to be used for modeling cratering problems from the foregoing brief review of the literature. Furthermore, it seems that no model tests of pavement cratering have been conducted so far.

## 2. PRELIMINARY MODEL STUDY

### a. Pavement System Modeling

This study consisted of modeling the rigid pavement system (reported in ref. 1) which was tested in the field using C-4 explosives. Figure 60 shows this rigid pavement system. One-half of the section consisted of a 14-in.-thick Portland cement concrete slab on a 6-in.-thick gravel base course; the other half consisted of an 8-in.-thick Portland cement concrete slab on a

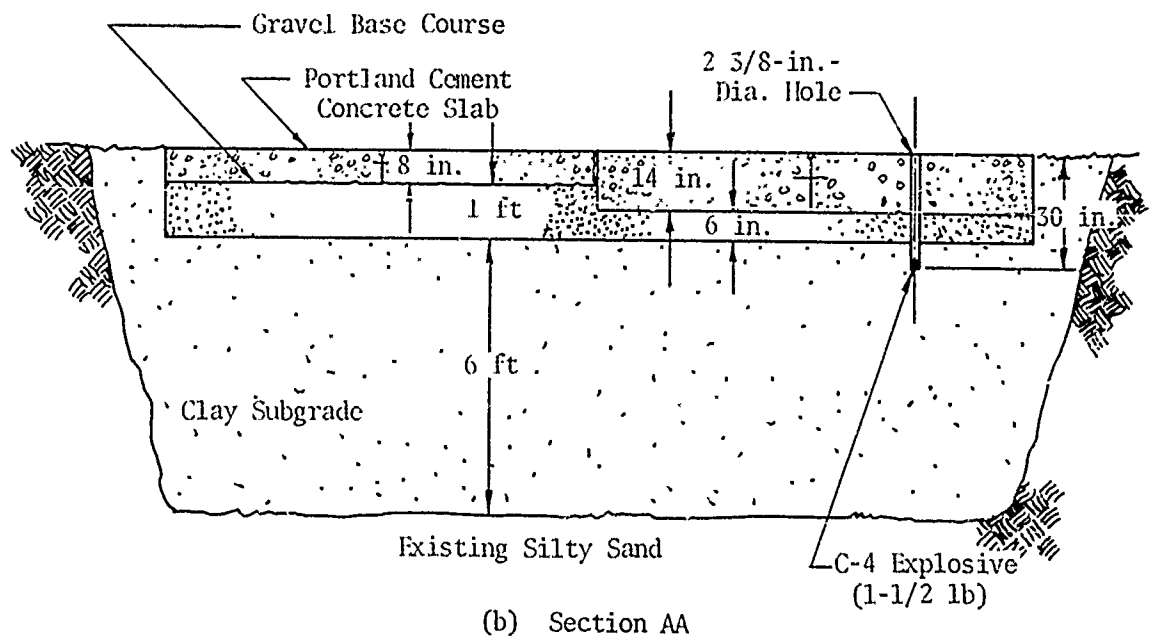
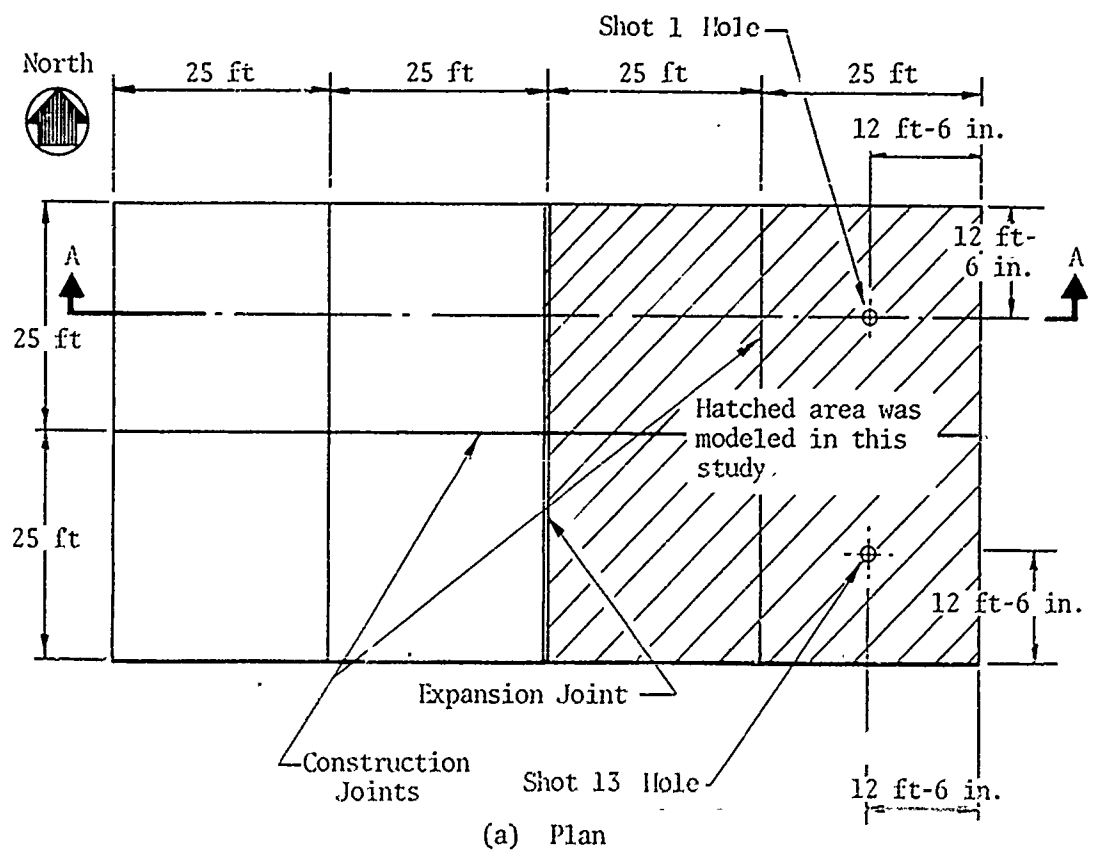


Figure 60. Full-Scale Rigid Pavement System  
[after Pichumani (ref. 1)]

12-in.-thick gravel base course. The entire section rested on a 6-ft-thick clay subgrade.

The scaling relationships mentioned in the literature survey seem to have been established for explosives in more or less homogeneous media. However, the objective of the present research was to model the cratering events on airfield pavement systems which consist of several layers of different materials. Therefore, preliminary dimensional analysis was performed on a cratering event in a pavement section consisting of two layers. From this analysis it was observed that the cube-root scaling was valid even for the layered pavement system when gravity was neglected. Consequently, it was decided to model the rigid pavement system (fig. 60) using the cube-root law for scaling.

The original rigid pavement system was 100 by 50 ft. This pavement was divided by joints into eight 25- by 25-ft panels. The positions of two shots fired in the original pavement are shown in figure 60a. Figure 61a shows the test section which was built to model the 25- by 25-ft panel located at the northeast corner of the original pavement shown in figure 60a. This panel was chosen to keep the model pavement as small as possible and also because the shot in this panel did not affect the adjacent panels of the 50- by 50-ft section of the prototype. Figure 61b shows the model of the 50- by 50-ft test section which consisted of four panels. The first eight tests were conducted on the model pavement section shown in figure 61a; the last two tests, 9 and 10, were conducted on two of the panels of the model test section shown in figure 61b. The K-4 panel was used for test 9 and the K-2 panel for test 10.

By using cube-root scaling and neglecting gravity effects, the following relationship between linear dimensions and quantity of explosive charge was obtained for craters produced by buried explosives (ref. 3):

$$\frac{C_1}{C_2} = \left( \frac{\rho_1}{\rho_2} \right)^{1/3} \left( \frac{W_1}{W_2} \right)^{1/3} \quad (4)$$

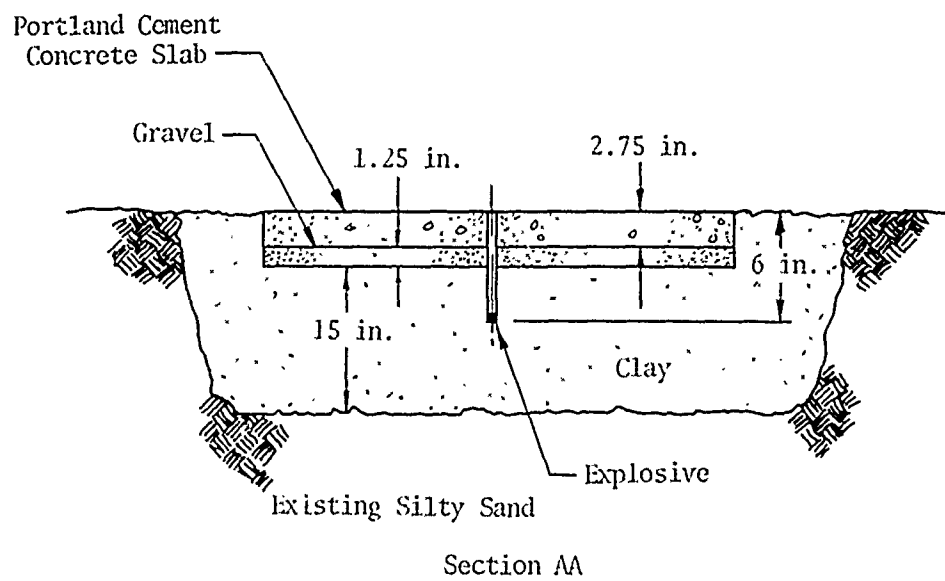
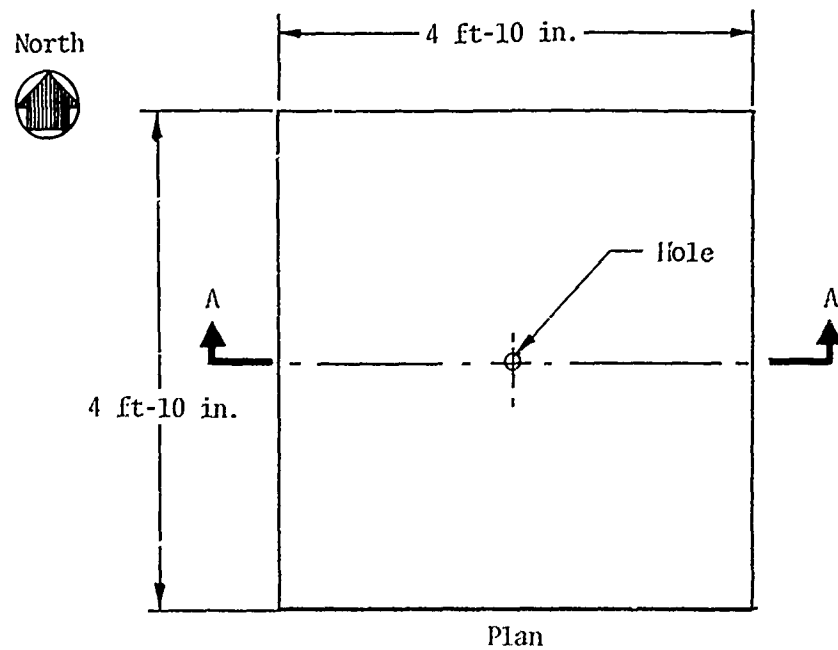
where

C = linear dimension

$\rho$  = density of medium

W = weight of charge

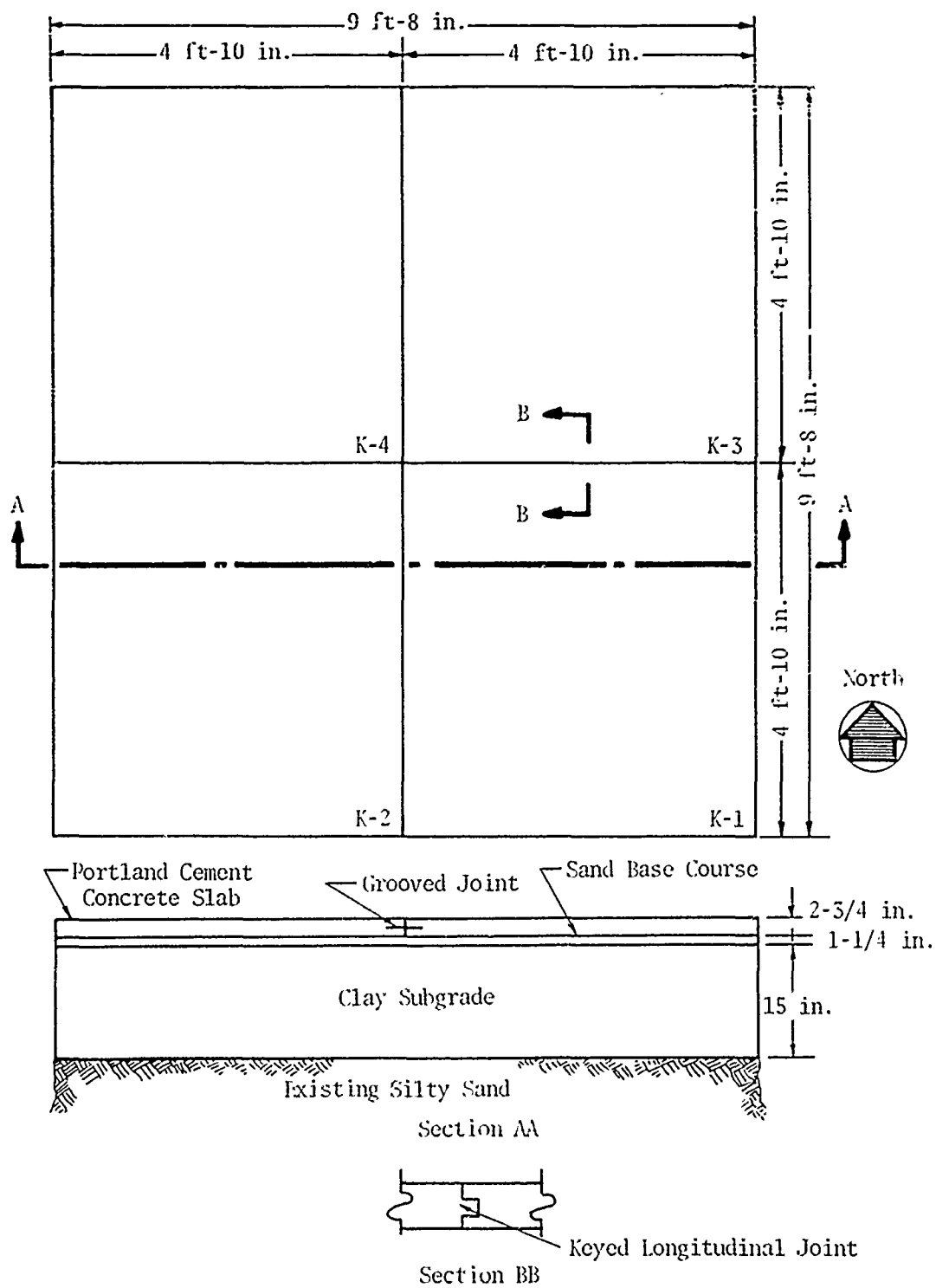
1, 2 = prototype and model, respectively.



(a) Test Section for Tests 1 Through 8

Figure 61. Models of Rigid Pavement System





(b) Test Section for Tests 9 and 10

Figure 61---Concluded

If the densities of the materials used for the model and the prototype are the same, i.e.,  $\rho_1 = \rho_2$ , eq. (4) becomes

$$\left(\frac{C_1}{C_2}\right) = \left(\frac{W_1}{W_2}\right)^{1/3} \quad (5)$$

In the original pavement system,  $C_1$  was 25 ft for tests 1 through 8 and 50 ft for tests 9 and 10; and  $W_1$  was 1.5 lb (C-4 explosive). A model charge of 5 gm of C-4 explosive was used to obtain the linear dimensions of the model test sections,  $C_2$ , shown in figure 61.

b. Construction of Model Test Sections

Processed clay was used as the subgrade material overlying the existing silty sand. The base course consisted of 1-1/4-in.-thick compacted gravel underlying a 2-3/4-in.-thick Portland cement concrete slab. Keyed longitudinal joints were constructed along the centerline of the pavement for tests 9 and 10. In addition, grooved transverse joints were provided. Oiled dowel bars, 1/8 in. in diameter and 6 in. long, were placed on 3-in. centers across these transverse sections during the concreting operation.

The 1.5-lb C-4 explosive charge which simulated the air-dropped cratering weapon in the prototype tests was modeled by electrically detonating the scaled quantity of uncased explosives at the bottom of a 6-in.-deep hole in the center of the pavement slab.

c. Results

Physical measurements of the pertinent variables such as the concrete crater and concrete repair volumes, the true soil crater volume, the surface diameter, and the maximum crater diameter were made to evaluate the effect of small cratering charges on pavements. Each shot was also photographically recorded. The crater volume was calculated from the approximate linear measurements of the crater shape. In addition, the in-place soil density,  $\gamma$ , and the moisture content,  $w$ , at the bottom of the crater were determined by taking tube samples after the crater was excavated. The compressive strength of the concrete cylinders,  $f'_c$ , was determined by testing on the day of detonation. These laboratory test data are given in table IX.

Table IX  
MODEL STUDY TEST DATA

Test	Charge Weight, gm	Soil		Concrete	
		Density ( $\gamma$ ), pcf	Moisture Content (w), %	Compressive Strength ( $f'_c$ ), psi	Curing Time, days
1	5.0	111.5	9.8	4050	17
2	11.3	111.2	7.8	4023	8
3*	9.0	112.8	11.6	3395	8
4	11.5	112.8	11.6	3395	8
5	13.0	112.8	11.6	3395	8
6**	7.0	112.8	11.6	3550	8
7	17.5	112.8	11.6	3550	8
8	15.0	112.8	11.6	3550	8
9†	17.5	112.0	10.4	3373	9
10††	17.5	108.3	12.2	4772	28

- \*Models for tests 3, 4, and 5 were prepared on the same day.  
 \*\*Models for tests 6, 7, and 8 were prepared on the same day.  
 †Test 9 was conducted on the northwest panel of the slab.  
 ††Test 10 was conducted on the southwest panel of the slab after the northwest panel was repaired.

The craters caused by the different quantities of explosive charges used in the model tests are presented in appendix V. Table X summarizes the true crater damage for these tests. In test 1, a 5-gm charge of C-4 explosive was used. The concrete slab was not damaged. Since the 5-gm shot did not cause any damage, test 2 was conducted using a model test section similar to the one used in test 1 and an explosive charge of 11.3 gm which corresponds to an n value of 2.5 in eq. (1). This shot produced radial cracks, but no

Table X  
SUMMARY OF TRUE CRATER DAMAGE FOR MODEL TESTS

Test:	Charge Weight, gm	Concrete Volume, ft <sup>3</sup>		True Soil Crater Volume, ft <sup>3</sup>		Concrete and True Soil Crater Volume, ft <sup>3</sup>		True Crater Depth, ft	Crater Radius, ft	
		Crater	Repair	Crater	Repair	Crater	Repair		R <sub>1</sub>	R <sub>3</sub>
1	5.0	0.00	0.00	0.00	0.00	0.00	0.00	0.00	0.00	0.00
2	11.3	0.00	0.00	0.07	0.07	0.07	0.07	0.83	0.03	0.25
3	9.0	0.00	0.00	0.04	0.04	0.04	0.04	0.83	0.03	0.25
4	11.5	0.00	0.00	0.09	0.09	0.09	0.09	0.79	0.03	0.30
5	13.0	0.00	0.00	0.10	0.10	0.10	0.10	0.77	0.03	0.32
6	7.0	0.00	0.00	0.04	0.04	0.04	0.04	0.71	0.03	0.23
7	17.5	0.03	5.35	0.19	0.19	0.22	5.54	1.18	0.20	0.20
8	15.0	0.00	0.00	0.13	0.13	0.13	0.13	0.77	0.03	0.67
9	17.5	0.72 * (0.91)	5.35 * (5.35)	0.23 * (0.20)	0.23 * (0.20)	0.95 * (1.10)	5.58 * (5.55)	1.04 * (0.98)	1.00 * (1.13)	1.00 * (1.13)
10	17.5	1.10	5.35	0.16	0.16	1.26	5.51	0.92	1.25	1.25

\* Average of tests 9 and 10.

Note: Depth-of-burst was 0.5 ft for all tests.

crater of the shape and size corresponding to those in the prototype test was formed. Therefore, two sets of three shots with different charges (i.e., tests 3, 4, and 5 with charges of 9.0, 11.5, and 13.0 gm, respectively; tests 6, 7, and 8 with charges of 7.0, 17.5 and 15.0 gm, respectively) were made to see if any of these shots would reproduce the damage parameters noted in the prototype test. These charges corresponded to different  $n$  values since  $C_1/C_2$  in eqs. (1) and (5) was constant by model construction. The 17.5-gm charge, used in test 7 produced damage quite similar to that in the prototype test. Therefore, tests 9 and 10 were conducted using a charge of 17.5 gm to check the reproducibility of these test results. The damage parameters visually observed in tests 9 and 10 were reasonably similar to those observed in tests 1 and 13 of the prototype study (ref. 1). Table XI summarizes the damage parameters pertaining to shots 1 and 13 of the prototype study. The explosive charge used in each prototype shot was 1.5 lb of C-4 explosive. From eq. (1), the scaling factor is given by

$$n = \frac{\log(W_1/W_2)}{\log(C_1/C_2)} \quad (6)$$

where

$W_{1,2}$  = weight of C-4 explosives in prototype (681 gm) and model, respectively

$C_{1,2}$  = linear parameters such as crater depth, etc., for prototype and model, respectively.

If  $C_1$  and  $C_2$  represent crater volumes,  $n$  will equal unity; if not, a distortion factor,  $m$ , will be obtained.

Table XII shows the computed scaling factor comparing the prototype data to the average values of damage parameters noted in tests 9 and 10. Although the model was scaled from the prototype by cube-root scaling using  $W_2 = 5$  gm, the same model was used for the larger charges up to 17.5 gm. The value of  $n$  in eq. (6) works out to 2.24 for the 17.5-gm charge when comparing crater depths of the prototype and model. However, as seen from table XII, a scaling factor of 3.09 is obtained against the theoretical value of 2.24. Comparison of the crater volumes of the prototype and model shows that the distortion factor,  $m$ , is 1.53, 0.67, and 1.28 for the concrete crater volume, the true soil crater volume, and the combined concrete and true soil crater volume, respectively.

Table XI

## SUMMARY OF TEST RESULTS FROM REFERENCE 1

Test*	Concrete Volume, ft <sup>3</sup>	Soil Volume, ft <sup>3</sup>	Concrete and Soil Volume, ft <sup>3</sup>	Crater Depth, ft	Compressive Strength (f' <sub>c</sub> ), psi
1	18.2	10.8	29.0	3.25	4996
13	28.0	12.3	40.3	3.17	7534
Average	23.1	11.6	34.7	3.21	

\* Both tests were conducted on adjacent panels of the same slab, base, and subgrade thickness from which the model thicknesses were determined using cube-root scaling.

Table XII

## COMPUTED SCALING FACTORS FROM MODEL STUDY

W <sub>1</sub> , gm	W <sub>2</sub> , gm	Concrete Volume, ft <sup>3</sup>			Soil Volume, ft <sup>3</sup>			Concrete and Soil Volume, ft <sup>3</sup>			Crater Depth, ft		
		V <sub>1</sub>	V <sub>2</sub>	m*	V <sub>1</sub>	V <sub>2</sub>	m*	V <sub>1</sub>	V <sub>2</sub>	m*	D <sub>1</sub>	D <sub>2</sub>	n
681	17.5	23.1	0.91	1.53	11.6	0.20	0.67	34.7	1.10	1.28	3.21	0.98	3.09

\*  $W_1/W_2 = m(V_1/V_2)$ , where  $m = 1.0$  if there is no distortion.

The above scaling factors were obtained from the results of only two small-scale model tests (9 and 10). However, this limited feasibility study indicates that, if large-scale models (say 1/2 scale instead of the 1/5 scale used here) were used and more tests were conducted with various depths-of-burst and charge sizes, reasonable correlation between the prototype and the model tests may be expected.

## SECTION IX

### CONCLUSIONS AND RECOMMENDATIONS

#### 1. CONCLUSIONS

Visual observation in the field revealed that there were three types of craters caused by the C-4 charges in the depth-of-burst range tested. These were as follows:

Type I ( $D/R_1 \leq 1.0$ )

These were shallow depth-of-burst craters of approximate hemispherical shape; the pavement beyond the crater was not appreciably heaved or cracked; and the ejecta was widely scattered with small concrete pieces, some of which measured a maximum 2 ft.

Type III ( $D/R_1 > 5.0$ )

These were deep depth-of-burst craters; there was no apparent crater and very little ejecta; a cavity was formed in the subgrade; and the overlying concrete slab was extensively heaved with the resultant radial cracks creating huge wedge-shaped pieces.

Type II ( $1.0 < D/R_1 \leq 5.0$ )

These were intermediate depth-of-burst craters which exhibited some of the characteristics of both types I and III craters; the apparent crater shape was conical with ejecta of intermediate size (between types I and III); and the true crater was bulb-shaped at the bottom with the frustum of a cone at the top.

This distinction of crater types is important in considering the possible repair techniques for bomb damage.

A general purpose bomb, usually detonated near the surface, will yield a type I crater; types II and III craters result only from detonation of special weapons having the capacity to penetrate deep beneath the pavement system. The relationships between crater parameters for the maximum damage depth-of-burst and the equivalent bomb sizes (fig. 54) will be valid only for special situations where the depth-of-burst is optimized; this optimization can be realized only when special cratering weapons are used. The relationships between the different crater damage conditions at shallower depths are

also shown in figure 54; these curves should approximate the damage that can be expected by near-surface detonation (general purpose bombs).

The true crater quantities from Fort Sumner were, in general, smaller than those from Hays for all C-4 charges. This was due to the difference in soil media at the two test sites, i.e., silty sand at Fort Sumner and silty clay at Hays. This finding is corroborated by similar crater data from reference 1 in which the crater quantities in pavement systems in the clay subgrade were over twice those in the silty sand subgrade. Pavement systems whose subgrades have a high percentage of clay will generally be damaged more than pavement systems with a lower clay content.

The concrete area in types II and III craters to be repaired because of cracks and heaves was a major part of the total concrete repair area. In general, the concrete repair area is maximized at a deeper depth-of-burst than are the other crater damage quantities.

The concrete area to be repaired was slightly larger for the 8-in.-thick concrete than for the 11-in.-thick concrete slabs for both the 5- and 15-lb charges. In general, the thickness effect is less significant with increasing charge size.

The volume of available material on the surface (i.e., the ejecta and concrete repair volume less the concrete crater volume) for all bombs tested at Hays was in general much larger than the apparent soil crater volume; hence, this material can possibly be used for backfilling the crater.

Apparent crater volumes for the bombs tested at Hays were found to be well predicted by the cone formula using the apparent crater height and the apparent crater radius. This relationship is useful for calculating volumes of backfill material needed so that the material can be transported from elsewhere.

Similitude analysis, using the crater results from the 25-lb charge at Hays as the prototype data and the results from the 5- and 15-lb charges as the model data, showed that the scaling factor varied rather widely for scaling the maximum damage depth-of-burst and the true surface crater radius. A similar analysis of the crater volumes showed a large distortion. This was expected since the existing pavement structure did not satisfy the similitude requirements for the different charge sizes. This analysis revealed that



cube-root scaling to determine the depth-of-burst for a given pavement system is not satisfactory.

The limited feasibility study showed that consistent data were not obtained with very small charges (such as 10 gm) probably because the materials of the various pavement layers were not scaled properly. If a smaller geometric scaling factor (say 1/2 scale) is used, it will be easier to scale down the material sizes.

Considering all the data obtained from the field tests at both sites, the authors feel that both simulation techniques using uncased C-4 charges and static detonation at a given depth-of-burst are valid experimental tools for defining crater damage parameters.

## 2. RECOMMENDATIONS

Analysis of the crater data obtained from the full-scale field tests reveals that further research is needed to establish the relationship between each dependent variable (i.e., concrete repair volume, true crater depth, etc.) and the independent variables such as the charge size, and the pavement and soil properties. Although empirical relationships between the dependent variables and a few independent variables such as the charge weight and depth-of-burst have been established in this report, it would be desirable to determine the significant effect of each independent parameter of the system on the crater damage quantities by a more formal method based on statistical analysis (i.e., regression analysis). Such an analysis will, hopefully, point out which of the independent parameters are not important and, therefore, could be excluded from further examination in crater studies.

The feasibility study of modeling pavement cratering including the literature survey performed at CERF indicates that a study using larger models (i.e., 1/2 scale) may yield important information regarding the scaling and distortion factors for the various charges in different pavement systems.

## APPENDIX I

### FORT SUMNER SUBSURFACE EXPLORATION DATA

Laboratory tests were conducted on soil and concrete samples from the test site in order to analyze the pavement crater data from the full-scale field tests at Fort Sumner. Figure 62 shows the locations on the test section from which these samples were taken.

#### 1. SOIL TESTING

Five test borings were conducted with a 2-in. ID, 2.5-in. OD California-type sampler with a 4-in. segmented brass liner. The sampler was dynamically driven by a 140-lb hammer with a 30-in. freefall. The blowcount, the dry density,  $\gamma_d$ , and the moisture content,  $w$ , were obtained every 2.5 ft down to a depth of 20 ft. Bag samples were also taken at each 2.5-ft interval during the boring operation for laboratory testing of the specific gravity,  $G_s$ , and the Atterberg limits for soil classification.

Three trenches were dug adjacent to the test section at stations S16, N15, and N44. Balloon density and moisture content were taken at 2.5-ft intervals down to a depth of about 14 ft. Bag samples, also taken at each 2.5-ft interval, were tested in the laboratory for the specific gravity,  $G_s$ , and the Atterberg limits for soil classification.

Three slabs (stations S11E2, S12E4, and N44E6) were cut out and balloon density, moisture content, and bag samples were taken directly under the slabs. The same tests were also conducted at 2.5-ft and 5-ft depths at stations S12E4 and N44E6. The results of these soil tests are given in table XIII.

#### 2. CONCRETE TESTING

Three concrete specimens were received from the test site (stations S15, N13, and N44). Four cylinders, each approximately 4 in. in diameter and 7 in. long, were core drilled from each of these samples. The ends of the cylinders were then milled down.

The density,  $\rho_c$ , was first determined. Sonic velocity tests were then performed using sonic testing equipment and a 300-lb compression load to obtain good contact at the ends. Uniaxial compression tests were performed on the cylinders to determine the ultimate compressive strength of the concrete,  $f'_c$ ,

from which the modulus of elasticity,  $E_c$ , was computed (ref. 12). These test data are given in table XIV. The concrete strengths reported here are probably on the high side because of the small cylinder size. (The concrete strengths given in the literature were obtained by testing 6- x 12-in. cylinders.)

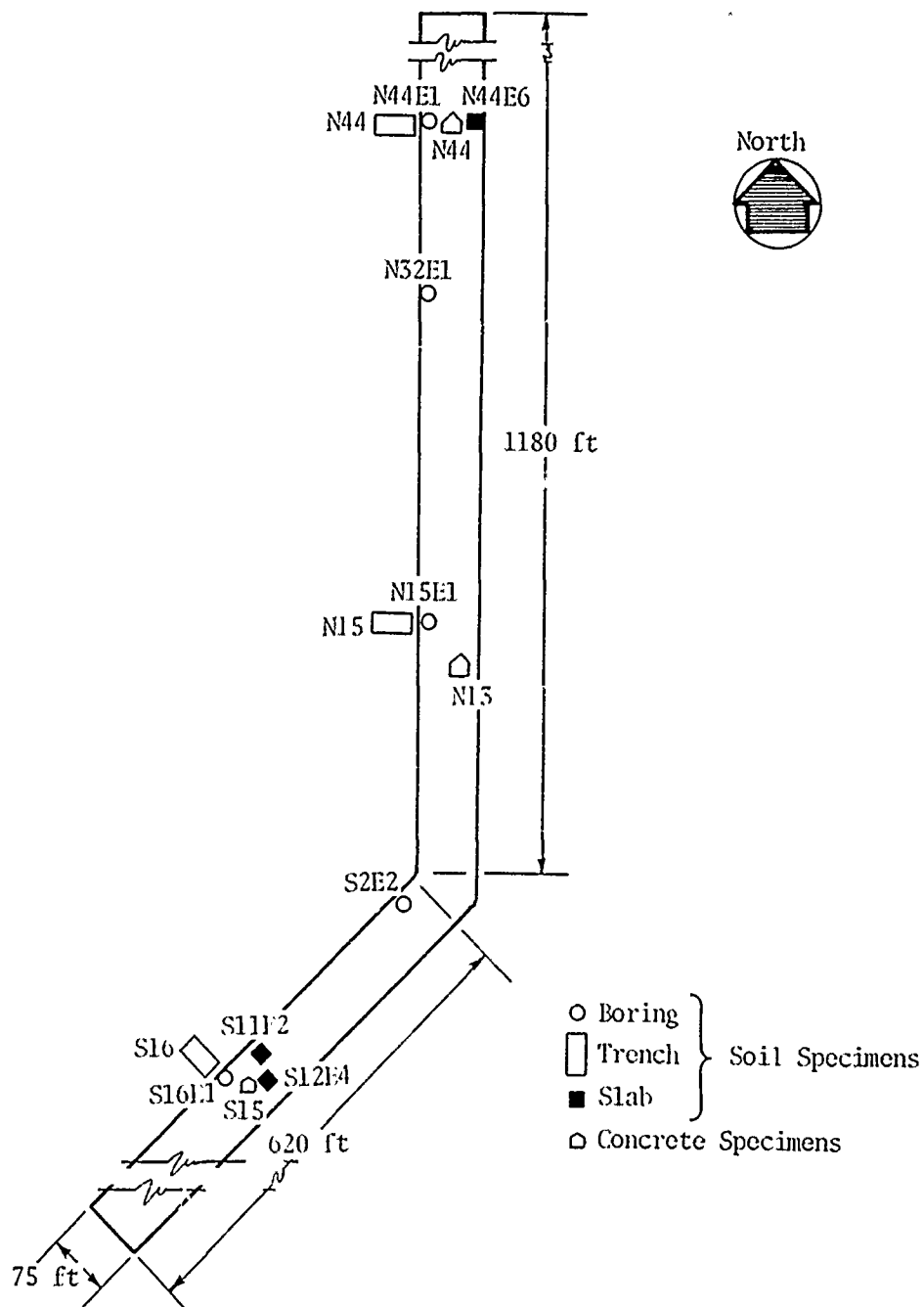


Figure 62. Location of Borings (Fort Sumner)

Table XIII

## SOIL TEST DATA (FORT SUMNER)

Depth, ft	Unified Classification	$\gamma_d$ , pcf	N/ft	$G_s$	Moisture Content, %	
					20	40
Station S11E2--Under Slab						
1	SM-SC			2.63	□ ○	
Station S12E4--Under Slab						
1	SM-SC			2.66	△ □ ○	
2					□	
3		111			□	
4						
5		109			□	
Station N44E6--Under Slab						
1	SM-SC			2.61	□ △ ○	
2					□	
3		96			□	
4						
5		108			□	
Station S16--Trench						
1						
2						
3	SC	101		2.66	△ □ ○	
4						
5	SM	105		2.67	□ △ ○	
6						
7						
8	SM	105		2.69	□	NP
9						
10	SP-SM	121		2.66	□	NP
11						

○ Liquid Limit (LL) △ Plastic Limit (PL) □ Natural Moisture Content (w)

Table XIII (Cont'd)

Depth, ft	Unified Classification	$\gamma_d$ , pcf	N/ft	$G_s$	Moisture Content, %	
					20	40
Station S16--Trench (Continued)						
13	SW-SM	110		2.66	□	NP
14						
15	CH	114		2.67	△	○
Station N15--Trench						
1						
2						
3	SC	90		2.64	□	△
4						
5	SM-SC	102		2.65	□	△
6						
7						
8	SM	109		2.68	□	NP
9						
10	SM	107		2.65	□	NP
11						
12						
13	SP-SM	115		2.66	□	NP
14						
15	SW	131		2.68	□	NP
Station N44--Trench						
1						
2						
3	SC	93		2.68	□	△
4						
5	SM-SC	116		2.74	□	△
6						

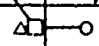
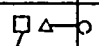
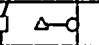
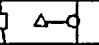


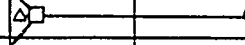
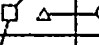


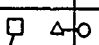
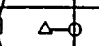
○ Liquid Limit (LL)    △ Plastic Limit (PL)    □ Natural Moisture Content (w)

Table XIII (Cont'd)

Depth, ft	Unified Classification	$\gamma_d$ , pcf	N/ft	$G_s$	Moisture Content, %	
					20	40
Station N44--Trench (Continued)						
8	SM	108		2.70	□	NP
9						
10	SP-SM	107		2.62	□	NP
11						
12						
13	SW	125		2.67	□	NP
14						
15	CL	113		2.72	△	○
Station S16E1--Boring 1						
1						
2	SC	127	23		△	○
3	SM-SC	99	8		△	○
4						
5	SC	102	6		□	○
6						
7						
8	SP	103	19		□	NP
9						
10	SW	113	28		□	NP
11						
12						
13	CL-CH	99	17		△	○
14						
15	CL	113	23		□	○
16						
17						
18	SC	122	18		△	○

○ Liquid Limit (LL) △ Plastic Limit (PL) □ Natural Moisture Content (w)

Table XIII (Cont'd)

Depth, ft	Unified Classification	$\gamma_d$ , pcf	N/ft	$G_s$	Moisture Content, %	
					20	40
Station S16E1--Boring 1 (Continued)						
20	CL	106		20		
Station S2E2--Boring 2						
1	SM-SC	124	13	2.65		
2						
3	SM-SC	97	6	2.74		
4						
5	SM-SC	107	10			
6						
7						
8	SM-SC	102	9			
9						
10	SP-SM	102	41			NP
11						
12						
13	CH	107	21			
14						
15	SC	119	17	2.62		
16						
17						
18	SM-SC	114	19			NP
19						
20	SP	105	17			NP
Station N15E1--Boring 3						
1	SM-SC	116	14			
2						
3	SC	112	7			

○ Liquid Limit (LL) △ Plastic Limit (PL) □ Natural Moisture Content (w)

Table XIII (Cont'd)

Depth, ft	Unified Classification	$\gamma_d$ , pcf	N/ft	$G_s$	Moisture Content,	
					20	40
Station N15E1--Boring 3 (Continued)						
5	ML-CL	117	12			
6						
7						
8	CL	114	12			
9						
10	SP	106	16			
11						
12	SP-SW	106	48			
13						
14						
15	SW	118	50			
16						
17	ML	122	18			
18						
19						
20	SM	94	14			
Station N32E1--Boring 4						
1	CL	110	10			
2						
3	CL	105	9			
4						
5	SM	110	9			
6						
7	SM	113	10			
8						
9						
10	SP-SW	114	40	2.65		

○ Liquid Limit (LL)    △ Plastic Limit (PL)    □ Natural Moisture Content (w)



Table XIII (Cont'd)

Depth, ft	Unified Classification	$\gamma_d$ , pcf	N/ft	$G_s$	Moisture Content, %	
					20	40
Station N32E1--Boring 4 (Continued)						
12						
13	SP	106	49	2.65	□	
14						
15						
16	SW	116	38		□	
17						
18	SM	109	18		□	
19						
20	CL-MI.	95	16		□	
Station N44E1--Boring 5						
1						
2	CL	113	40	2.74	□	
3	CL	102	15		□	
4						
5						
6	CL-ML	99	11	2.71	□	
7						
8	CL	103	16	2.65	□	
9						
10						
11	SP	117	53		□	
12						
13	SW	110	66		□	
14						
15	CL-CH	117	36			□
16						

○ Liquid Limit (LL)    △ Plastic Limit (PL)    □ Natural Moisture Content (w)

Table XIII (Concl'd)

[illegible]

- Liquid Limit (LL)  $\Delta$  Plastic Limit (PL)  $\square$  Natural Moisture Content (w)

Table XIV  
CONCRETE TEST DATA (FORT SUMNER)

Sample	Station	Density ( $\rho_c$ ), pcf	Sonic Velocity (c), fps	Compressive Strength ( $f'_c$ ), psi	Modulus of Elasticity ( $E_c$ ), psi **
1	S 15 E1*	150.66	13,500	5,966	4,713,617
2	S 15 E3	148.36	14,220	10,027	5,909,722
3	S 15 E5	149.12	14,030	9,470	5,847,650
4	S 15 E7*	149.75	14,550	7,242	5,144,201
Average		148.74	14,125	9,749	5,878,686
5	N 13 E1*	152.95	14,080	6,119	4,876,258
6	N 13 E2	154.35	15,100	11,317	6,731,460
7	N 13 E4	153.60	15,700	11,615	6,769,626
8	N 13 E6	151.28	15,080	11,618	6,619,093
Average		153.07	15,293	11,517	6,706,726
9	N 44 E1*	149.61	13,110	9,271	5,814,349
10	N 44 E3	149.56	15,290	10,823	6,280,655
11	N 44 E5	150.51	14,500	8,754	5,701,032
12	N 44 E7*	150.48	14,550	10,663	6,286,985
Average		150.18	14,780	10,081	6,089,558

\* Since pads E1 and E7 (fig. 2) were not tested with C-4 charges, these results were not used to obtain the average numbers given in this table.

\*\*  $E_c = 33 \rho_c^{1.5} \sqrt{f'_c}$ .

## APPENDIX II

### HAYS SUBSURFACE EXPLORATION DATA

Laboratory tests were conducted on soil and concrete samples from the test site in order to analyze the pavement crater data from the full-scale field tests at Hays. Figure 63 shows the locations on the test section from which the samples were taken. In addition to these tests, in-place densities were obtained from the crater wall, the thrown-out material, and the fallback material of some of the bomb craters.

#### 1. SOIL TESTING

The samples were furnished in Shelby tubes. The results of these soil tests are given in table XV.

Table XVI summarizes the in-place densities taken from the crater wall, the thrown-out material, and the fallback material of some of the MK-81, MK-82, and M-117 bomb craters. Either sand cone or balloon density tests were conducted.

#### 2. CONCRETE TESTING

Concrete specimens were received from three stations at the test site. Cylinders, 4 in. in diameter and approximately 8 in. long, were core drilled from the specimens. Each cylinder was milled down to approximately 7.5 in. The density,  $\rho_c$ , was first determined. Sonic velocity tests were then performed using sonic testing equipment and a 1200-lb compression load to obtain good contact at the ends. Uniaxial compression tests were performed on these cylinders to determine the ultimate compressive strength of the concrete,  $f'_c$ , from which the modulus of elasticity,  $E_c$  was computed (ref. 12). These test data are given in table XVII.

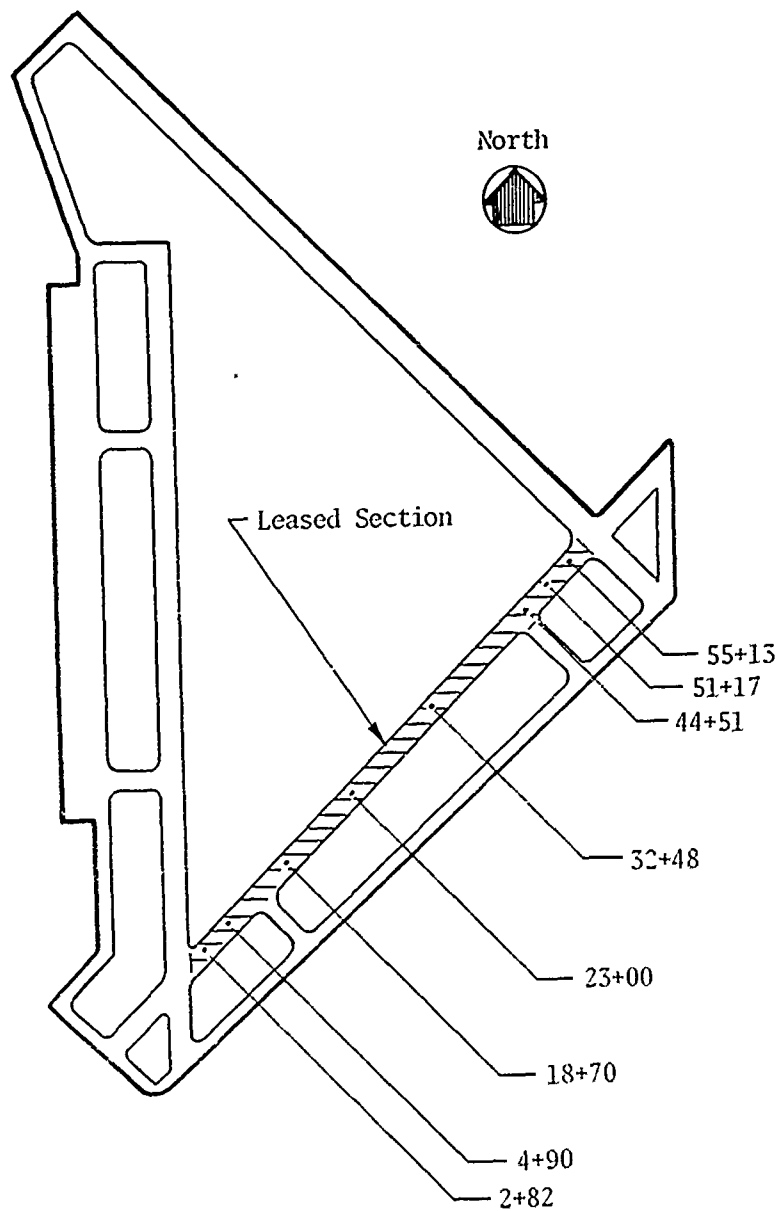




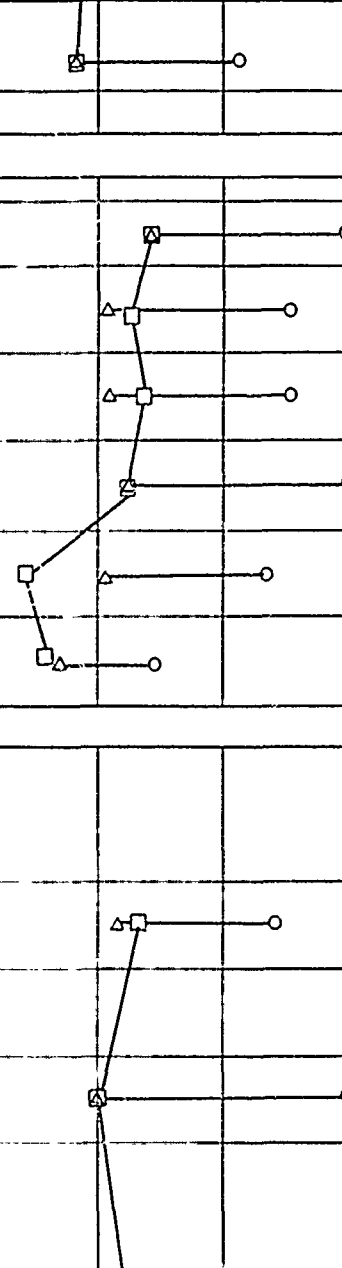
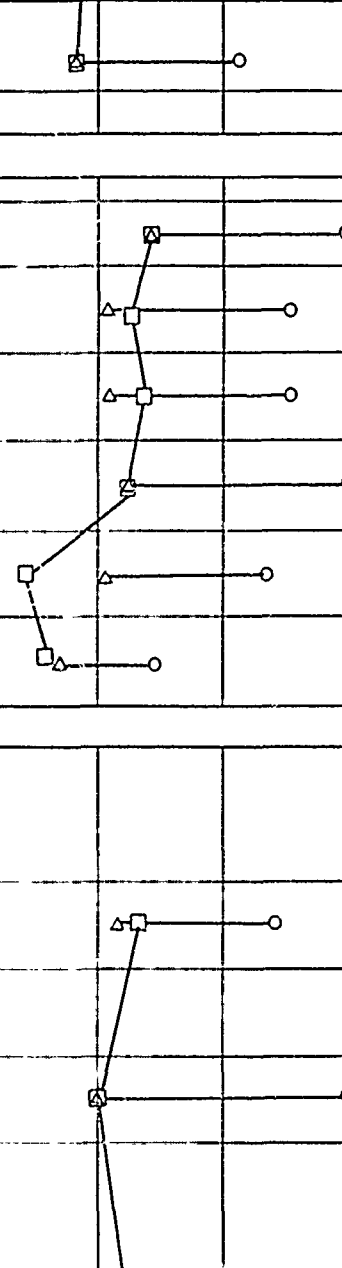
Figure 63. Location of Borings (Hays)

Table XV  
SOIL TEST DATA (HAYS)

Depth, ft	Unified Classification	$\gamma_d$ , pcf	N/ft	$G_s$	Moisture Content, %		
					20	40	
Station 2+82							
1							
2							
3	CH	98		2.63			
4							
5	CL	98		2.69			
6							
7	CH	113		2.72			
Station 4+90							
1							
2	CH	95		2.72			
3							
4	CL	104		2.69			
5							
6	CL	103		2.74			
7							
8	CH	105		2.73			
Station 18+70							
1							
2	CH	96		2.68			
3							
4	CH	103		2.69			
5							
6							
7	CH	98		2.70			
8							
9	CL	109		2.67			
10							
11							

○ Liquid Limit (LL) △ Plastic Limit (PL) □ Natural Moisture Content (w)

Table XV (Cont'd)

Depth, ft	Unified Classification	$\gamma_d$ , pcf	N/ft	$G_s$	Moisture Content, %	
					20	40
Station 18+70 (Continued)						
13	CL	116		2.67		
14						
Station 23+00						
1	CH	98		2.66		
2						
3	CL	100		2.66		
4						
5	CL	96		2.69		
6						
7	CH	99		2.66		
8						
9	CL	120		2.70		
10						
11	CL	112		2.73		
Station 32+48						
1						
2						
3						
4	CL	96		2.71		
5						
6						
7						
8	CH	111		2.68		
9						
10						
11						

○ Liquid Limit (LL)    △ Plastic Limit (PL)    □ Natural Moisture Content (w)








Table XV (Cont'd)

Depth, ft	Unified Classification	$\gamma_d$ , pcf	N/ft	$G_s$	Moisture Content, %	
					20	40
Station 32+48 (Continued)						
13	SW					
14	CH	102		2.68		
15						
16						
17						
18	CH	111		2.76		
Station 44+51						
1						
2						
3						
4						
5	CL	99		2.73		
6						
7						
8						
9	CL	103		2.70		
10						
11						
12						
13	CI	117		2.71		
14						
15						
16						
17						
18						
19	SW	112		2.65		
20						

○ Liquid Limit (LL)    Δ Plastic Limit (PL)    □ Natural Moisture Content (w)



Table XV (Concl'd)

Depth, ft	Unified Classification	$\gamma_d$ , pcf	N/ft	$G_s$	Moisture Content, %		
					20	40	
Station 51+17							
1							
2							
3	CH	99		2.69			
4							
5	CH	100		2.69			
6							
7	CH	95		2.68			
Station 55+13							
	CH	104		2.63			
2							
3	CL	99		2.68			
4							
5	CL	98		2.66			
6							
7	CH	98		2.64			
8							

○ Liquid Limit (LL) △ Plastic Limit (PL) □ Natural Moisture Content (w)

Table XVI

## SUMMARY OF IN-PLACE DENSITY TESTS (HAYS)

Shot	Depth-of-Burst, ft	Cylinder	Type of Density Test	Density, pcf	Comments
MK-81					
75	10	1	Sand Cone	123.14*	Ejecta
		2		114.89	
		3		105.61	
		4		110.61	
		5		107.37	
		6		116.76	
		7		111.81	Fallback
		8		109.10	
		9		112.36	
		10		120.95	
		11		110.03	
		12		120.86	
		13		131.09	
		14		107.08	Apparent Crater wall
		15		121.42	
		16		119.32	
MK-82					
81	18	1	Sand Cone	118.37	Fallback
		2		105.87	
		3		107.54	
		4		87.40	
		5		118.91*	
		6		123.16*	
		7		115.27*	
84	12	1	Sand Cone	121.80	Fallback
		2		115.32	
		3		108.81	
		4		120.18	
		5		87.23	
		6		114.26	Ejecta
		7		106.03	
		8		114.10	
		9		104.50	
		10		111.04	
		11		98.00	Crater wall
		12		127.81	
M-117					
90	15	1	Sand Cone	123.63	Crater wall
		2		124.22	
		3		126.90	
		4		120.64	
		5		122.42	
		6	121.24	Balloon	
		7	128.52		
		8	122.89		
		9	131.06		

\*Large chunk inside crater.

Table XVI (Concl'd)

Shot	Depth-of-Burst, ft	Cylinder	Type of Density Test	Density, pcf	Comments
M-117 (Continued)					
91	12	1	Sand Cone	91.22	Fallback
		2		115.49	
		3		110.49	
		4		120.17	
		5		96.50	
		6		128.20*	
		7		111.74*	
		8		118.94*	
92	15	1	Sand Cone	88.94	Fallback
		2		91.04	
		3		95.36	
		4		114.89	
		5		96.05	
		6		91.15	
		7		94.10	
		8		112.23	
		9		90.98	
		10		109.30	
		11		117.84	
		12		120.49	
		13		121.81	
		14		119.10	
93	18	1	Sand Cone	107.85	Fallback
		2		107.69	
		3		115.82	
		4		120.18	
		5		113.78	
		6		122.85*	
		7		114.00	
		8		120.39	
		9		119.54	
		10		115.86	
		11		118.32	
		12		117.69	
		13	Balloon	119.50	
		14		118.40*	
95	21	1	Sand Cone	95.19	Fallback
		2		126.63	
		3		92.62	
		4	Balloon	105.20	
		5		104.40	
		6		118.50	

\* Large chunk inside crater.

Table XVII  
CONCRETE TEST DATA (HAYS)

Sample	Station	Density ( $\rho_c$ ), pcf	Sonic Velocity (c), fps	Compressive Strength (f'), psi	Modulus of Elasticity ( $E_c$ ),*
1	5+00	145.92	17,539	9,168	5,567,460
2		145.41	17,488	8,817	5,435,054
3		147.43	17,586	8,356	5,396,640
4		150.19	19,195	12,892	6,898,074
Average		147.24	17,952	9,808	5,824,307
1	28+00	147.49	17,762	8,611	5,484,490
2		147.14	18,316	10,186	5,941,698
3		149.37	18,955	10,465	6,164,308
Average		148.00	18,344	9,754	5,863,499
1	52+00	146.05	18,077	9,768	5,756,539
2		147.31	17,584	11,937	6,446,574
Average		146.68	17,830	10,853	6,101,557

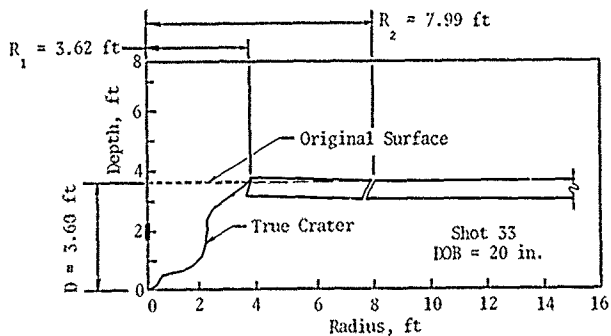
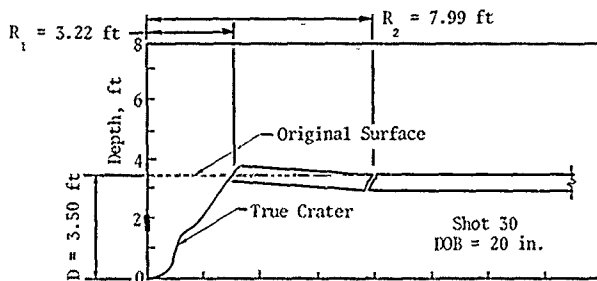
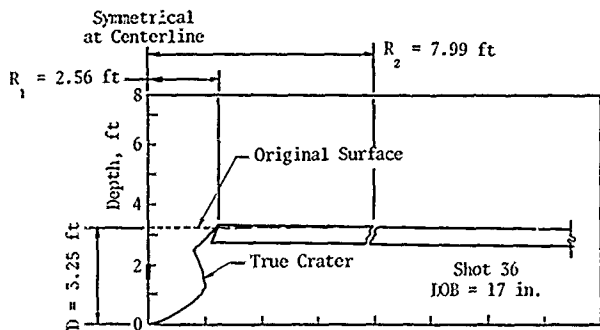
$$* E_c = 33 \rho_c^{1.5} \sqrt{f'_c}$$

APPENDIX III  
FORT SUMNER CRATER DATA

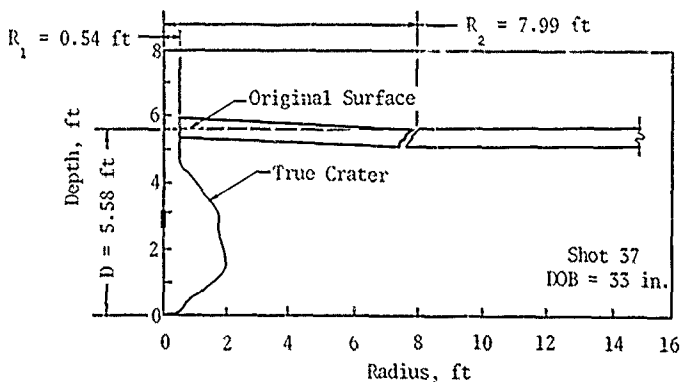
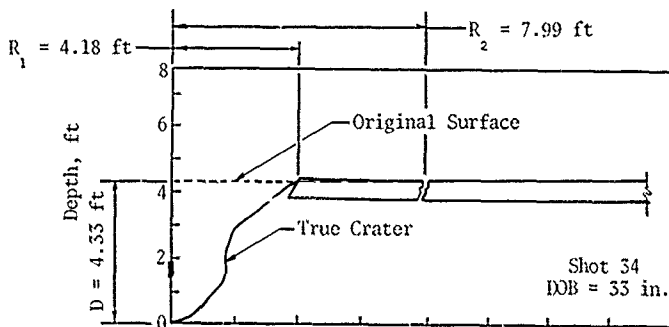
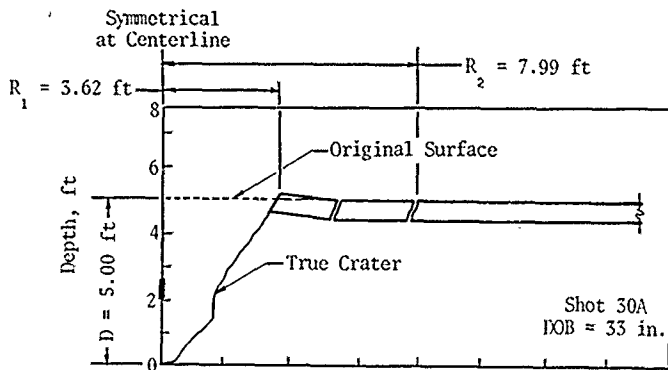
	<u>Page</u>
5-1b Charge, 7-Inch-Thick Concrete	120
15-1b Charge, 7-Inch-Thick Concrete	124
25-1b Charge, 7-Inch-Thick Concrete	130

### DAMAGE QUANTITIES FOR C-4 CHARGES (FORT SUMNER)

[illegible]<sup>a</sup> Data from various sources are plotted.

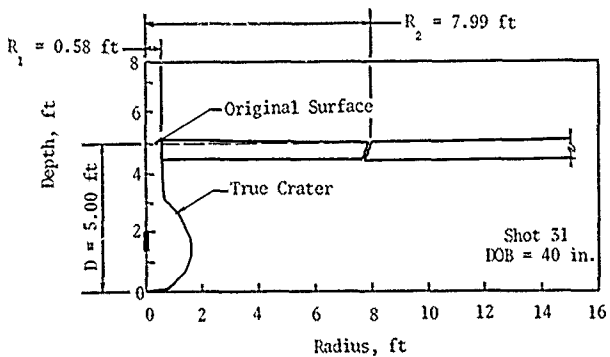
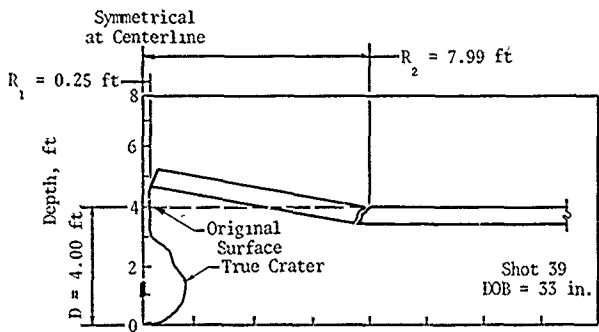


5-lb Charge, 7-Inch-Thick Concrete

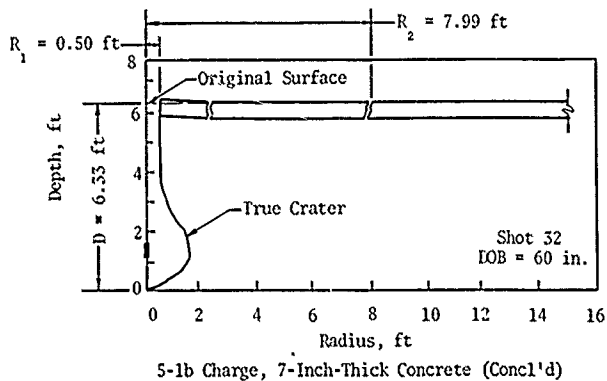
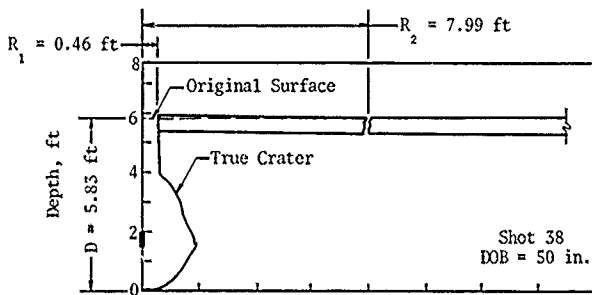
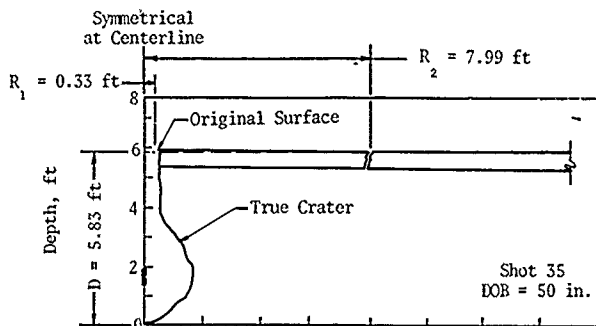


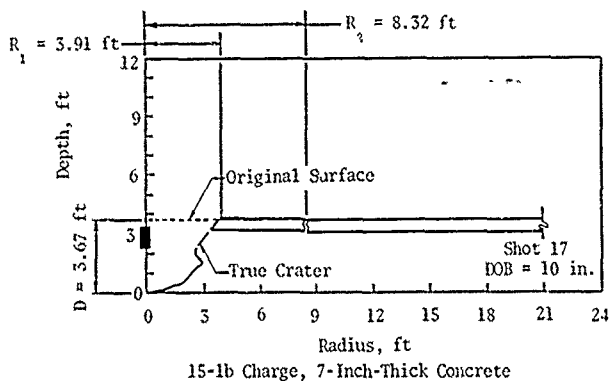
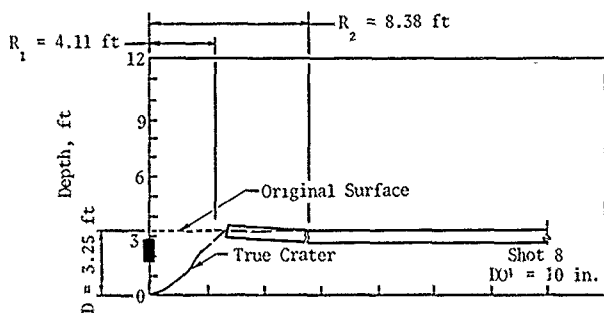
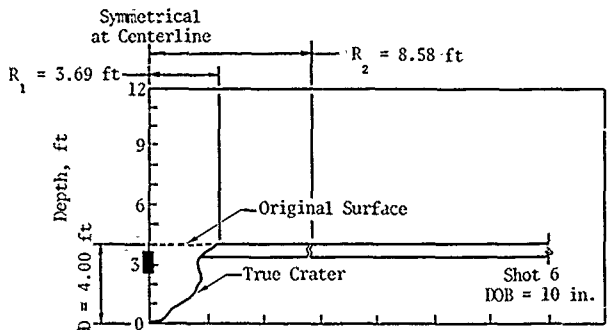
5-lb Charge, 7-Inch-Thick Concrete (Cont'd)

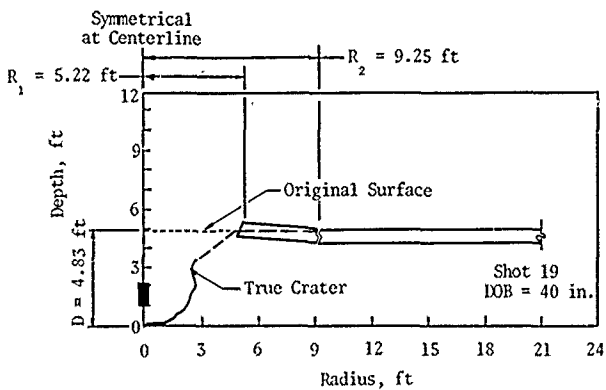




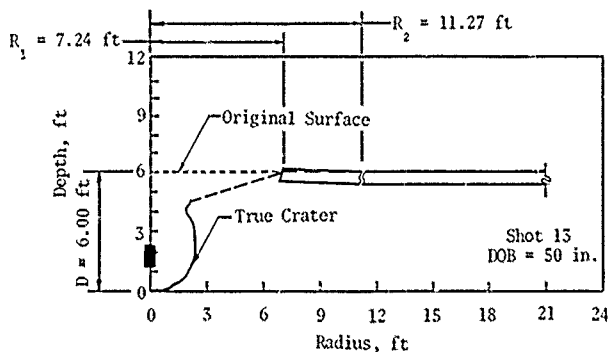
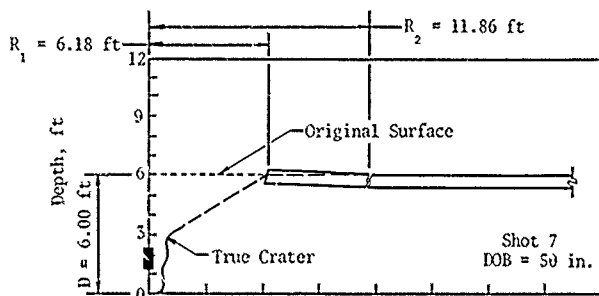
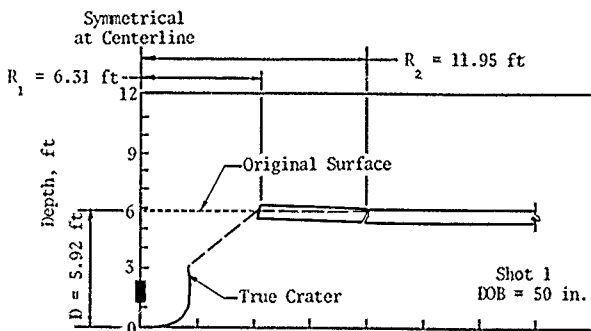
5-lb Charge, 7-Inch-Thick Concrete (Cont'd)



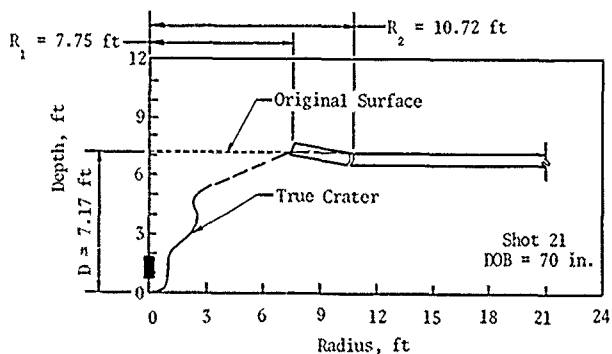
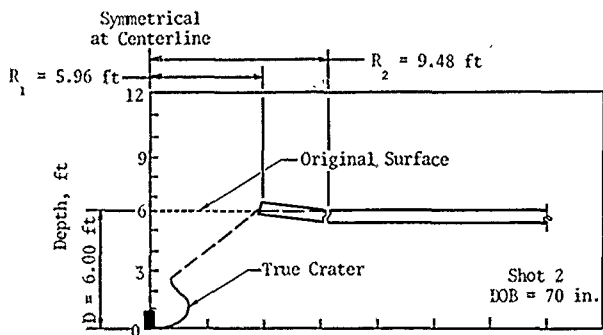




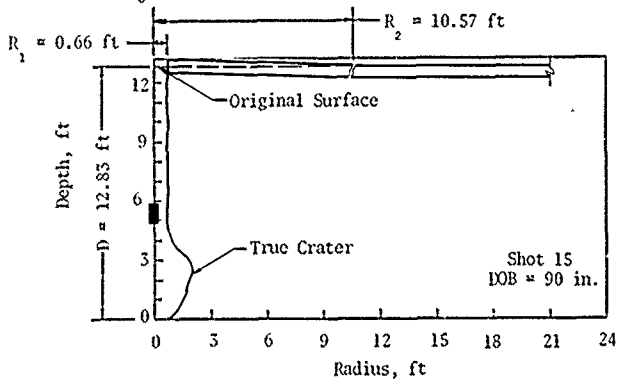
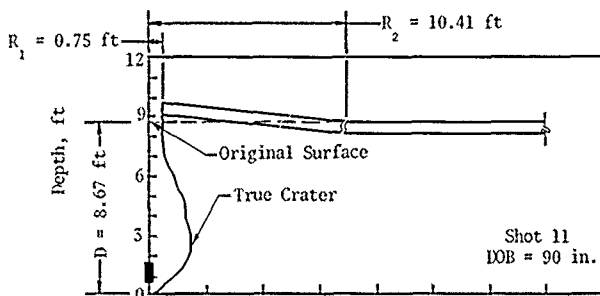
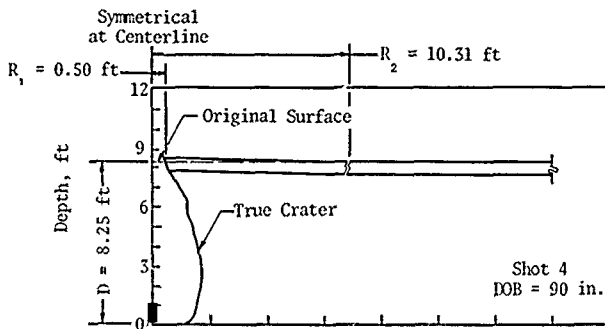
15-lb Charge, 7-Inch-Thick Concrete (Cont'd)



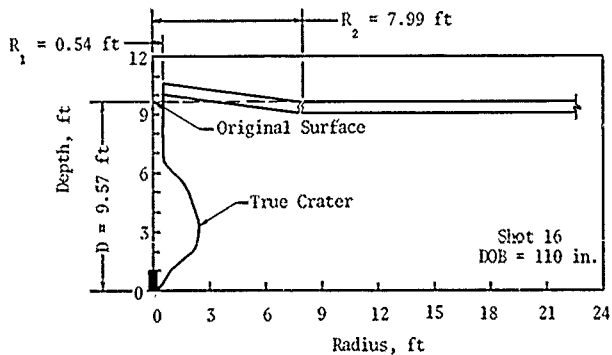
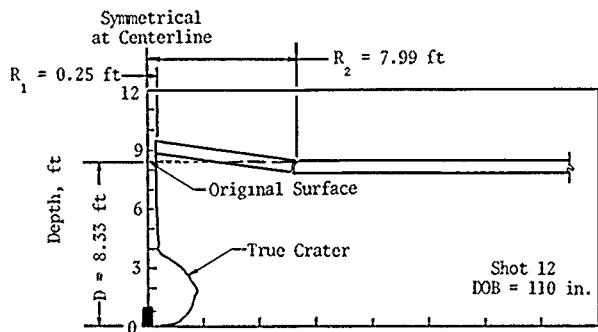
15-lb Charge, 7-Inch-Thick Concrete (Cont'd)



15-lb Charge, 7-Inch-Thick Concrete (Cont'd)

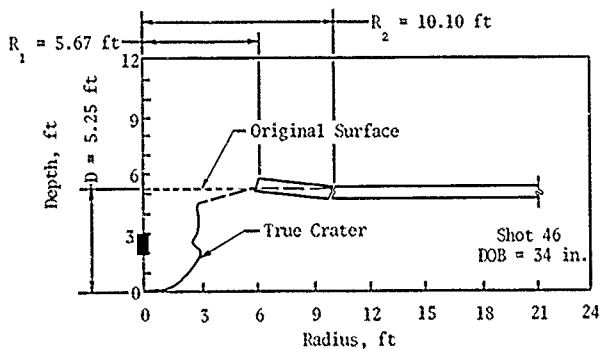
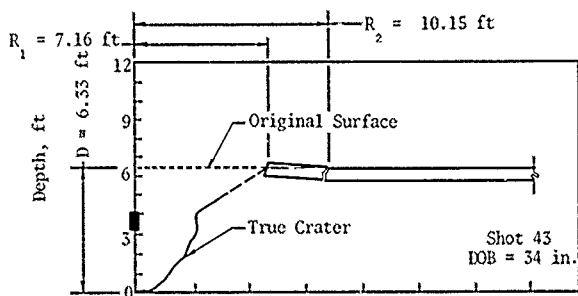
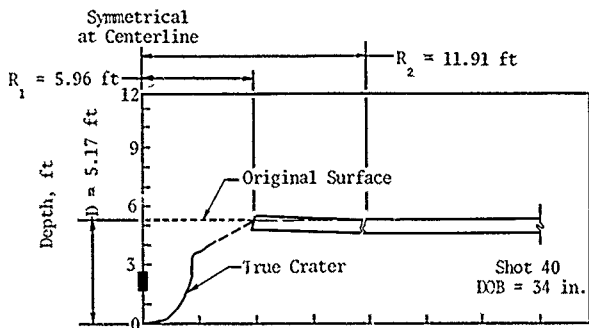


15-lb Charge, 7-Inch-Thick Concrete (Cont'd)

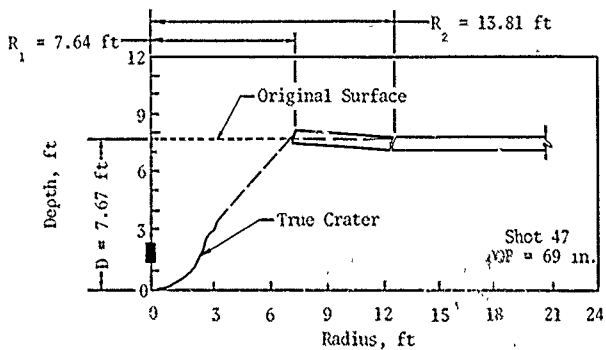
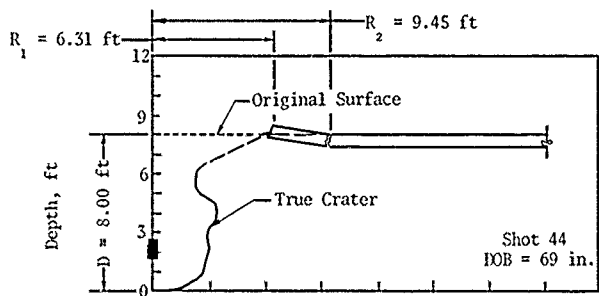
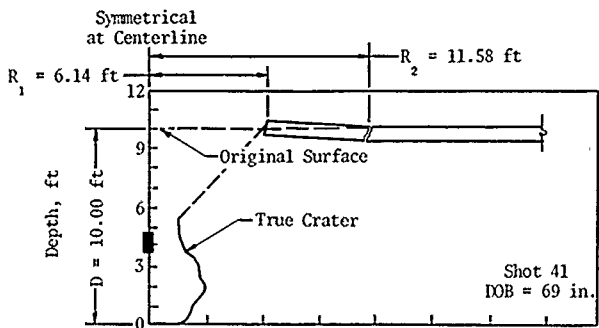


15-lb Charge, 7-Inch-Thick Concrete (Concl'd)





25-lb Charge, 7-Inch-Thick Concrete



25-lb Charge, 7-Inch-Thick Concrete (Concl'd)

APPENDIX IV  
HAYS CRATER DATA

	<u>Page</u>
5-1b Charge, 8-Inch-Thick Concrete	134
5-1b Charge, 11-Inch-Thick Concrete	141
15-1b Charge, 8-Inch-Thick Concrete	143
15-1b Charge, 11-Inch-Thick Concrete	149
25-1b Charge, 8-Inch-Thick Concrete	155
MK-81 (250-1b Bomb), 11-Inch-Thick Concrete	158
MK-82 (500-1b Bomb), 11-Inch-Thick Concrete	160
M-117 (750-1b Bomb), 11-Inch-Thick Concrete	162

Table XIX

[illegible]

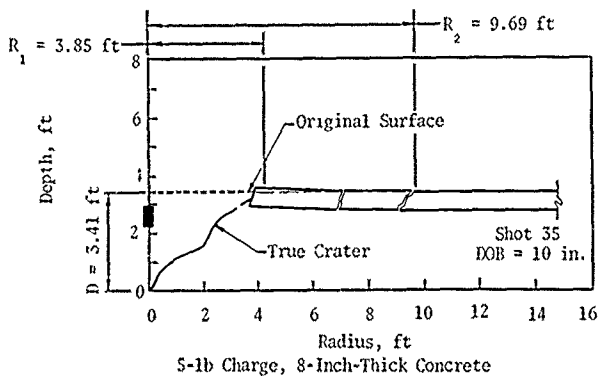
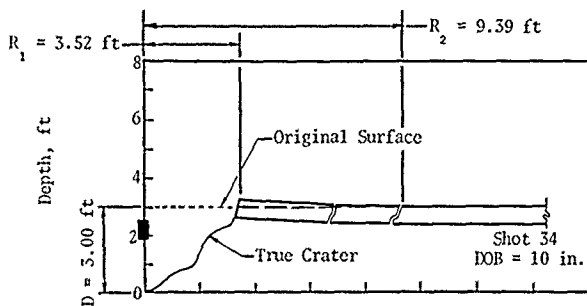
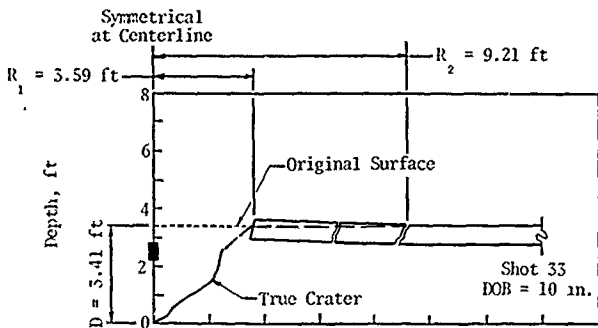
Table XX

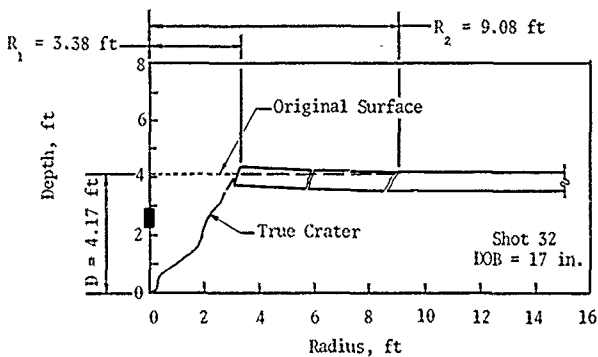
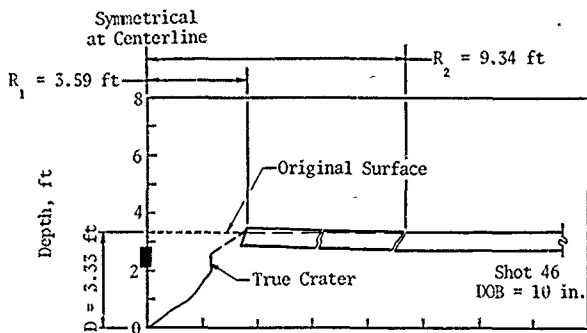
DAMAGE QUANTITIES FOR BOMBS (HAYS)

[illegible]

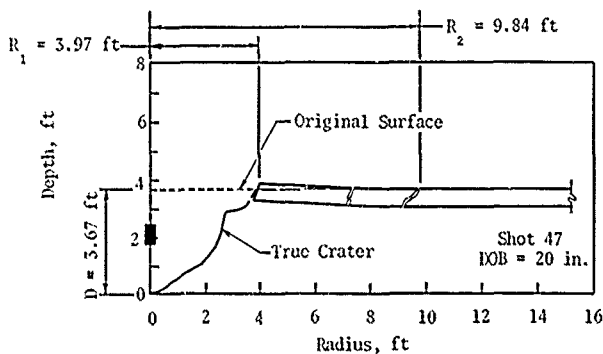
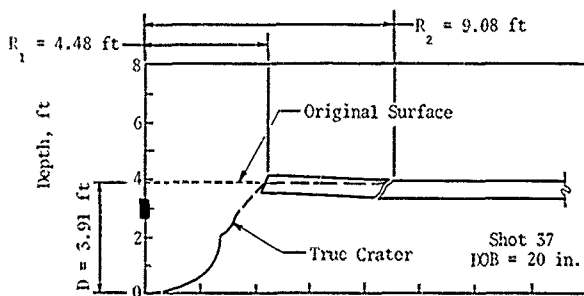
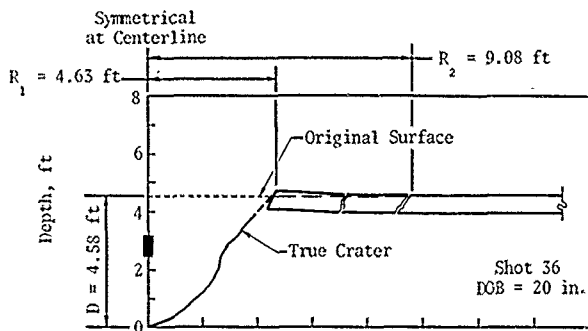
average value of  $\mu$  and (5) of the

<sup>a</sup> = null set; not stated.

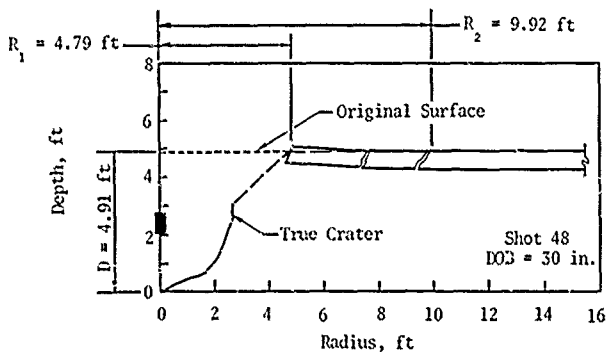
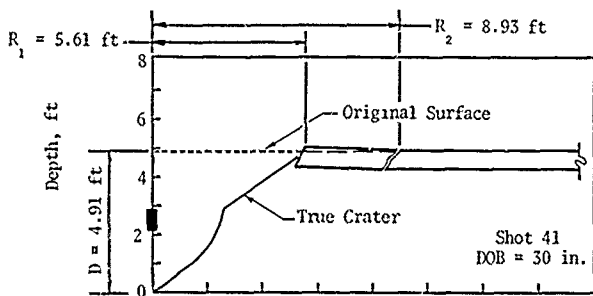
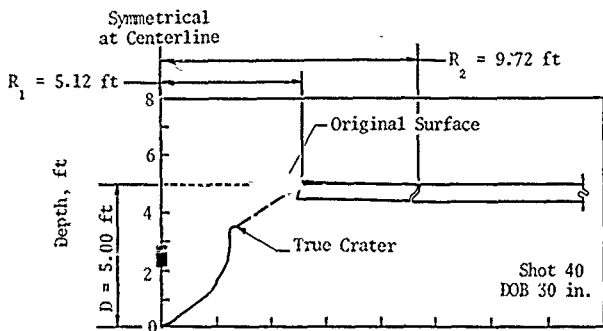




5-lb Charge, 8-Inch-Thick Concrete (Cont'd)

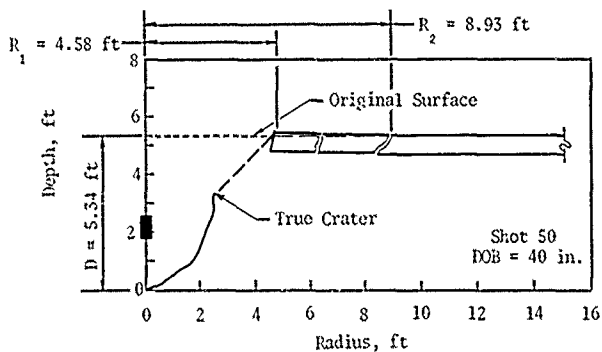
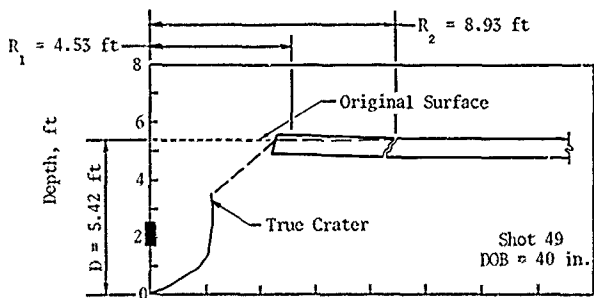
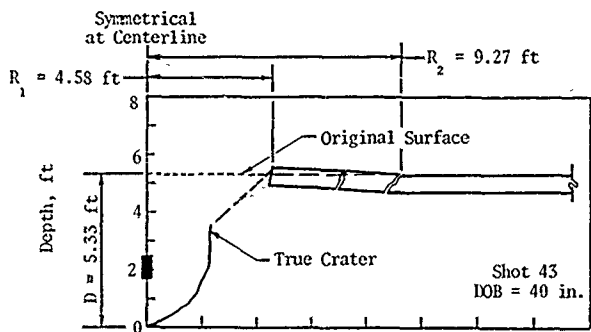


5-lb Charge, 8-Inch-Thick Concrete (Cont'd)

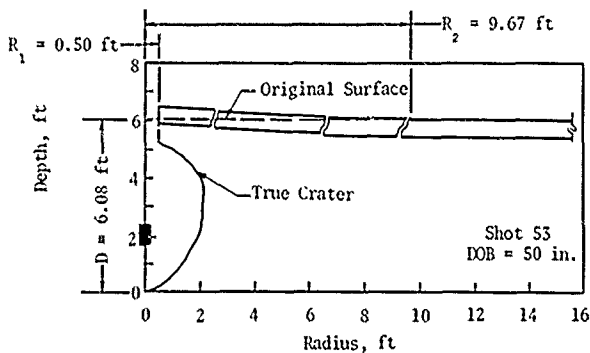
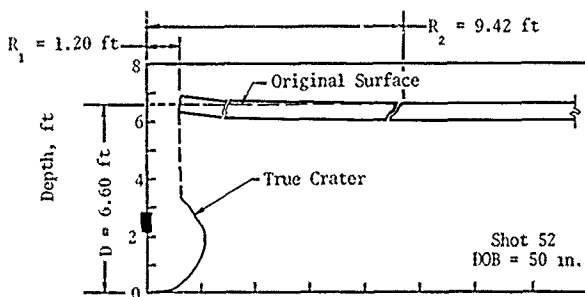
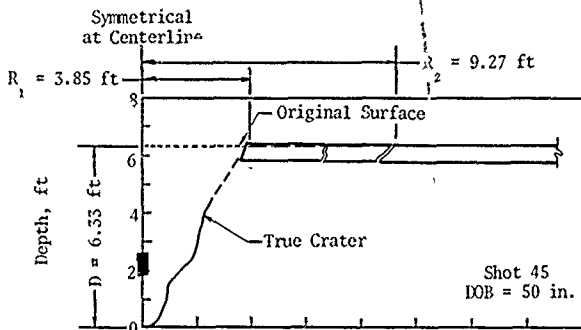


5-lb Charge, 8-Inch-Thick Concrete (Cont'd)

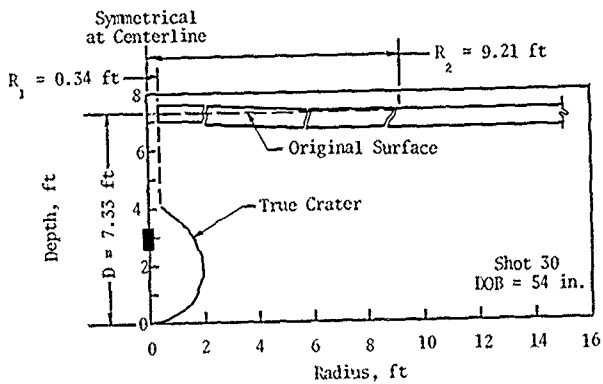




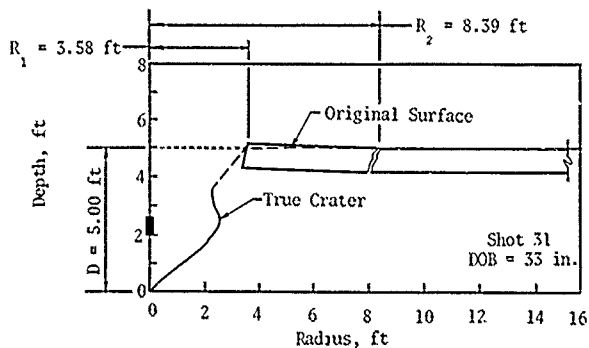
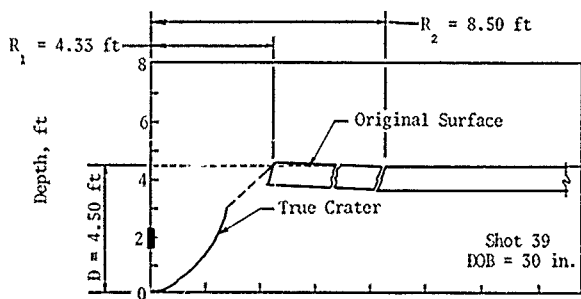
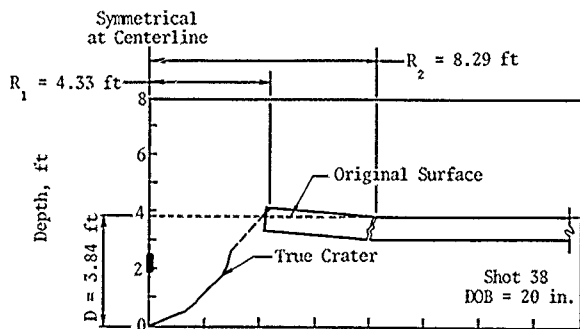
5-lb Charge, 8-Inch-Thick Concrete (Cont'd)



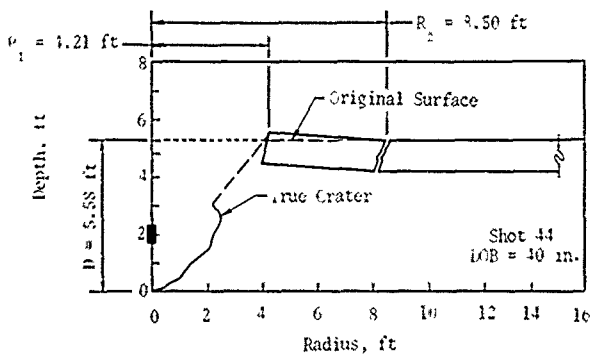
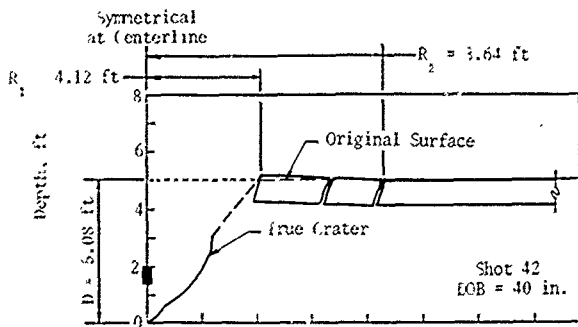
5-lb Charge, 8-Inch-Thick Concrete (Cont'd)



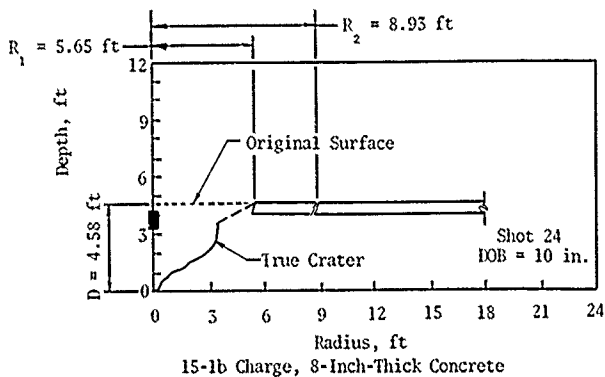
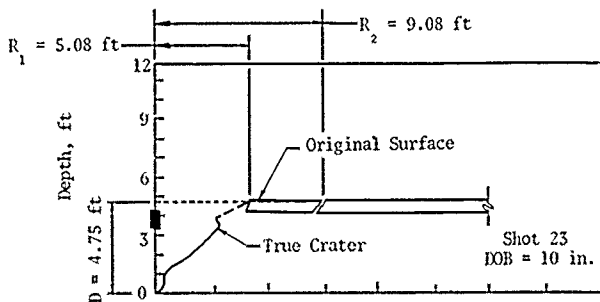
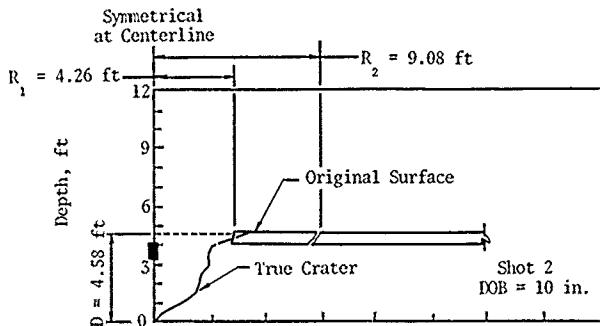
5-1b Charge, 8-Inch-Thick Concrete (Concl'd)

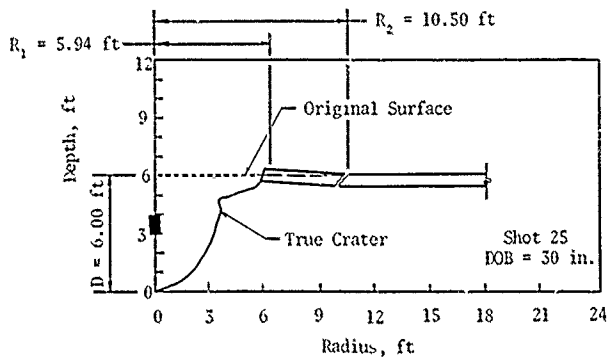
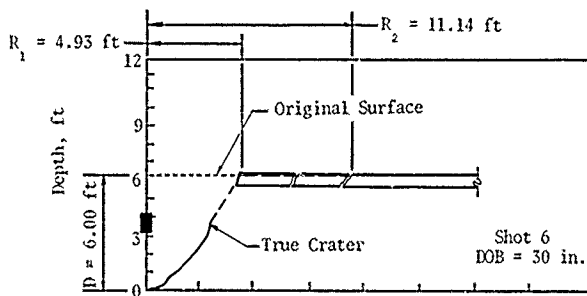
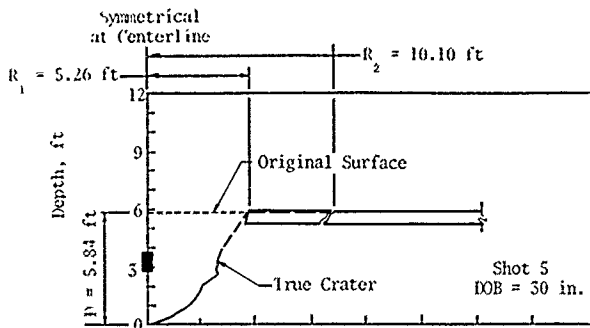


5-lb Charge, 11-Inch-Thick Concrete

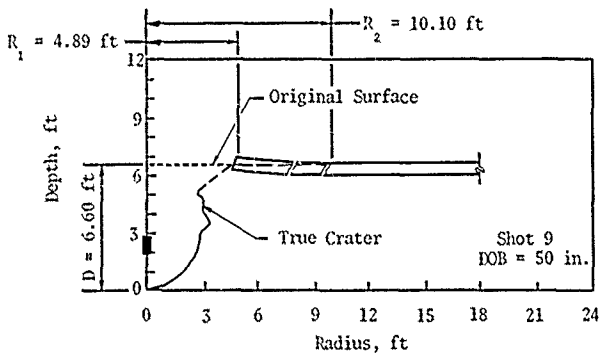
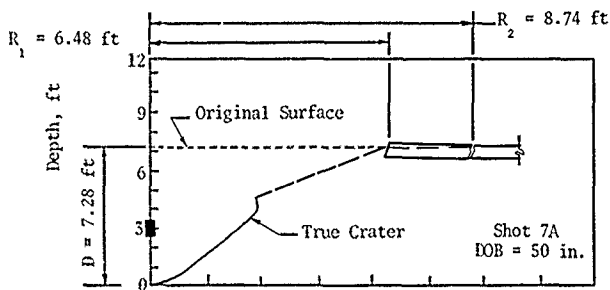
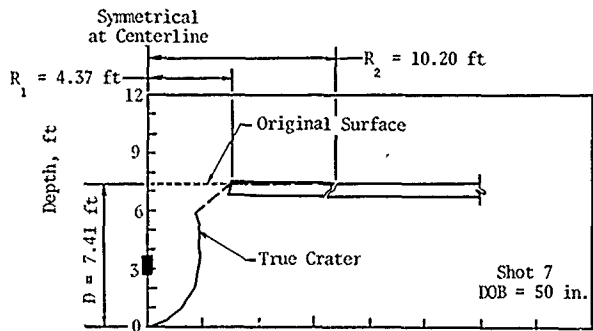


5-lb Charge, 11-Inch-Thick Concrete (Concl'd)



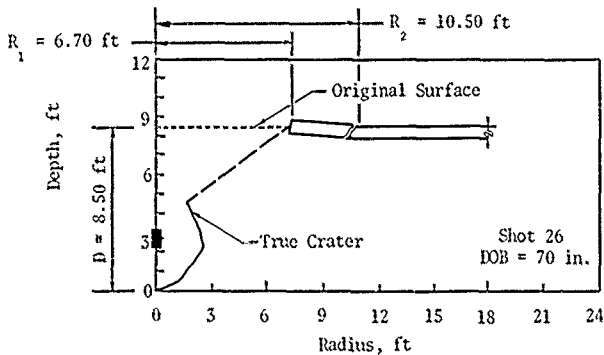
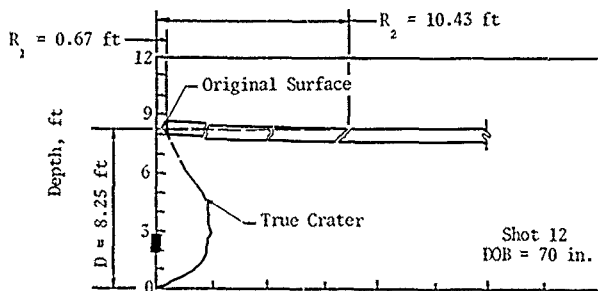
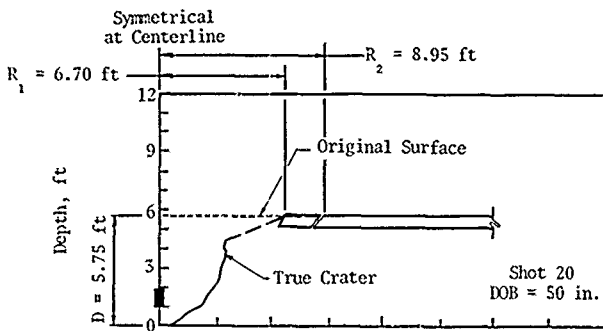


15-lb Charge, 8-Inch-Thick Concrete (Cont'd)

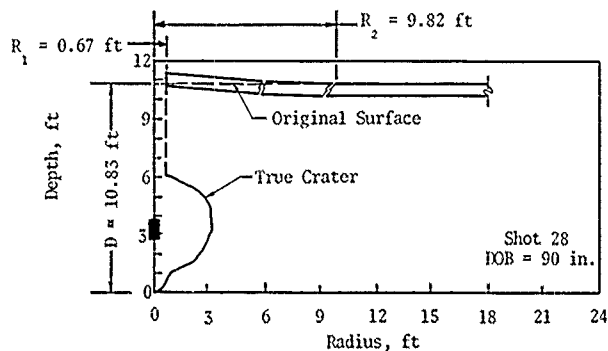
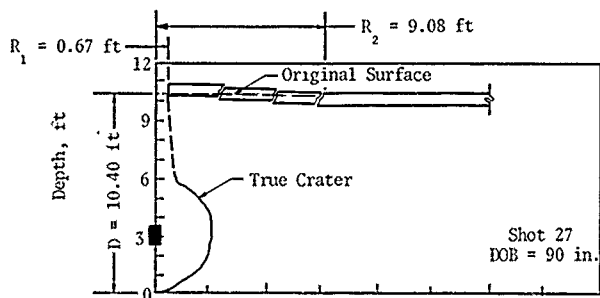
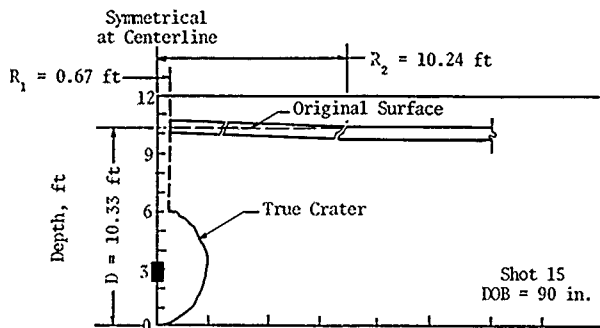


15-lb Charge, 8-Inch-Thick Concrete (Cont'd)

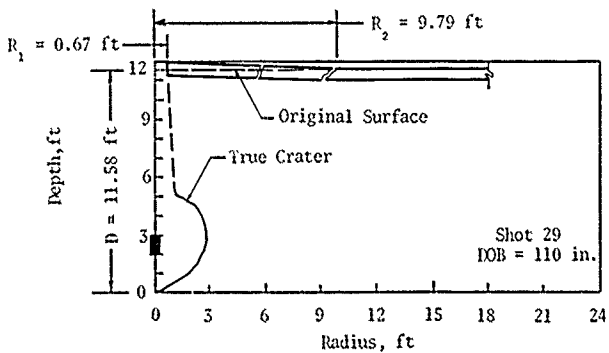
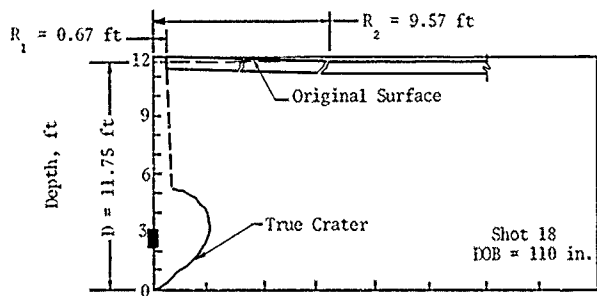
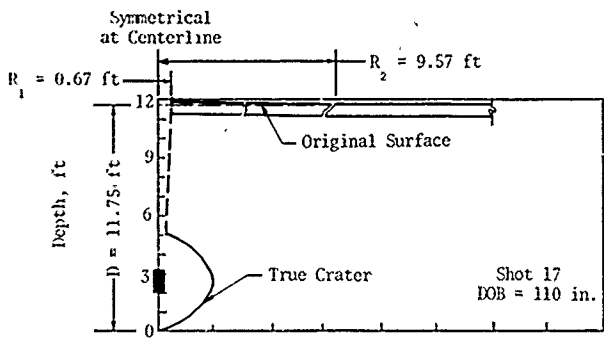




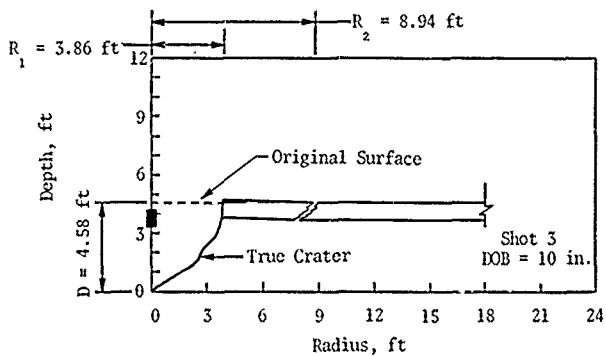
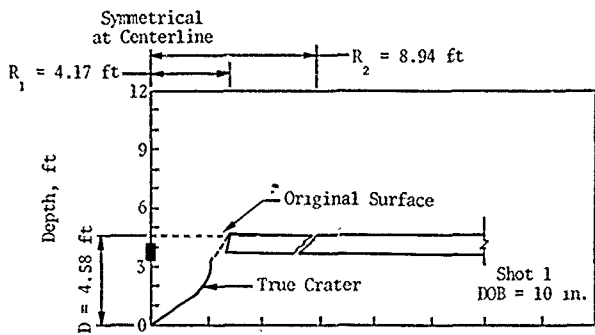
15-lb Charge, 8-Inch-thick Concrete (Cont'd)



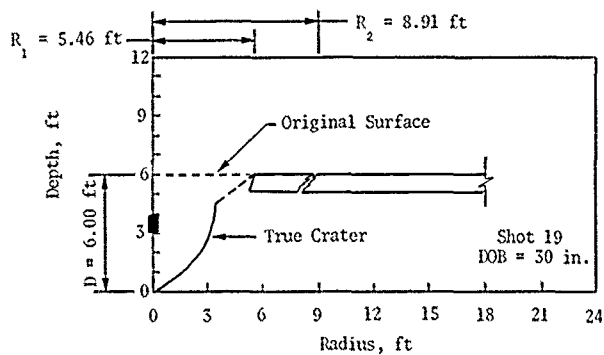
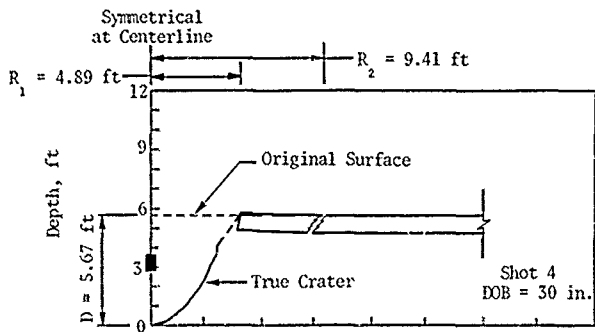
15-lb Charge, 8-Inch-Thick Concrete (Cont'd)



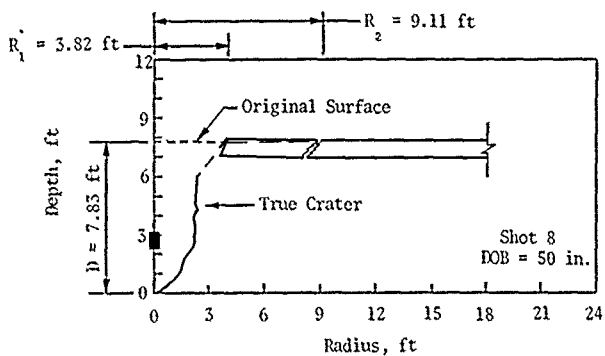
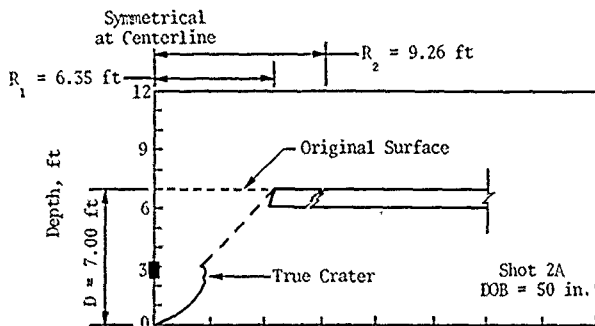
15-lb Charge, 8-Inch-Thick Concrete (Concl'd)



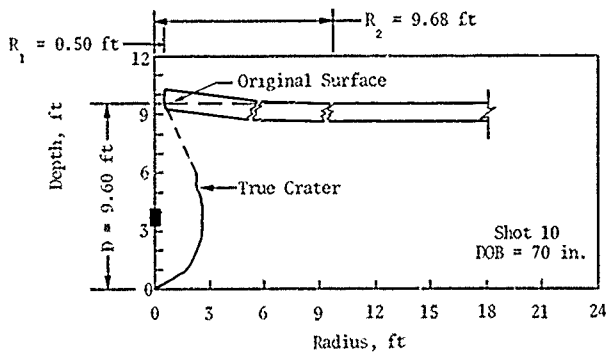
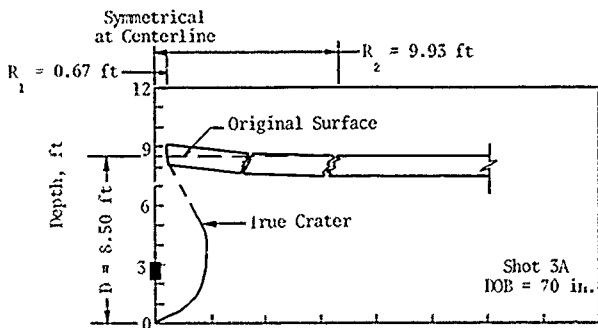
15-lb Charge, 11-Inch-Thick Concrete



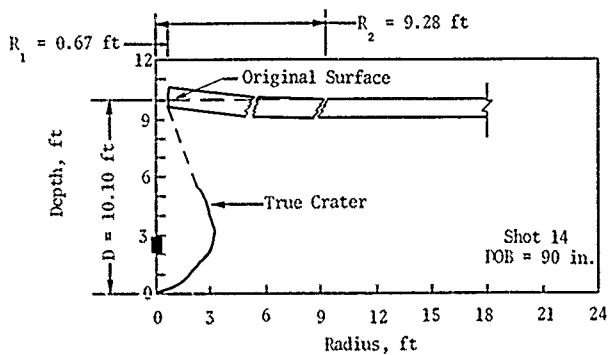
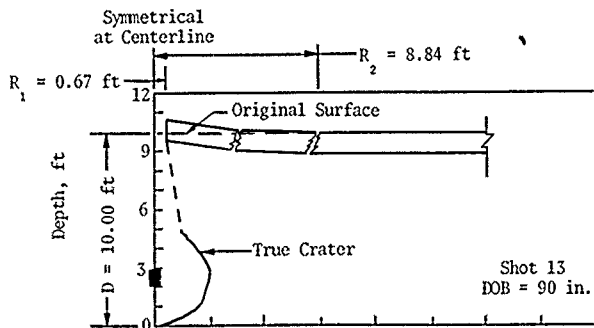
15-lb Charge, 11-Inch-Thick Concrete (Cont'd)



15-lb Charge, 11-Inch-Thick Concrete (Cont'd)

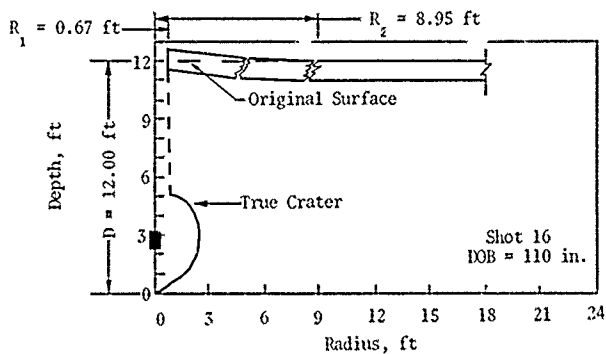
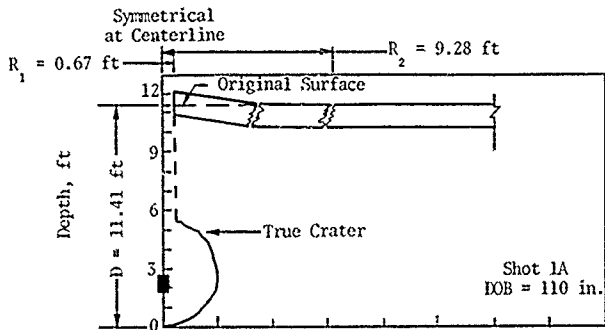


15-lb Charge, 11-Inch-Thick Concrete (Cont'd)

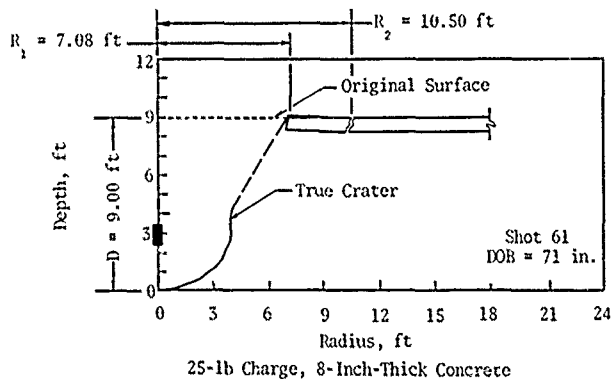
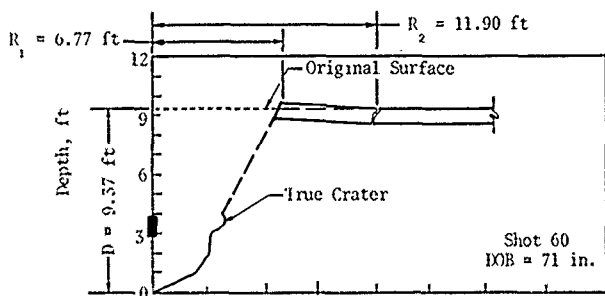
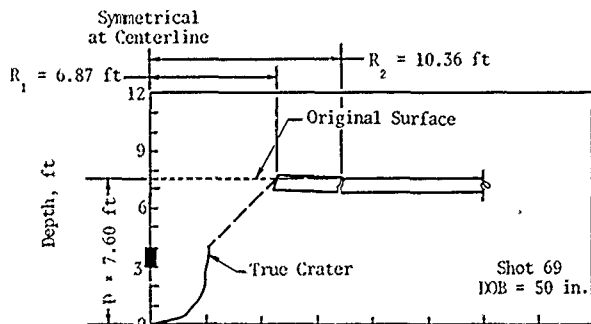


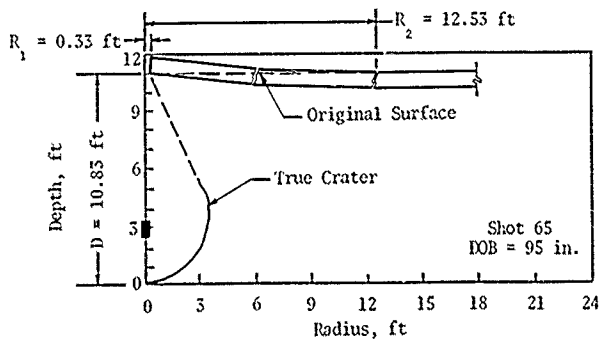
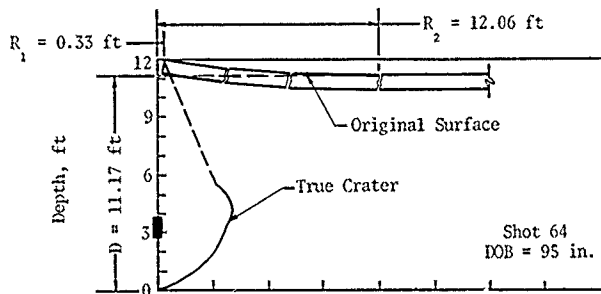
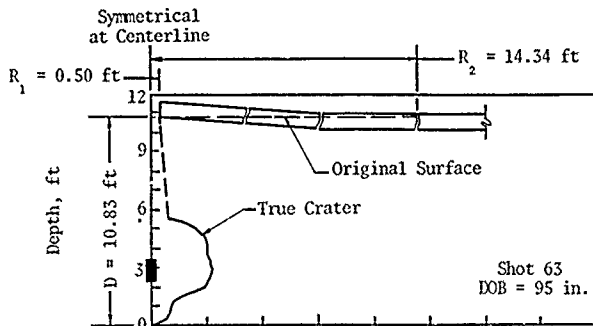
15-1b Charge, 11-Inch-Thick Concrete (Cont'd)



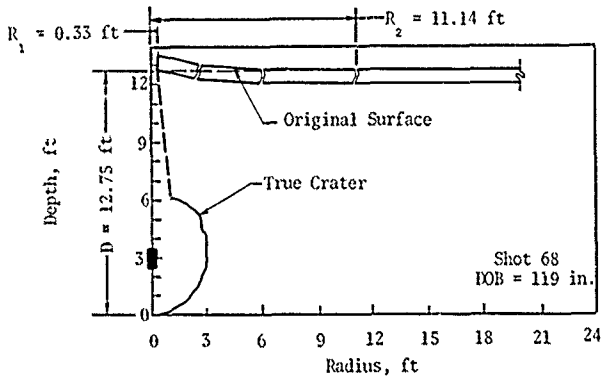
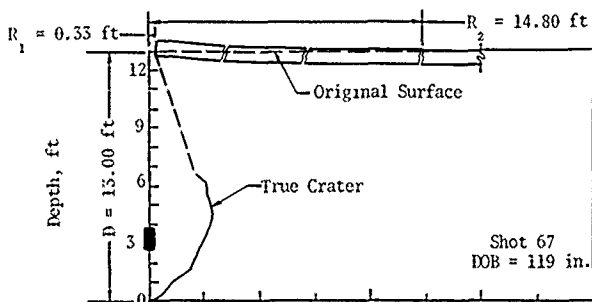
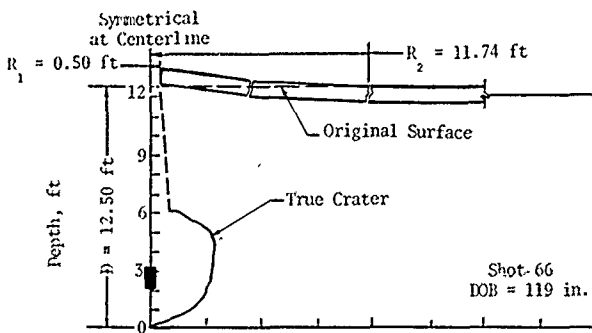


15-lb Charge, 11-Inch-Thick Concrete (Concl'd)

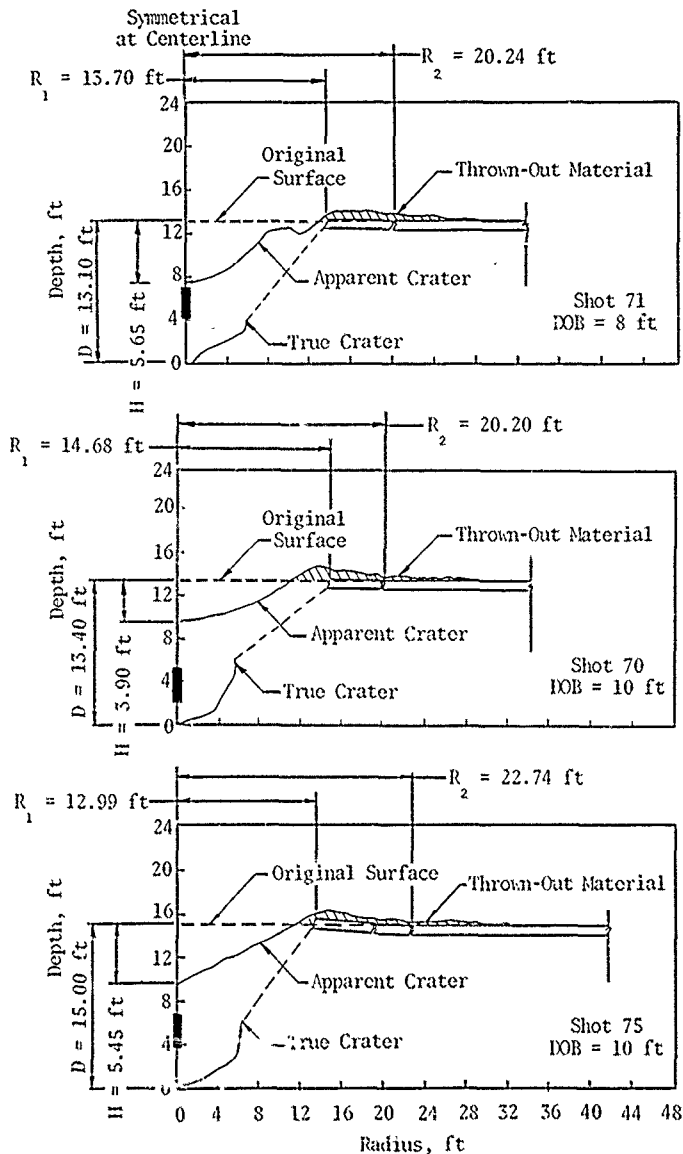




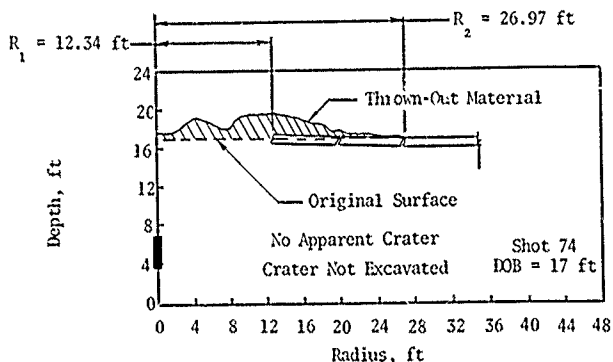
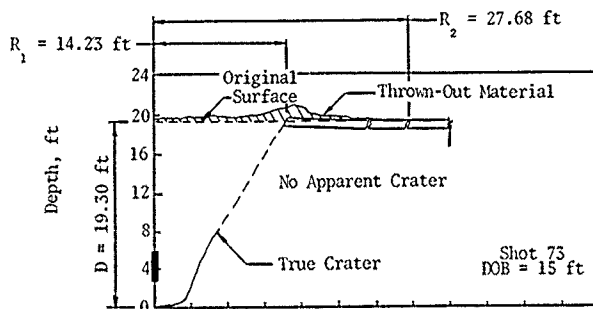
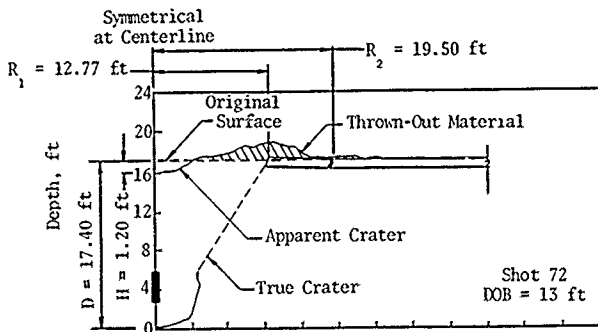
25-lb Charge, 8-Inch-Thick Concrete (Cont'd)



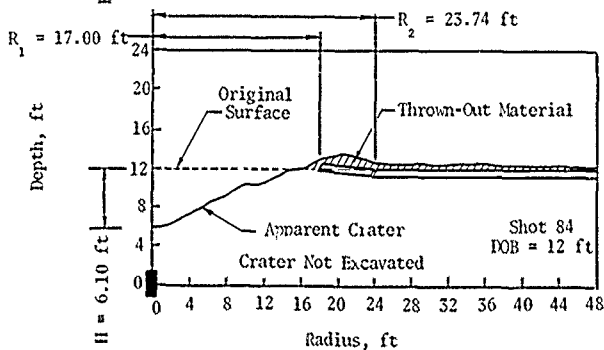
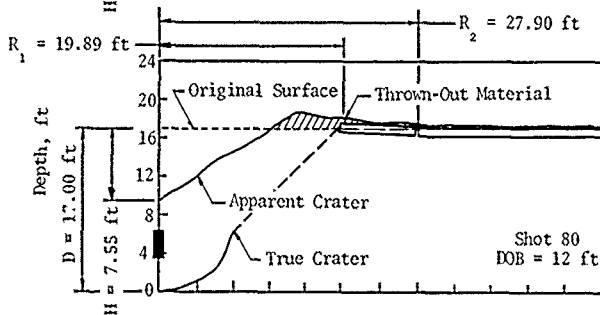
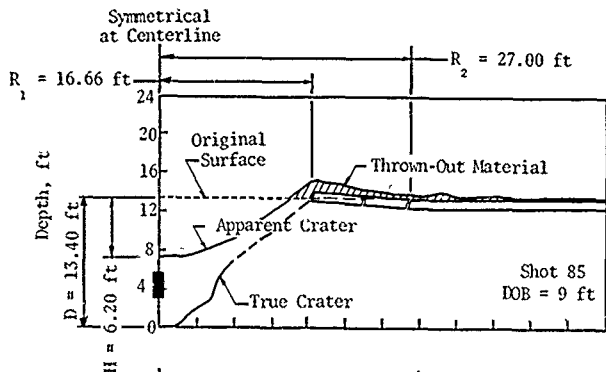
25-lb Charge, 8-Inch-Thick Concrete (Concl'd)



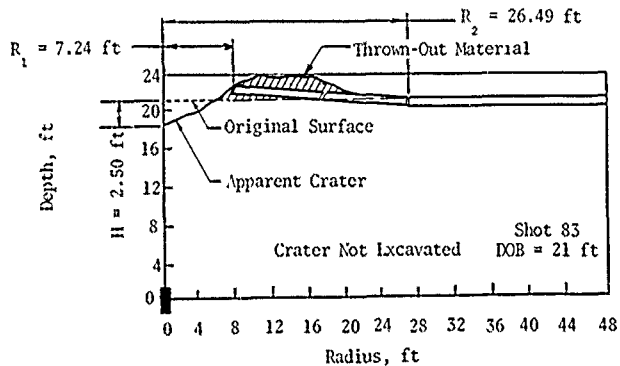
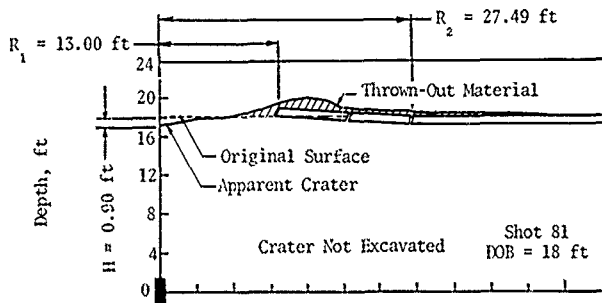
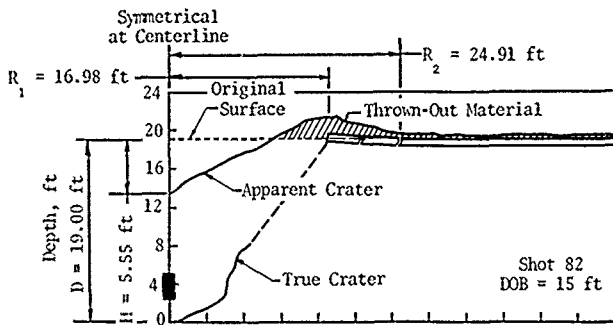
MK-81 (250-lb Bomb), 11-Inch-Thick Concrete



MK-81 (250-lb Bomb), 11-Inch-Thick Concrete (Concl'd)

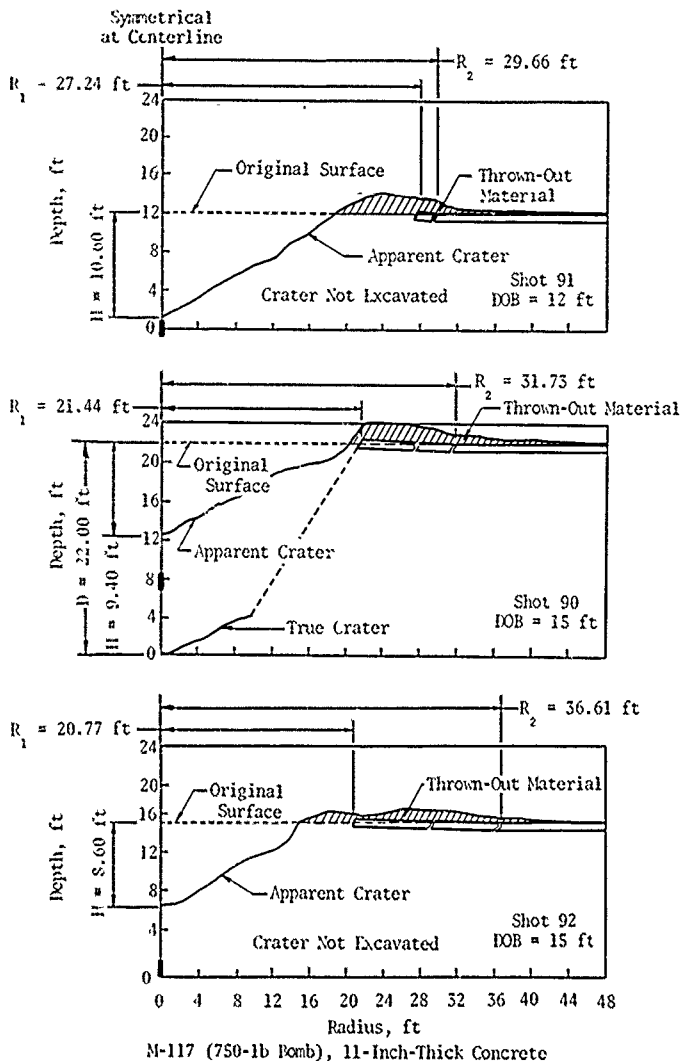


MK-82 (500-lb Bomb), 11-Inch-Thick Concrete

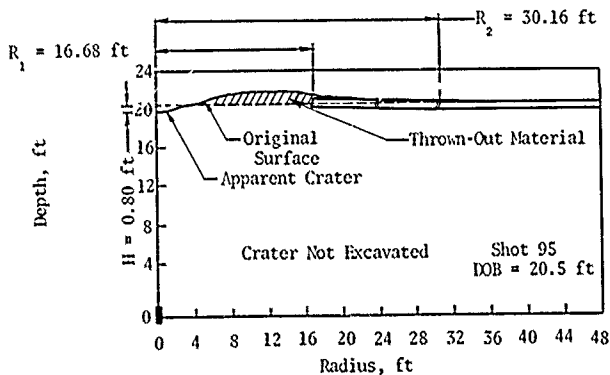
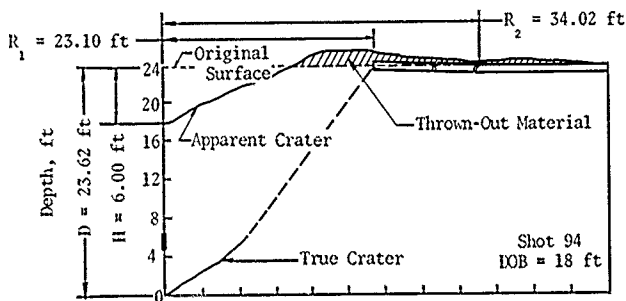
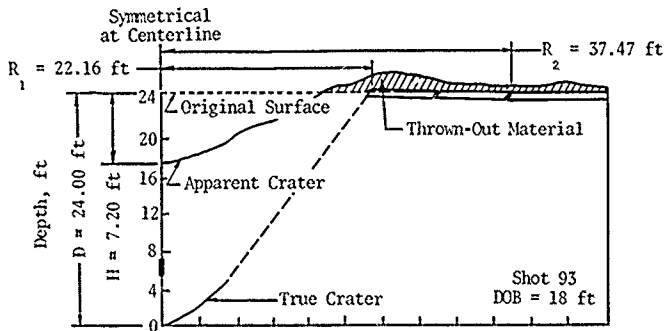


MK-82 (500-lb Bomb), 11-Inch-Thick Concrete (Concl'd)





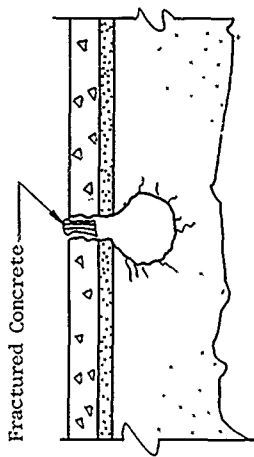
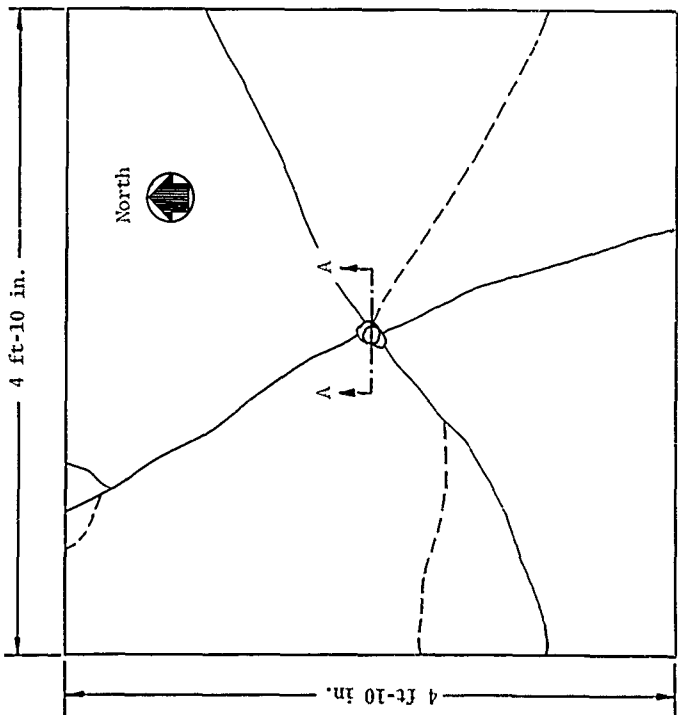
M-117 (750-lb Bomb), 11-Inch-Thick Concrete



M-117 (750-lb Bomb), 11-Inch-Thick Concrete (Concl'd)

APPENDIX V  
MODEL STUDY DATA

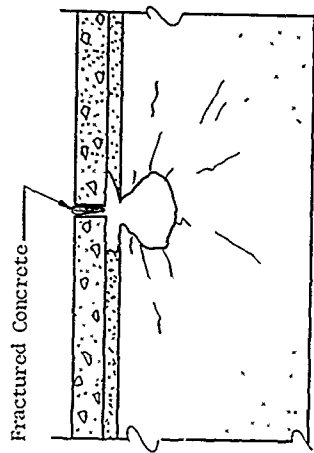
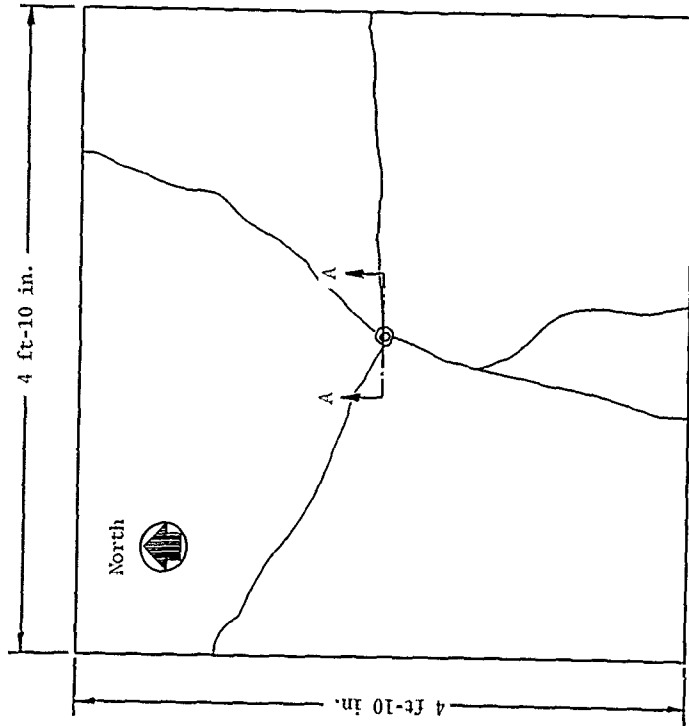
	<u>Page</u>
Test 2: 11.3-gm Charge	165
Test 3: 9-gm Charge	166
Test 4: 11.5-gm Charge	167
Test 5: 13-gm Charge	168
Test 6: 7-gm Charge	169
Test 8: 15-gm Charge	170
Test 9: 17.5-gm Charge	171
Test 10: 17.5-gm Charge	172



Section AA



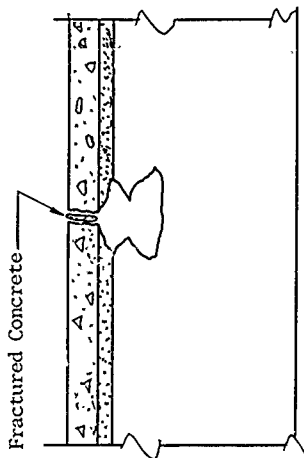
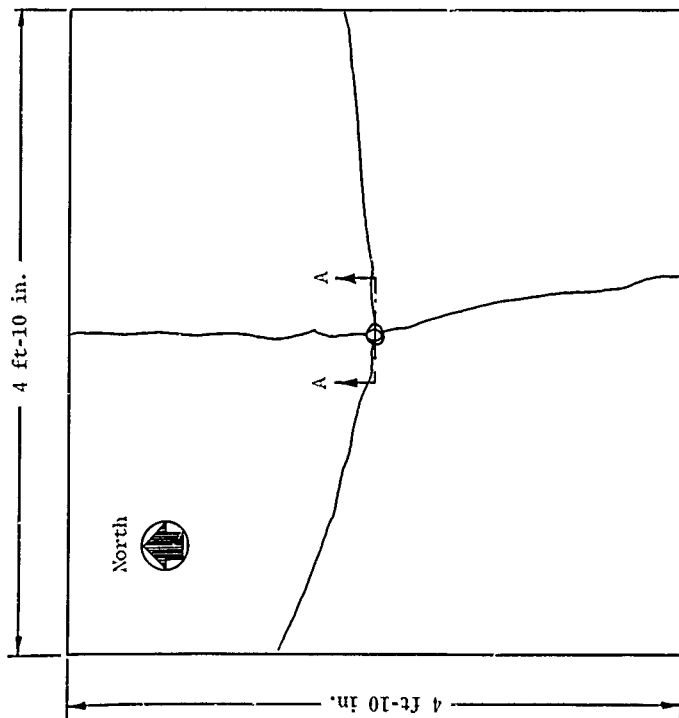
**Test 2: 11.3-gm Charge**



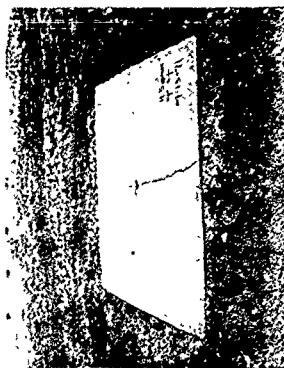
Section AA



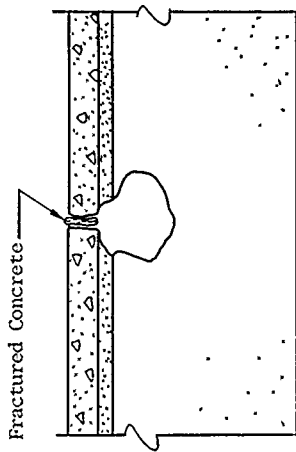
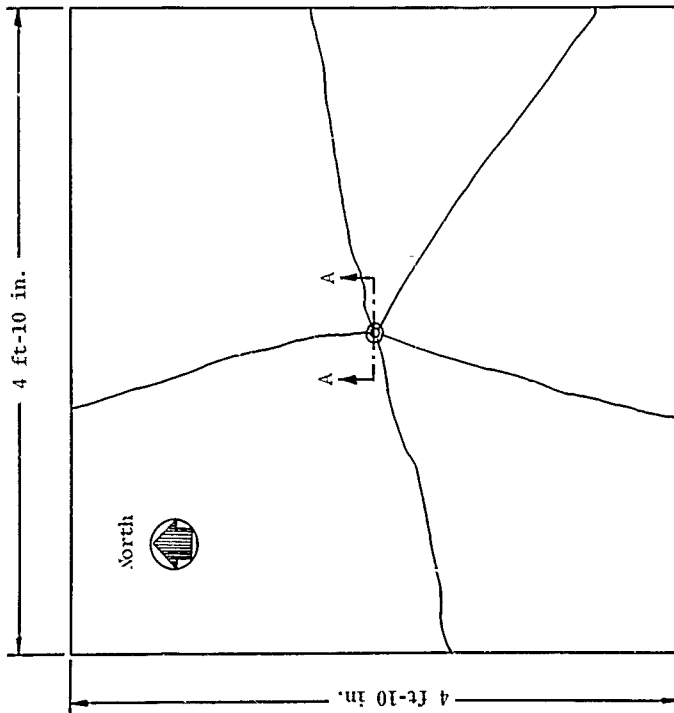
Test 3: 9-gm Charge



Section AA



Test 4: 11.5-gm Charge

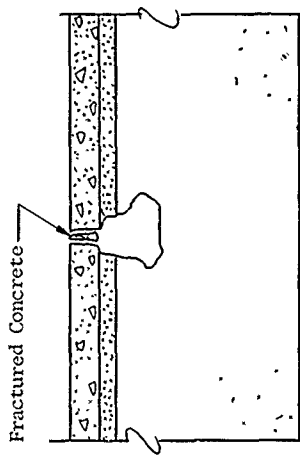
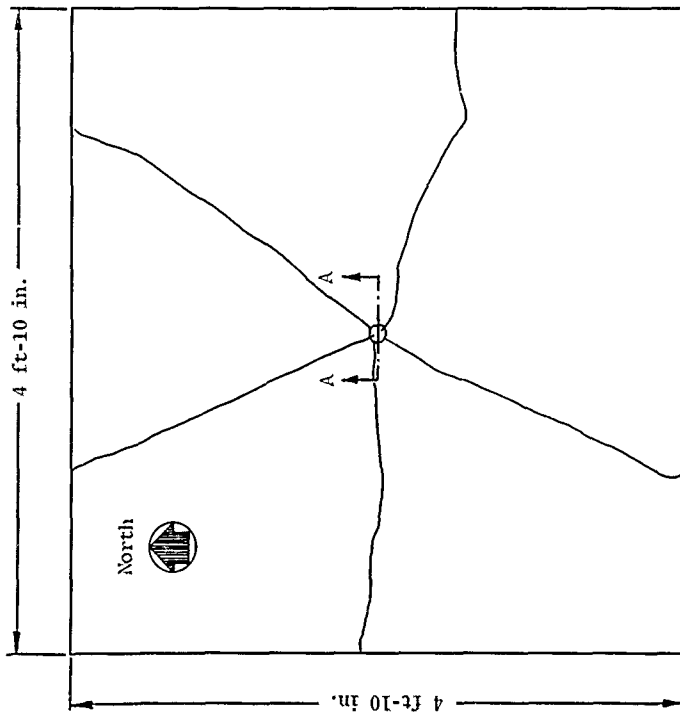


Section AA



Test 5: 15-gm Charge

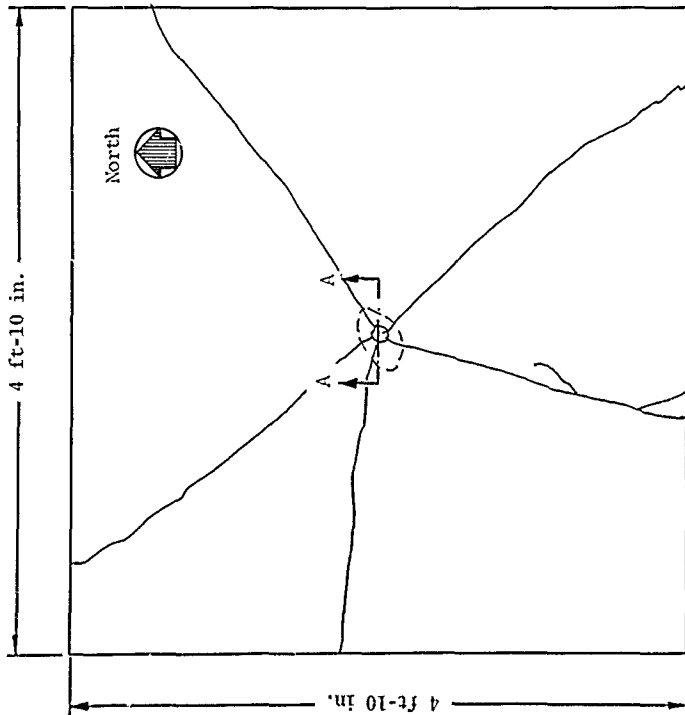




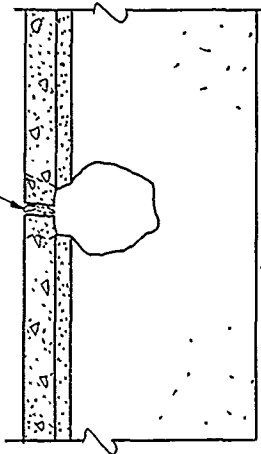
Section AA



Test 6: 7-gm Charge



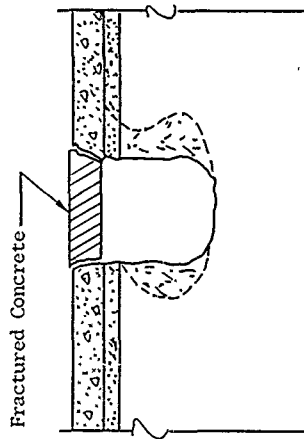
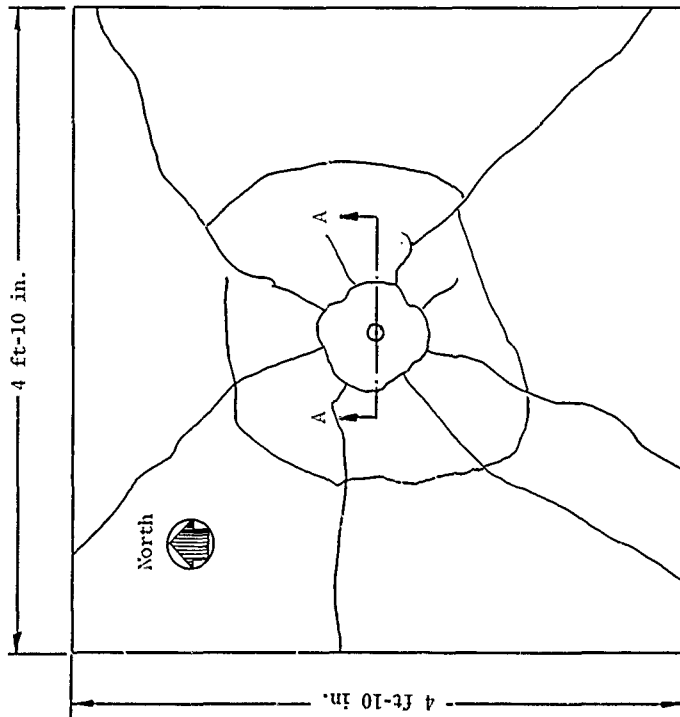
Fractured Concrete



Section AA



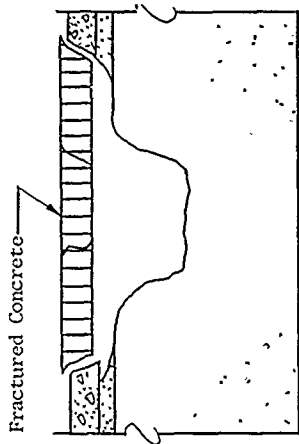
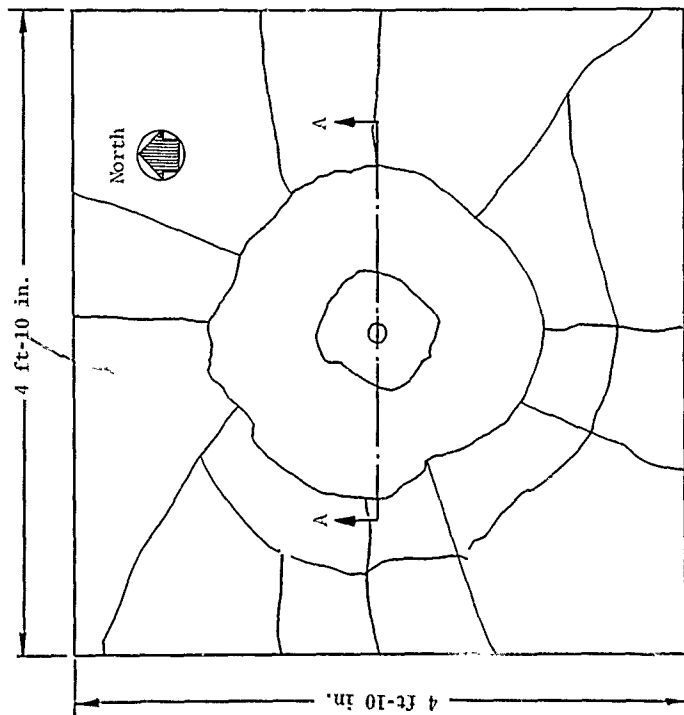
Test 8: 15-gm Charge



Section AA



Test 9: 17.5-gm Charge



Section AA



Test 10: 17.5-gm Charge

## REFERENCES

1. Pichumani, R., and Dick, Jr., J. L., *Effects of Small Cratering Charges on Airfield Pavements*, AFWL-TR-70-66, Kirtland Air Force Base, New Mexico, December 1970.
2. Vesić, A. B., and Barksdale, R. D., *Theoretical Studies of Cratering Mechanisms Affecting the Stability of Cratered Slopes*, Final Report, Project No. A-655, U.S. Army Engineer Waterways Experiment Station, Mississippi, September 1963.
3. Chabai, A. J., *Scaling Dimensions of Craters Produced by Buried Explosions*, SC-RR-65-70, Sandia Laboratories, Albuquerque, New Mexico, February 1965.
4. Johnson, J. B., and Fischer, R. L., *Effects of Mechanical Properties of Material on Cratering: A Laboratory Study*, U.S. Department of the Interior, Bureau of Mines, 1963.
5. Moraski, L. K., and Feal, D. J., *An Investigation of the Effects of Gravity on Crater Formation in a Cohesionless Medium*, Air Force Institute of Technology, Wright-Patterson Air Force Base, Ohio, September 1965.
6. Divoky, D., Comments on a Paper by A. J. Chabai, "The Equivalence of Mass and Energy Scaling of Crater Dimensions," *Journal of Geophysical Research*, Vol. 71, No. 10, May 15, 1966.
7. Saxe, H. C., and DelManzo, D. D., Jr., "A Study of Underground Explosion Cratering Phenomena," *Proceedings, Symposium on Engineering with Nuclear Explosives*, Las Vegas, Nevada, January 14-16, 1970.
8. Galbraith, B. G., *Hot's Analysis of Small Explosion Cratering Events in Dry Ottawa Sand*, M.S. Thesis, Air Force Institute of Technology, Wright-Patterson Air Force Base, Ohio, June 1970.
9. Bessert, G. C., *The Effects of Variation of Charge Size and Depth-of-Burst in Laboratory Sand Cratering Experiments*, M.S. Thesis, Air Force Institute of Technology, Wright-Patterson Air Force Base, Ohio, June 1970.
10. Carlson, R. H., and Newell, R. L., *Effects from Single-Charge Cratering, Explosions*, SC-RR-69 1, Sandia Laboratories, Albuquerque, New Mexico, June 1970.
11. D'Andrea, D. V., Fischer, R. L., and Hendrickson, A. D., *Crater Sealing in Granite for Small Charges*, Report No. 7409, U.S. Department of the Interior, Bureau of Mines, July 1970.
12. *ACI Standard Building Code Requirements for Reinforced Concrete* (ACI 318-63), American Concrete Institute, Detroit, Michigan, June 1963.

UNCLASSIFIED

Security Classification

DOCUMENT CONTROL DATA - R & D

1. ORIGINATING ACTIVITY (Corporate author) The Eric H. Wang Civil Engineering Research Facility University of New Mexico Albuquerque, New Mexico 87106			2a. REPORT SECURITY CLASSIFICATION UNCLASSIFIED	
3. REPORT TITLE PAVEMENT CRATERING STUDIES			2b. GROUP	
4. DESCRIPTIVE NOTES (Type of report and inclusive dates) January 1971 through January 1972				
5. AUTHOR(S) (First name, middle initial, last name) Ashbjorn Kvammen, Jr.; Raman Pichumani; James L. Dick, Capt, USAF				
6. REPORT DATE December 1972		7a. TOTAL NO. OF PAGES 186		7b. NO. OF REFS 12
8a. CONTRACT OR GRANT NO. F29601-72-C-0024		9a. ORIGINATOR'S REPORT NUMBER(S) AFWL-TR-72-61		
b. PROJECT NO. 6834		9b. OTHER REPORT NO(S) (Any other numbers that may be assigned this report)		
10. DISTRIBUTION STATEMENT Distribution limited to US Government agencies only because of test and evaluation (1 Dec 72). Other requests for this document must be referred to AFWL (DEZ), Kirtland AFB, NM 87117.				
11. SUPPLEMENTARY NOTES		12. SPONSORING MILITARY ACTIVITY AFWL (DEZ) Kirtland AFB, NM 87117		
13. ABSTRACT (Distribution Limitation Statement B) The objectives of this research effort were twofold: (1) to define the damage to air-field pavement systems caused by a wide range of C-4 charges and bombs when detonated at various depths below the pavement surface (i.e., determine the extent of damage expected from these explosives), and (2) to investigate the feasibility of scaling pavement systems and explosives in order to more economically study cratering effects on different pavement systems. The first objective was implemented by a series of tests using 5, 15, and 25-lb C-4 charges placed at various depths under pavement surfaces in two abandoned airfields (Fort Sumner and Hays) and three sizes of bombs at the Hays test site. Damage such as the repair volumes, true crater depths, etc., were plotted as a function of charge size and depth of-burst. Three types of craters were found: (1) shallow depth-of-burst craters of hemispherical shape, (2) deep depth-of-burst craters with no apparent crater and little ejecta, and (3) intermediate depth-of-burst craters exhibiting some of the characteristics of both the shallow and the deep craters. The crater dimensions from Fort Sumner (sandy silt subgrade) were, in general, smaller than those from Hays (clay subgrade) for all C-4 charges. A similitude analysis was conducted using the test data from the C-4 charges (Hays) to ascertain if a scaling factor or a distortion factor could be determined. The study revealed that the scaling factor varied widely when scaling the maximum damage depth-of-burst, the radius of the crater at the surface, and the crater volumes. To accomplish the second objective, small-scale tests were conducted modeling the full-scale experimental test performed at CLRF in 1969. This study also indicated variations in scaling factors.				

14	KEY WORDS	LINK A		LINK B		LINK C	
		ROLE	WT	ROLE	WT	ROLE	WT
	Cratering of rigid pavements Airfield pavement cratering Bomb damage on pavements Full-scale pavement cratering tests Apparent craters True craters Small-scale pavement cratering studies						